DEFENSE DOCUMENTATION CENTER

FOR

SCIENTIFIC AND TECHNICAL INFORMATION

CAMERON STATION. ALEXANDRIA. VIRGINIA

ASD-TDR-62-696

Mission Analysis for Controlled Fusion Propulsion System

Richard L. Verga

Robert F. Cooper

D D C

JUN 19 1963

TISIA B

NO OTS

NOTICES

When Government drawings, specifications, or other data are used for any purpose other than in connection with a definitely related Government procurement operation, the United States Government thereby incurs no responsibility nor any obligation whatsoever; and the fact that the Government may have formulated, furnished, or in any way supplied the said drawings, specifications, or other data, is not to be regarded by implication or otherwise as in any manner licensing the holder or any other person or corporation, or conveying any rights or permission to manufacture, use, or sell any patented invention that may in any way be related thereto.

ASTIA release to OTS not authorized.

Qualified requesters may obtain copies of this report from the Armed Services Technical Information Agency, (ASTIA), Arlington Hall Station, Arlington 12, Virginia.

Copies of this report should not be returned to the Aeronautical Systems Division unless return is required by security considerations, contractual obligations, or notice on a specific document.

D

ASD-TDR-62-696

FOREWORD

This report was prepared by the Electric and Advanced Propulsion Branch, Propulsion Laboratory, Directorate of Aeromechanics, Deputy for Technology, Aeronautical Systems Division, Wright-Patterson Air Force Base, Ohio, under AFSC Project 5350, "Advanced Concepts for Propulsion," with Robert F. Cooper as project engineer for the laboratory.

The studies presented began 1 February 1962 and were concluded in May 1962.

The application of controlled thermonuclear reactions for the propulsion of a space vehicle has been subject to an intensive in-house investigation under AFSC Project 5350. Three technical reports are to be published, which will summarize the results of these efforts. The first deals with the conceptual feasibility of the application. It will be published as ASD Technical Documentary Report 62-698, "Controlled Fusion for Space Application." The second, in providing preliminary development of design philosophy, will give a detailed analysis of the physics and engineering problems that will be encountered in designing a controlled fusion thrustor for space application. This report, to be titled "An Analysis of Controlled Fusion for Space Propulsion Systems," has not yet been assigned a number. This report, the third of the series, discusses the mission capabilities of a typical controlled fusion propulsion device. It is being published as ASD Technical Documentary Report 62-696, "Mission Analysis for a Controlled Fusion Propulsion System."

ASD-TDR-62-696

ABSTRACT

This report presents a discussion of the relationships existing between engine, vehicle, and mission parameters of a typical controlled-fusion propulsion (CFP) system. The low specific weight (α) obtainable with a CFP device allows extremely high payload fractions in large vehicles. The CFP system is compared with other electric propulsion systems, and the CFP system is shown to possess inherent advantages for the performance of high ΔV missions.

PUBLICATION REVIEW

This technical documentary report has been reviewed and is approved.

FOR THE COMMANDER:

ROBERT SUPP
Chief, Electric and Advance Propulsion
  Branch
Propulsion Laboratory

TABLE OF CONTENTS

LIST OF ILLUSTRATIONS

LIST OF ILLUSTRATIONS (Continued)

LIST OF ILLUSTRATIONS (Continued)

LIST OF SYMBOLS

W_o = total initial mass of vehicle

W_E = mass of electric engine

W_P = mass of propellant

W_L = mass of payload

W_S = mass of structure that is associated with vehicle and payload

W_{L+S} = $W_L + W_S$

W_G = mass of generator (or engine, for CFP system)

ΔV = total velocity increment that is required for accomplishment of the mission; ΔV is the sum of escape from earth ΔV_e, orbit to orbit transfer ΔV_t, and planet capture ΔV_p, etc.

a = acceleration (constant)

t_b = burn time of engine

η = efficiency

P = beam power

C = expellant exhaust velocity

C_o = optimum initial exhaust velocity

C_f = optimum final exhaust velocity

V_c = $218\sqrt{\dfrac{\eta t_b}{a}}$ = characteristic velocity. This is the maximum achievable exhaust velocity.

f_{L+S} = payload fraction $\dfrac{W_{L+S}}{W_o}$

f_G = generator (or CFP engine) fraction = $\dfrac{W_G}{W_o}$

f_P = propellant fraction = $\dfrac{W_P}{W_o}$

$W(t)$ = mass of vehicle as a function of time

α = specific weight of power plant (pounds per kilowatt)

I_{sp}^{o} = optimum initial specific impulse

I_{sp}^{f} = optimum final specific impulse

F = thrust level of the propulsion device

g = acceleration of gravity

For a CFP device, $W_o = W_L + W_P + W_G + W_S$.

For an electric system, $W_o = W_L + W_P + W_G + W_E + W_S$

ix

where $W_E \ll W_o$ and may be neglected. The propulsive package for CFP and for electric is W_G and $W_G + W_E$ respectively.

INTRODUCTION

Fusion propulsion, or the application of controlled thermonuclear reactions to the propulsion of a space vehicle, has heretofore been considered a "far-future" approach to the problem of obtaining high-power propulsion systems for use in space. Recent advances in sustained superconductivity indicate that the fabrication of low-weight magnetic coils that require negligible power for operation will be possible. These advances will permit the generation of fields as high as several hundred kilogauss without huge coils and unfeasibly heavy cooling systems. This savings in weight now makes fusion power for space propulsion extremely attractive. Under the assumption that controlled fusion will be realized in the near future, a number of engineering studies have been made recently concerning the application of this process to space propulsion. For the purposes of this report, representative values of the operating parameters for propulsion systems have been obtained from these analyses, and a set of equations for missions of electric propulsion systems have been modified and used to study the mission capabilities of a typical controlled fusion propulsion (CFP) system. The motivation for the writing of this report was provided by the apparently obvious capacity of a CFP device for the performance of ultra-high ΔV missions. Detailed analyses have been found to confirm this assumption.

The weight of the power supply that is required to put a certain amount of energy into the exhaust jet is frequently used in fission-electric systems to express the characteristics of the propulsion system. Fission-electric and CFP systems have been compared on this specific weight(α), which is expressed in pounds per kilowatt. A realistic α of 10 pounds per kilowatt is used for an advanced electric system. For CFP systems, conservative values of 1 and 3 pounds per kilowatt are used.

The assumption has been made that controlled fusion will be realized in the near future. Because of the general optimism of that portion of the scientific community engaged in thermonuclear research and because of continuing advances in superconductivity, an urgent need exists for further study and analysis of fusion propulsion. Irrecoverable years, so vital in this time of national need, may be lost in the transition from concept to usable device unless the groundwork for this development has been laid previously. The primary purpose of this study is to assist in providing the urgently needed impetus for further work in the field of fusion propulsion.

Questions arise concerning the advisability of undertaking large-scale mission analyses for a vehicle whose operating parameters are at best only roughly estimated. Because of the apparently enormous potential of such devices for the performance of a number of high energy missions, some efforts are most certainly justified at this time. The studies presented in this report are based on a large number of simplifying assumptions and are admittedly of a preliminary nature. The purposes of the studies are to establish general trends, rather than to predict exact values. More detailed analyses will be justified only when the operating parameters of a proposed system can be predicted with an accuracy greater than the order-of-magnitude estimates that are presently possible.

ANALYTICAL APPROACH

The various propulsion systems presently existing or under development embrace a wide spectrum of thrust and specific impulse (I_{sp}) values. Providing any reasonable common denominator for the comparison of the potential of several propulsion devices for the performance of various missions proves extremely difficult. For purposes of illustration, such a comparison might be effected on the general basis of mission energy, the total energy increment that must be given to the vehicle for accomplishment of the mission. This rather arbitrary quantity is a function of the total weight of the vehicle (W_o) and total required velocity increment (ΔV).

The equation

$$\frac{P}{W_o} = \frac{1}{2} g \left(\frac{F}{W_o}\right) I_{sp}$$

gives the power-to-weight ratio in terms of the more common thrust-to-weight ratio and I_{sp}. The power-to-weight ratios for various propulsion systems are plotted as a function of mission energy in Figure 1. From these curves, one can see that a propulsion system of large minimum weight is severely penalized for low energy missions. For high energy missions, this disadvantage soon vanishes and the relative efficiencies of the systems become apparent. Only electric and CFP systems are competitive for missions of very high energy (large payloads and long distances in short time). In this regime, the electric systems are limited only by the total fuel inventory of the reactor.

The ($\frac{P}{W_o}$) curves of Figure 1 are plotted without coordinates. The points of intersection of the various curves will shift with variations in the parameters of the individual systems; the curves merely indicate general trends.

With the preceding philosophical arguments in mind, round trip and one-way missions to the Moon and to Mars, Venus, and Jupiter are analyzed for a CFP device, and results are compared with typical electric propulsion systems. All missions are assumed to originate in a 200-nautical-mile orbit of the earth and to terminate, in the case of one-way missions, in an orbit of altitude that is 1/10 the radius of the planet. Round trip missions terminate in a 200-nautical-mile orbit of the earth. Constant acceleration, with variable thrust and specific impulse, is assumed for all missions.

The weight of the engine has been neglected for all calculations for the electric systems. This is valid at low power levels, but is questionable for the higher power (i.e., 10 megawatts or greater) systems. Here the weight of the engine may become a sizable fraction of the total weight of the vehicle.

"Normalization" of a sort has been accomplished. The total power of the CFP system is taken to be 10 megawatts. Since all weights of the vehicles are linear with power, actual weights may, therefore, be conveniently found for any power level. The specific weight of the CFP system (3 pounds per kilowatt) is the result of a first look at the vehicles. Further optimization should result in an α of the order of unity. Values less than unity are not unrealistic. Relationships have been derived allowing calculations for any α using the values for $\alpha = 1$.
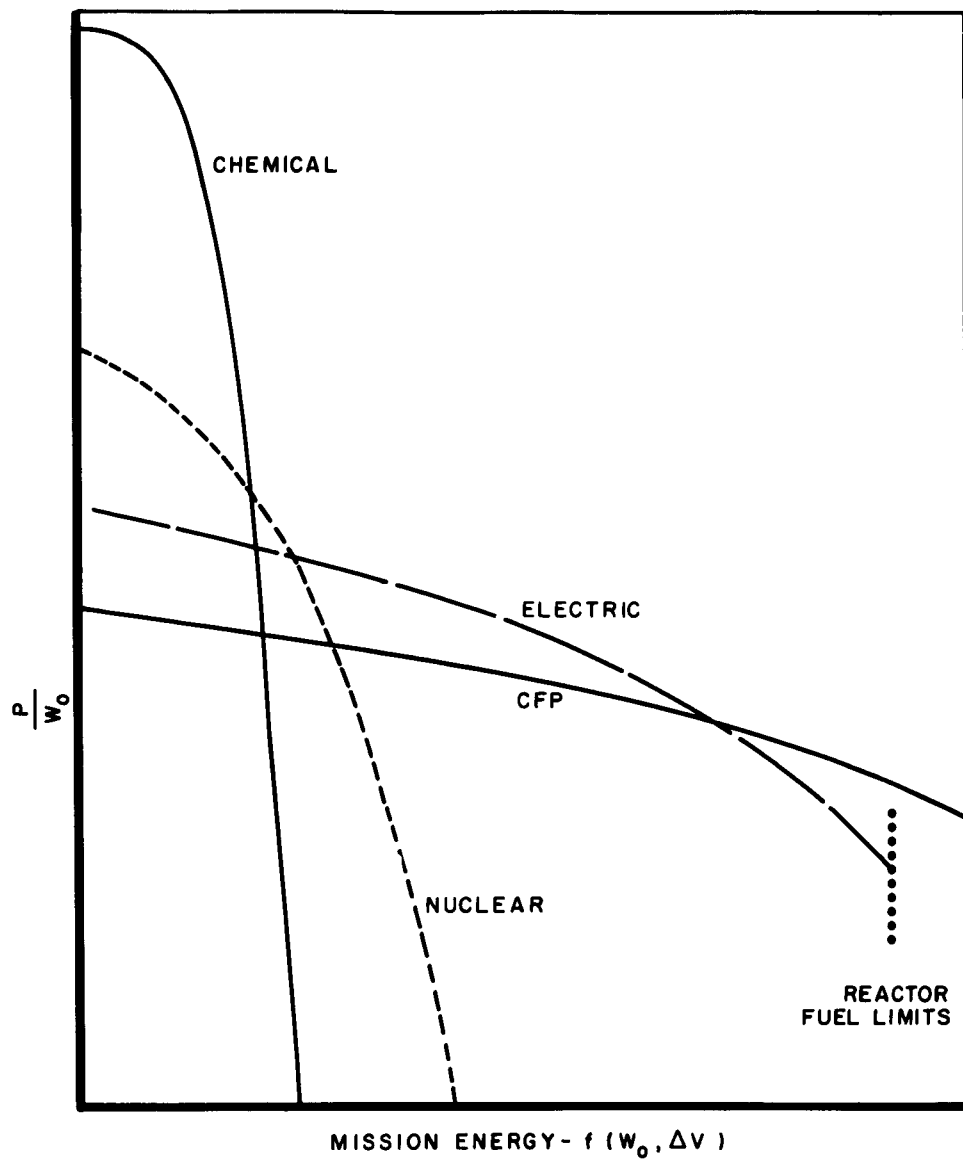
Figure 1. Power-to-Weight Ratio Versus Mission Energy for Four Propulsion Systems

DERIVATION OF ENGINE PARAMETERS

The derivation of engine parameters follows that given in Reference (1).

In general, the total initial weight of the vehicle (W_o) may be divided into

$$W_o = W_G + W_P + W_{L+S} \tag{1}$$

where

$$W_G = \alpha P . \tag{2}$$

For the case of constant acceleration, the velocity increment of the vehicle (ΔV) is given by the product of the acceleration of the vehicle and the burn time

$$\Delta V = a\, t_b \tag{3}$$

and the mass of propellant that is consumed in achieving this ΔV is

$$W_P \ (\text{pounds}) = 4.75 \times 10^4 \ \eta \ P \int_0^{t_b} \frac{1}{c^2} \ dt . \tag{4}$$

A number of optimization procedures are possible. For the purpose of this study, the payload fraction, or

$$f_{L+S} = 1 - f_G - f_P \ , \tag{5}$$

is "maximized" subject to the condition that

$$a = \frac{\Delta V}{t_b} = \frac{F(t)}{W(t)} = \text{constant}$$

where

F (t) is given by

$$F(t) \ (\text{pounds f}) = 1.476 \times 10^3 \ \frac{\eta P}{c} \quad (\text{see Reference 2}). \tag{6}$$

The mass of the vehicle as a function of time is just the initial mass minus the mass of the propellant used, or

$$W(t) = W_o - \frac{4.75 \times 10^4}{g} \ \eta P \int_0^{t_b} \frac{1}{c^2} \ dt. \tag{7}$$

Solving for the exhaust velocity as a function of t and P gives

$$c' = \left(\frac{\Delta V}{t_b}\right) t + \frac{4.75 \times 10^4 \ \eta P t_b}{\Delta V \ W_o} \ , \tag{8}$$

4

where the primed symbolism is used to designate unoptimized values. This says that for a constant acceleration program, C is a linear function of time with initial value C_o' given by

$$C_o' = \frac{4.75 \times 10^4 \, \eta \, P \, t_b}{\Delta V \, W_o} \tag{9}$$

The exhaust velocity at the completion of the mission is then

$$C_f' = C_o' + \Delta V \tag{10}$$

Combining and rewriting Equations (2), (4), and (5) yields

$$f_{L+S} = 1 - \frac{\alpha \, P}{W_o} - \frac{4.75}{W_o} \times 10^4 \int_0^{t_b} \frac{1}{C^2} \, dt. \tag{11}$$

Substituting the value of C from Equation (8) gives

$$f_{L+S} = -\frac{\alpha P}{W_o} + \frac{1}{1 + \dfrac{2.101 \times 10^{-8} \, (\Delta V)^2}{t_b \, \eta \, \left(\dfrac{P}{W_o}\right)}} \tag{12}$$

To obtain the maximum values of the payload fraction, one must set the derivative of f_{L+S}, with respect to $\dfrac{P}{W_o}$, equal to zero. Then

$$\frac{d f_{L+S}}{d\left(\dfrac{P}{W_o}\right)} = -\alpha - \frac{\dfrac{2.101 \times 10^{-8} \, (\Delta V)^2}{t_b \, \eta \, \left(\dfrac{P}{W_o}\right)^2}}{\left[1 + \dfrac{2.101 \times 10^{-8} \, (\Delta V)^2}{t_b \, \eta \, \dfrac{P}{W_o}}\right]^2} = 0. \tag{13}$$

Introducing

$$V_c = 218 \sqrt{\eta \frac{t_b}{\alpha}}$$

and solving for $\dfrac{P}{W_o}$ gives

$$\frac{P}{W_o} = \frac{2.101 \times 10^{-8}}{\eta(t_b)} \, \Delta V \, (V_c - \Delta V) \cdot \tag{14}$$

When this equation is substituted into the value of C' found in Equation (8), the optimum exhaust velocity (the exhaust velocity that is associated with the maximized payload) is given by

$$C_{op} = \left(\frac{\Delta V}{t_b}\right) t - V_c - \Delta V \quad , \tag{15}$$

with the initial and final values given by

$$c_o = V_c - \Delta V \tag{16}$$

and

$$c_f = V_c \tag{17}$$

Figure 2 shows a plot of $\dfrac{C_o}{V_c}$ and $\dfrac{C_f}{V_c}$ versus $\dfrac{\Delta V}{V_c}$.
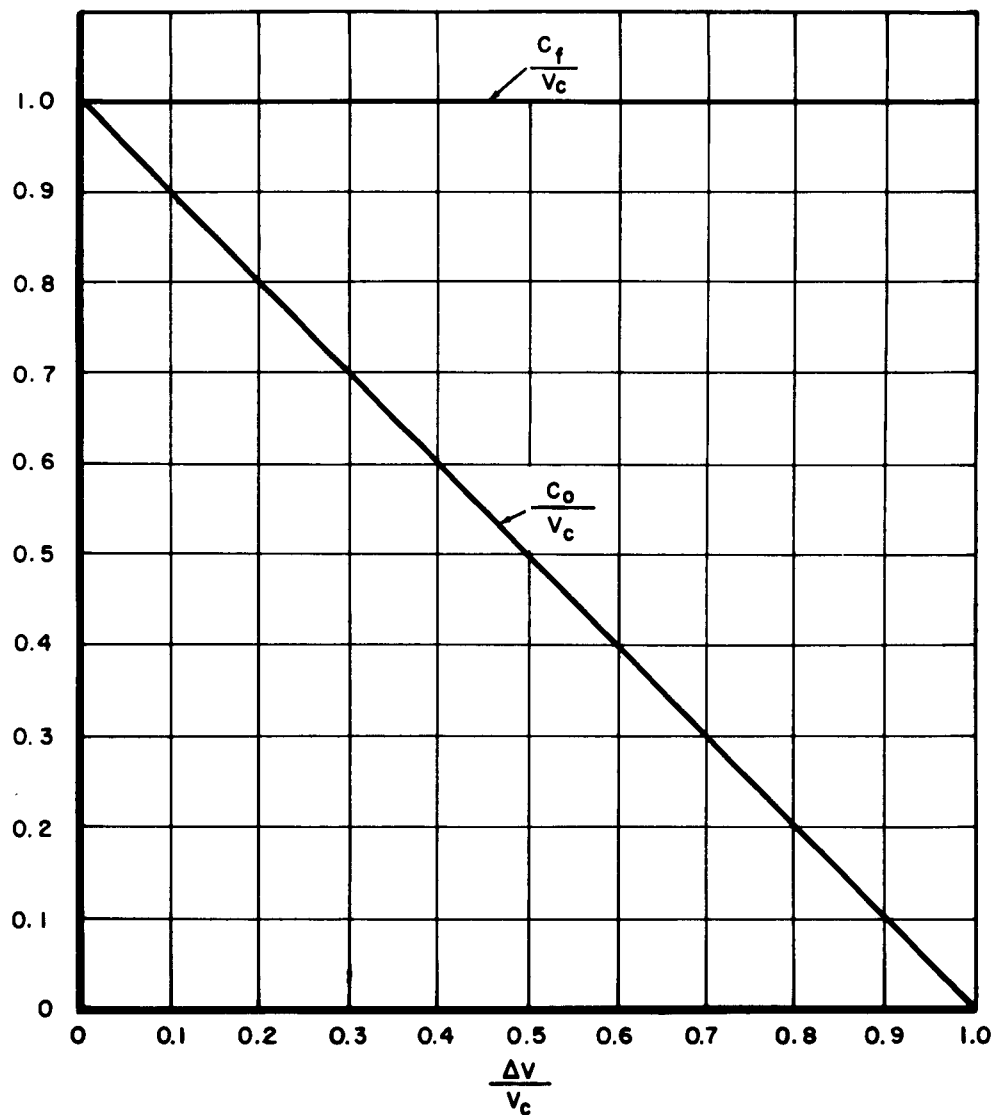
Figure 2. $\dfrac{C_f}{V_c}$ and $\dfrac{C_o}{V_c}$ Versus $\dfrac{\Delta V}{V_c}$

Equations (12), (13), and (14) may be combined to yield the maximum payload fraction. That is

$$(f_{L+S}) = \left(\frac{\Delta V}{V_c} - 1\right)^2 \tag{18}$$

From Equations (2) and (5),

$$f_G = \frac{\Delta V}{V_c}\left(1 - \frac{\Delta V}{V_c}\right) \tag{19}$$

Adding Equations (18) and (19) gives

$$f_G + f_{L+S} = 1 - \frac{\Delta V}{V_c} \tag{20}$$

Figure 3 shows a plot of f_{L+S} and $f_G + f_{L+S}$ as a function of $\frac{\Delta V}{V_c}$.

METHOD OF PLOTTING CURVES

The energy required for the successful completion of a given mission is measured in terms of ΔV, or total velocity increment. This ΔV is an inverse function of time; Figures 4 through 6 give ΔV for the missions discussed in this report (References 3, 4, and 5).

By using Figures 4 through 6 one may formulate a simplified method of computing mission parameters as follows:

a. ΔV is read from Figures 4, 5, or 6

b. V_c is calculated from

$$V_c = 218\sqrt{\frac{\eta t_b}{\alpha}}$$

In this report, optimistically projected efficiencies are used for all engines.

c. $\frac{\Delta V}{V_c}$ is computed

d. $\frac{C_o}{V_c}$ is read from Figure 2

e. $C_o = \frac{C_o}{V_c} \times V_c$ is calculated, giving the optimum initial exhaust velocity for the particular mission

f. $C_f = V_c$ is determined from Equation (16)

g. $I_{sp}^* = \frac{C_o}{32.2}$ is calculated

h. $I_{sp}^f = \frac{V_c}{32.2}$ is calculated
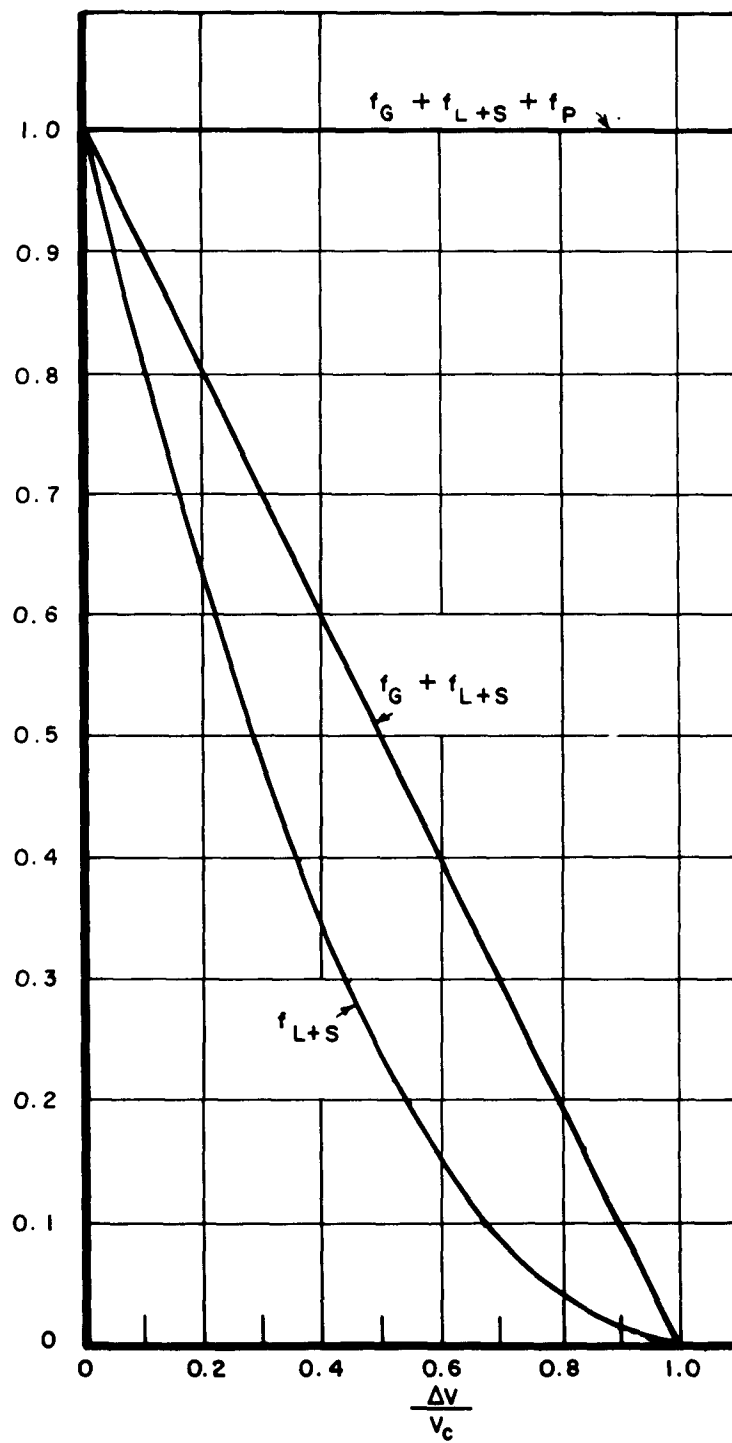
Figure 3. f_{L+S} and $f_G + f_{L+S}$ Versus $\dfrac{\Delta V}{V_c}$
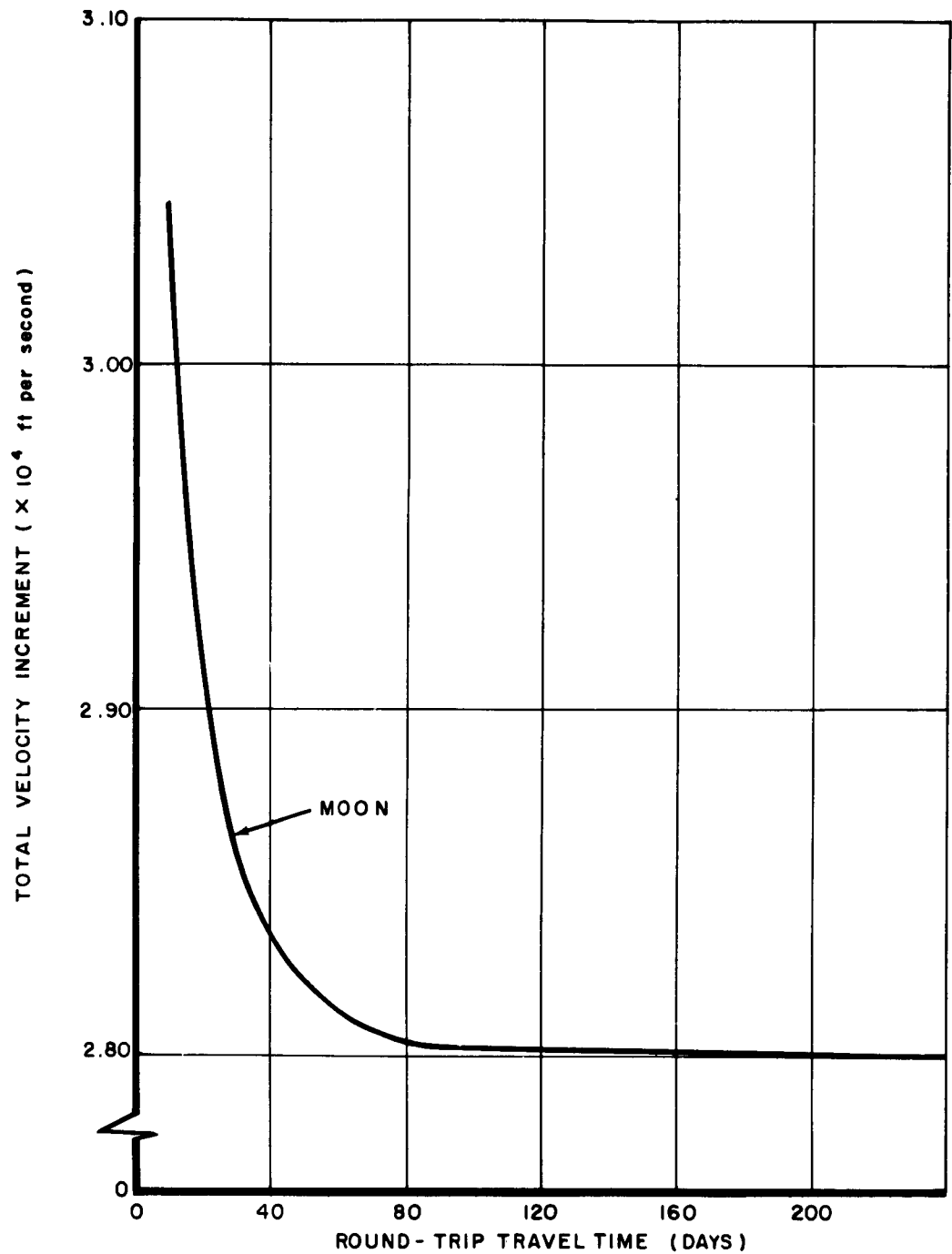
Figure 4. Total Velocity Increment for Round Trip Mission to Moon
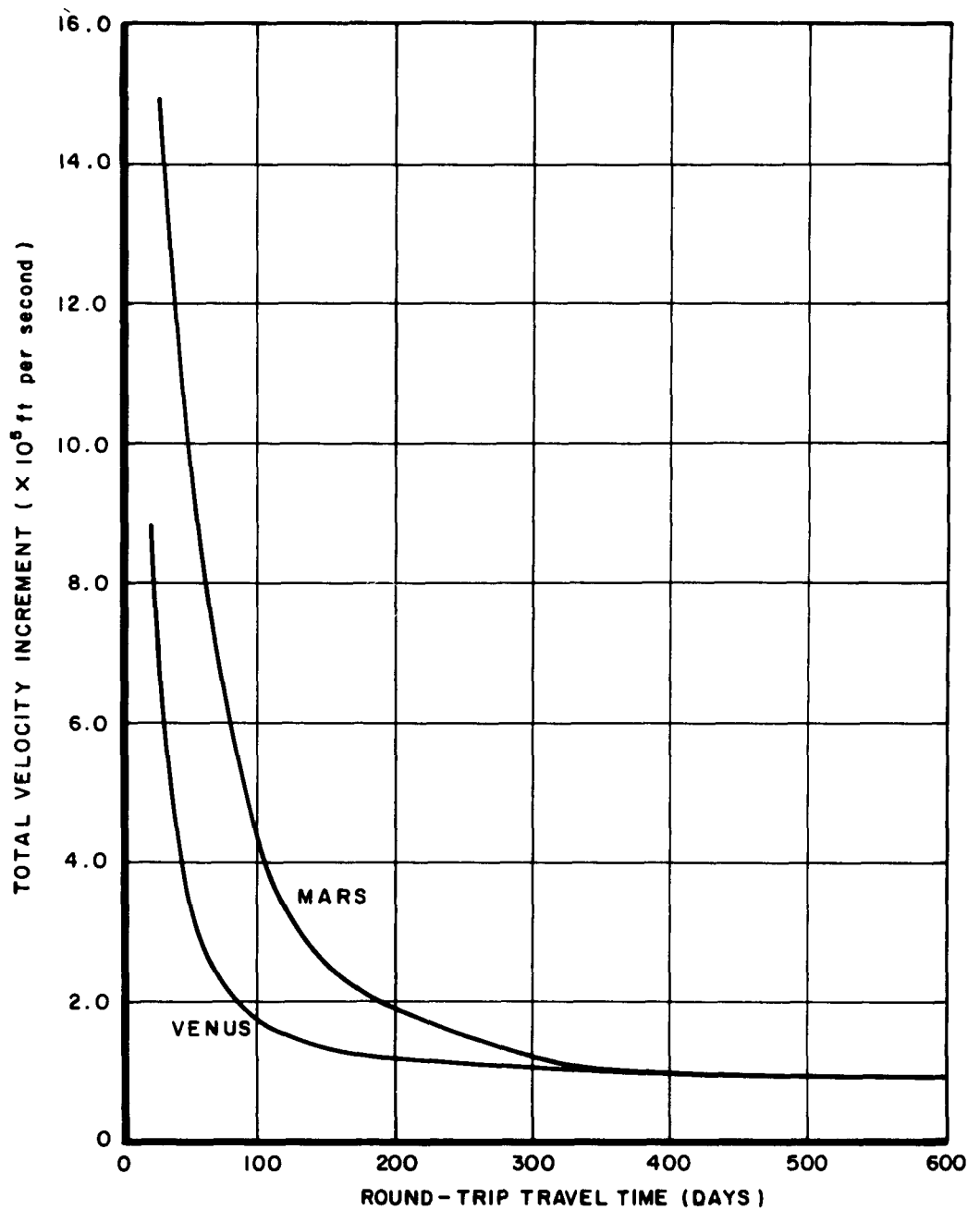
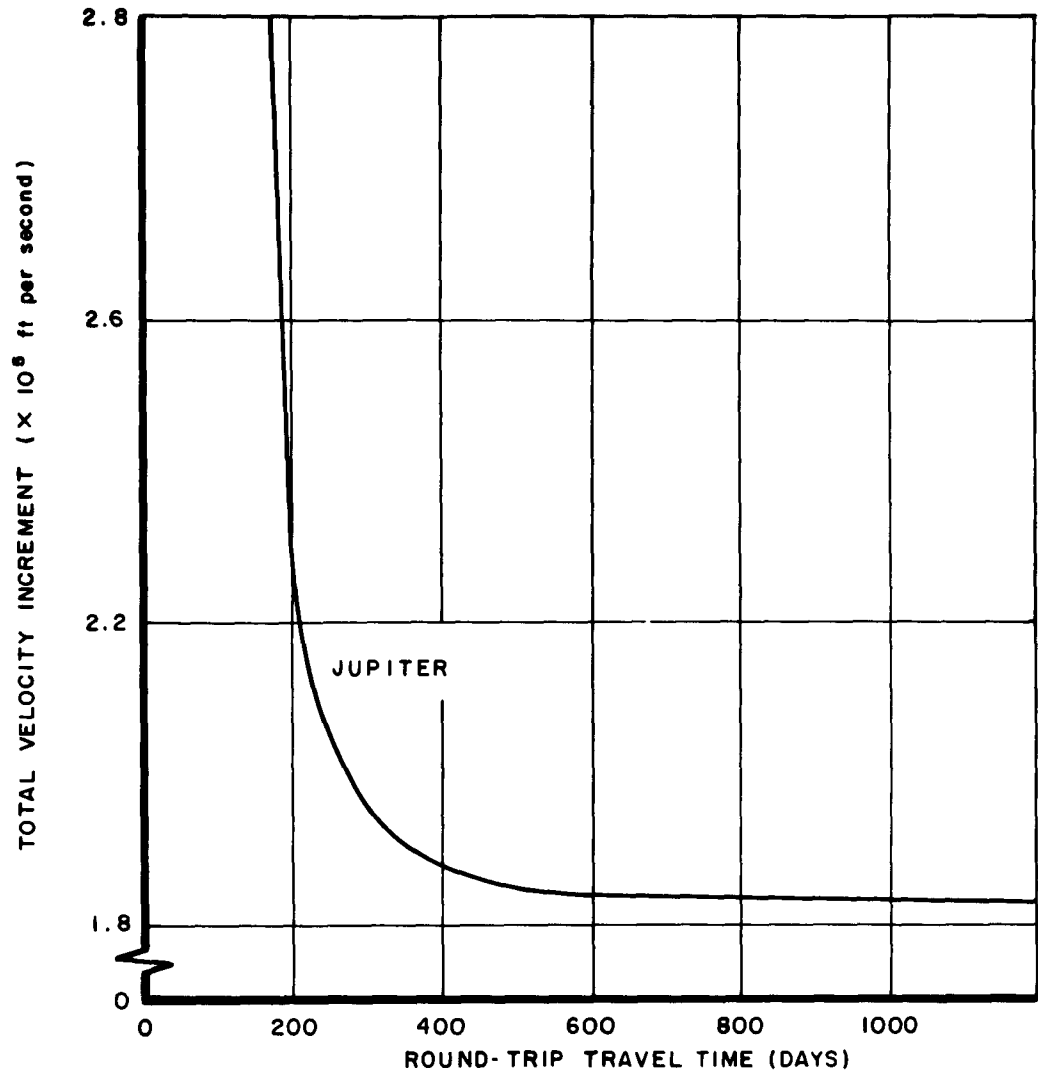Figure 5.   Total Velocity Increment for Round Trip Missions to Mars and Venus

Figure 6. Total Velocity Increment for Round Trip Mission to Jupiter

i. $f_{L + S}$ is read from Figure 3. This yields the payload fraction associated with the optimum specific impulse found previously.

j. $f_G + f_{L + S}$ is read from Figure 3. $f_{L + S}$ is subtracted from this value to give f_G, the power-plant fraction that is associated with the optimum I_{sp}.

k. $f_p = 1 - f_{L + S} - f_G$ is calculated.

The foregoing arguments do not depend on many of the system parameters. The fractions of the total vehicle mass that have been derived depend only upon the efficiency, burn time, and specific weight; they do not depend on any actual weights and power limits. When the weight of the power plant (W_G) is known, an initial weight of the vehicle and an associated weight of the payload may be found as a function of the optimum I_{sp}. For systems possessing certain definite characteristics, the calculations of the weights of the vehicles and payloads are given as follows:

a. For a CFP system, $W_o = \dfrac{W_G}{f_G}$

and

$$W_{L+S} = f_{L+S} \times W_o$$

b. For an electrical system to deliver a payload of identical weight,

$$W_o' = \dfrac{W_{L+S}}{f_{L+S}'}$$

and

$$P' = \dfrac{f_G' \, W_o'}{\alpha'}$$

where primed symbols refer to electrical systems.

c. Conversely, for an electrical system with the same initial vehicle weight,

$$W_{L+S}' = f_{L+S}' \times W_o$$

$$W_G' = f_G' \, W_o$$

and

$$P' = \dfrac{W_G'}{\alpha'} \quad .$$

The plots of mission parameters may be further simplified by effecting some sort of normalization. In the equations that follow, the quantities subscripted with a zero refer to the value calculated on the basis of $\alpha = 1$. The relationships give the parameter values for any α in terms of the value corresponding to $\alpha = 1$.

From Equation (16),

$$(C_o)_o = (V_c)_o - \Delta V \qquad \text{for } \alpha = 1.$$

For any α ,

$$C_0 = \frac{(V_c)_0}{\sqrt{\alpha}} - \Delta V = (C_0)_0 + (V_c)_0 \left(\frac{1}{\sqrt{2}} - 1 \right) . \qquad (21)$$

Also, for any α,

$$I_{sp}^{\bullet} = (I_{sp}^{\bullet})_0 + (V_c)_0 \left(\frac{1}{\sqrt{2}} - 1 \right) \qquad (22)$$

and

$$I_{sp}^{f} = \frac{(I_{sp}^{f})_0}{\sqrt{\alpha}} . \qquad (23)$$

Similarly from Equation (18),

$$(f_{L+S})_0 = \left[\left(\frac{\Delta V}{V_c} \right)_0 - 1 \right]^2 \quad \text{for} \quad \alpha = 1.$$

For any α,

$$f_{L+S} = \left[\left(\frac{\Delta V}{V_c} \right)_0 \sqrt{\alpha} - 1 \right]^2 = \left[\sqrt{\alpha (f_{L+S})_0} + (\sqrt{\alpha} - 1) \right]^2. \qquad (24)$$

From Equation (20),

$$(f_G + f_{L+S})_0 = 1 - \left(\frac{\Delta V}{V_c} \right)_0 \quad \text{for} \quad \alpha = 1.$$

For any α,

$$f_G + f_{L+S} = 1 - \left(\frac{\Delta V}{V_c} \right) \sqrt{\alpha} = 1 - \sqrt{\alpha} \left[1 - (f_G + f_{L+S})_0 \right]$$

$$f_P = 1 - (f_G + f_{L+S}) = \sqrt{\alpha} \left[1 - (f_G + f_{L+S})_0 \right]$$

$$f_P = \sqrt{\alpha} (f_P)_0. \qquad (25)$$

PRESENTATION OF RESULTS

The CFP system is compared with the electrical system on the basis of the time required to complete one-way and round trips to the Moon and to Mars, Venus, and Jupiter. First, the two systems are compared as to their basic system parameters. Then they are compared on the bases of identical initial weights of the systems and on identical weights of the payloads delivered. These comparisons are shown in Figures 7 through 70.

All graphs are plotted as functions of durations of the missions. For each mission, there exists a minimum time for accomplishment, which corresponds to the delivery of zero payload. Also in all cases, there is another minimum time limit, which is determined by the initial specific impulse. That is, the specific impulse of the propulsion device is assumed to be variable only within certain limits. For the CFP system, these limits are assumed to be 5000 seconds and upward. For the electrical system, these limits are assumed to be 1000 seconds and upward. In almost all cases, the inability to operate below 5000 seconds is the limiting factor for thermonuclear systems. For electric systems, the minimum time for accomplishment of a mission is, in all cases, determined by the zero payload limit.

COMPARISONS ON BASES OF BASIC PARAMETERS OF SYSTEMS

The data of Figures 7 through 38 do not depend on any actual system weights; they depend only upon η, t_b, and α.

Figures 7 through 14 show that portion of the total mass of the vehicle that is usable payload. These curves are of primary importance since they provide the simplest and most straightforward means of effecting a valid comparison among various propulsion systems. The difference in the horizontal asymptotes of the curves for long times emphasizes the advantage in η possessed by the CFP system. The extremely large difference in f_{L+S} at shorter times points up the inherent advantage of the CFP device for high energy missions.

Figures 15 through 22 are straightforward plots of propellant requirements.

Figures 23 through 30 show the value of I_{sp} that is used initially at launch from orbit.

Figures 31 through 38 show the value of I_{sp} that is used at the completion of the mission.
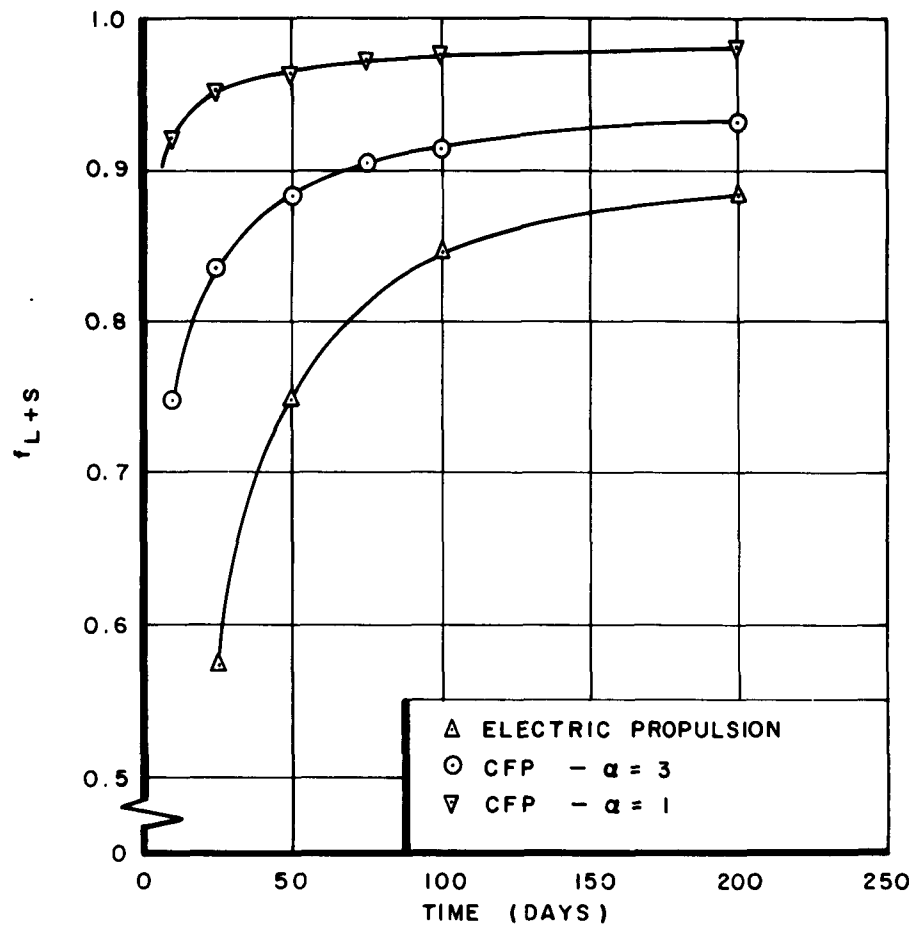
Figure 7. Comparison of CFP System with Electric System Based on Usable Payload:
One-Way Trip to Moon
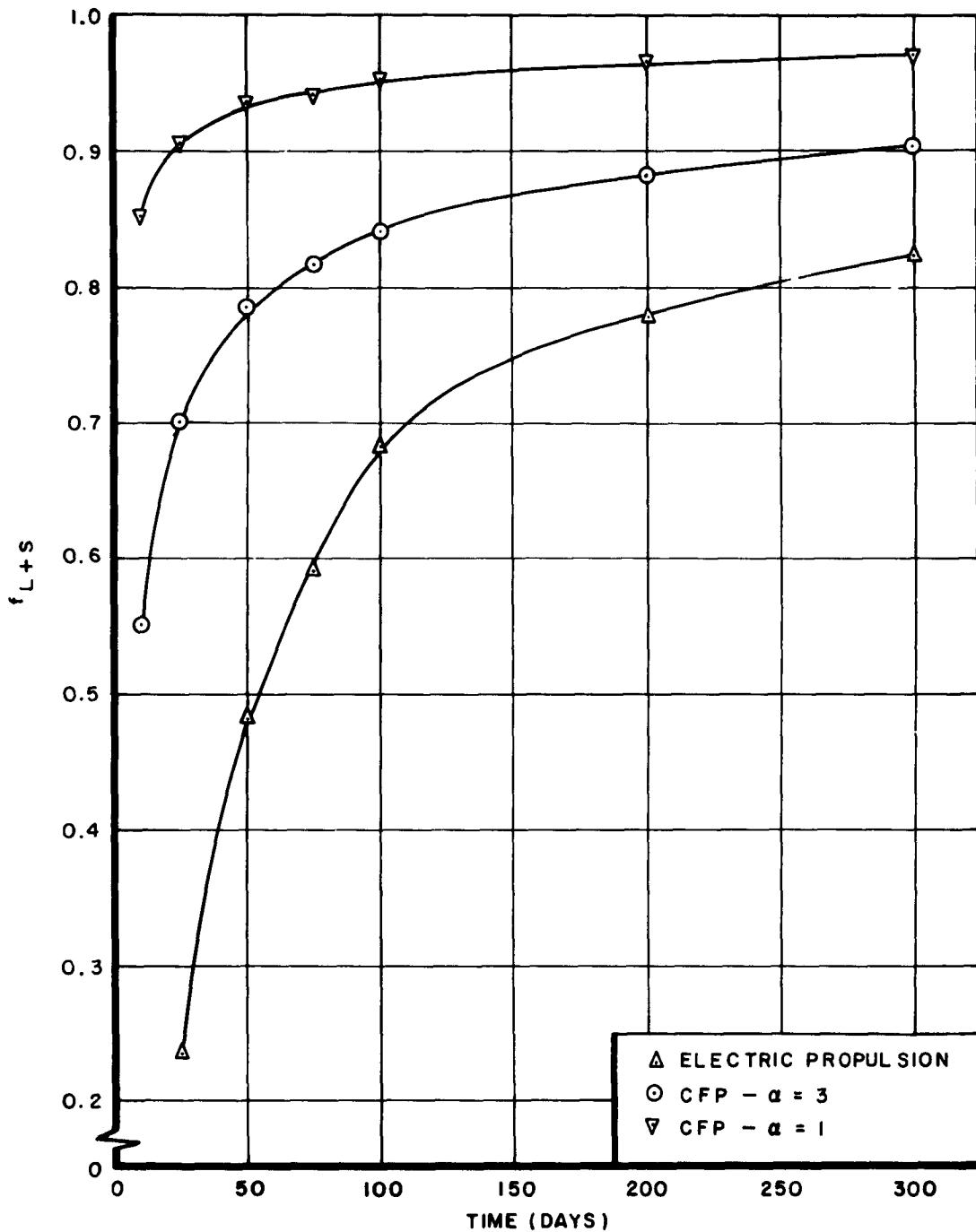
Figure 8.   Comparison of CFP System with Electric System Based on Usable Payload:
Round Trip to Moon
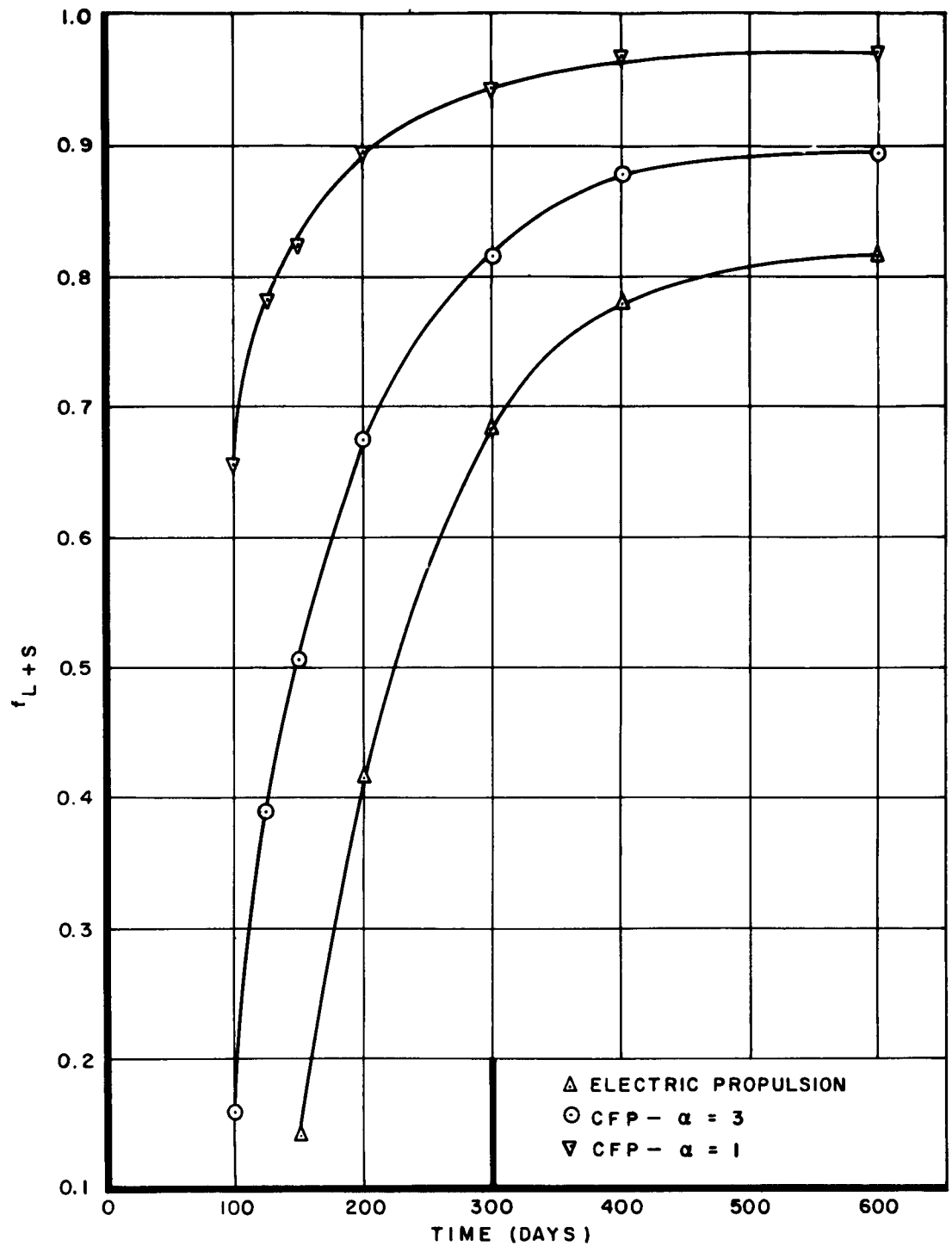
Figure 9.   Comparison of CFP System with Electric System Based on Usable Payload:
One-Way Trip to Mars
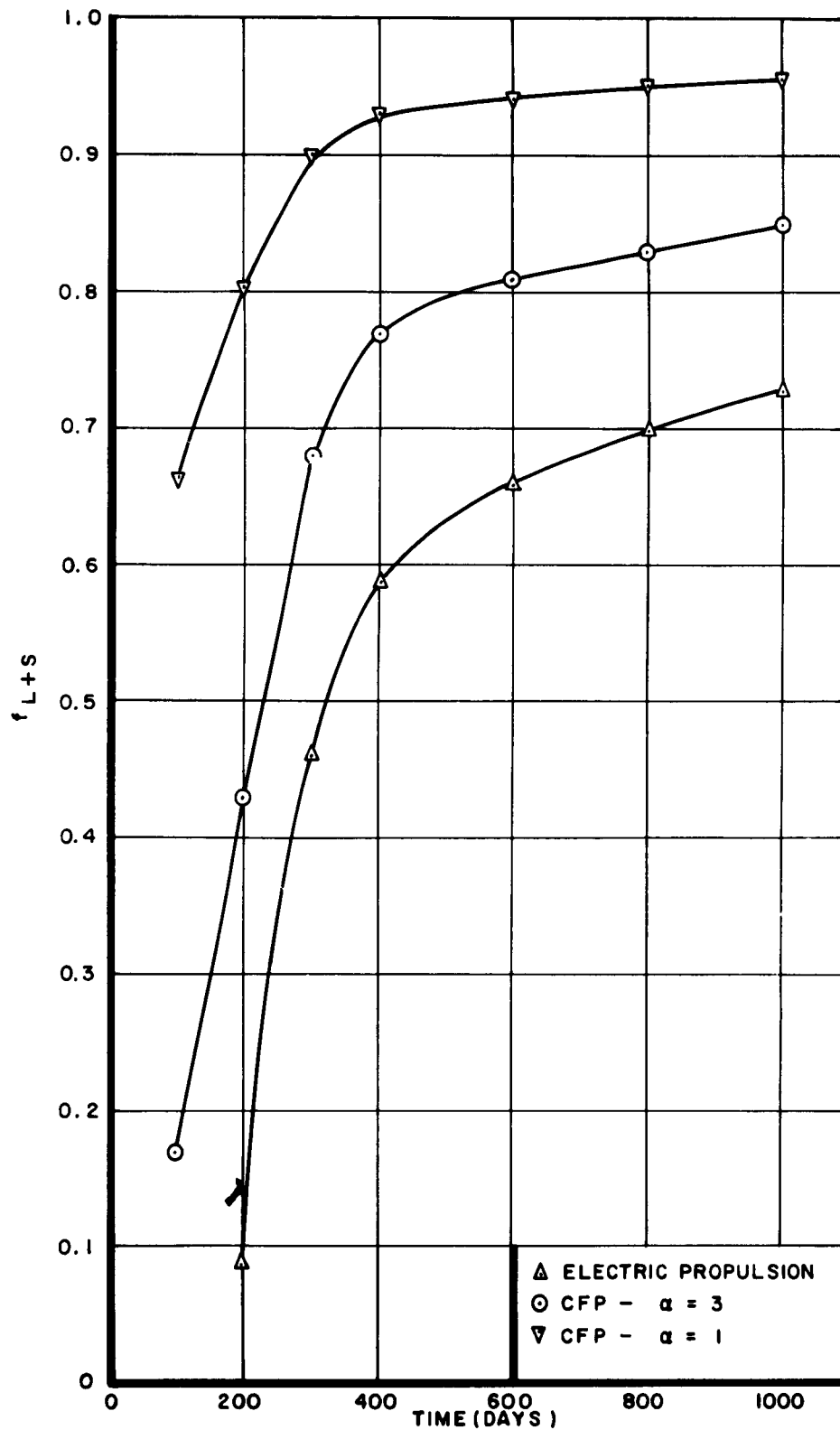
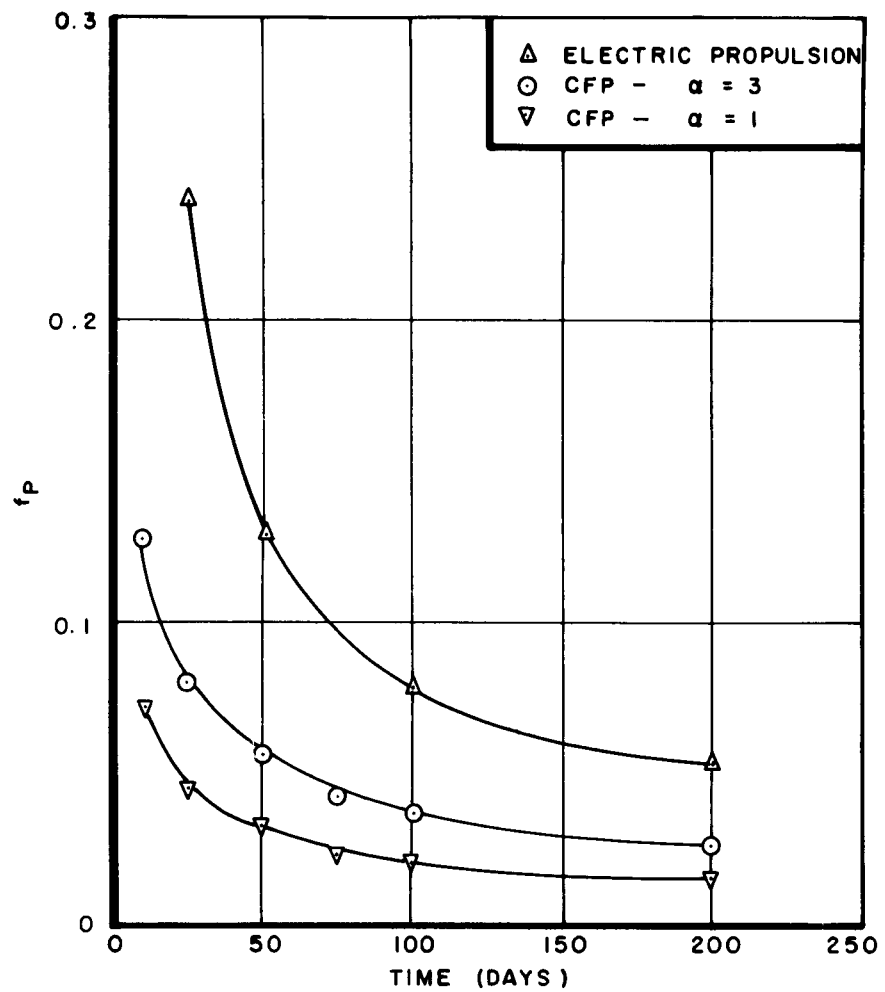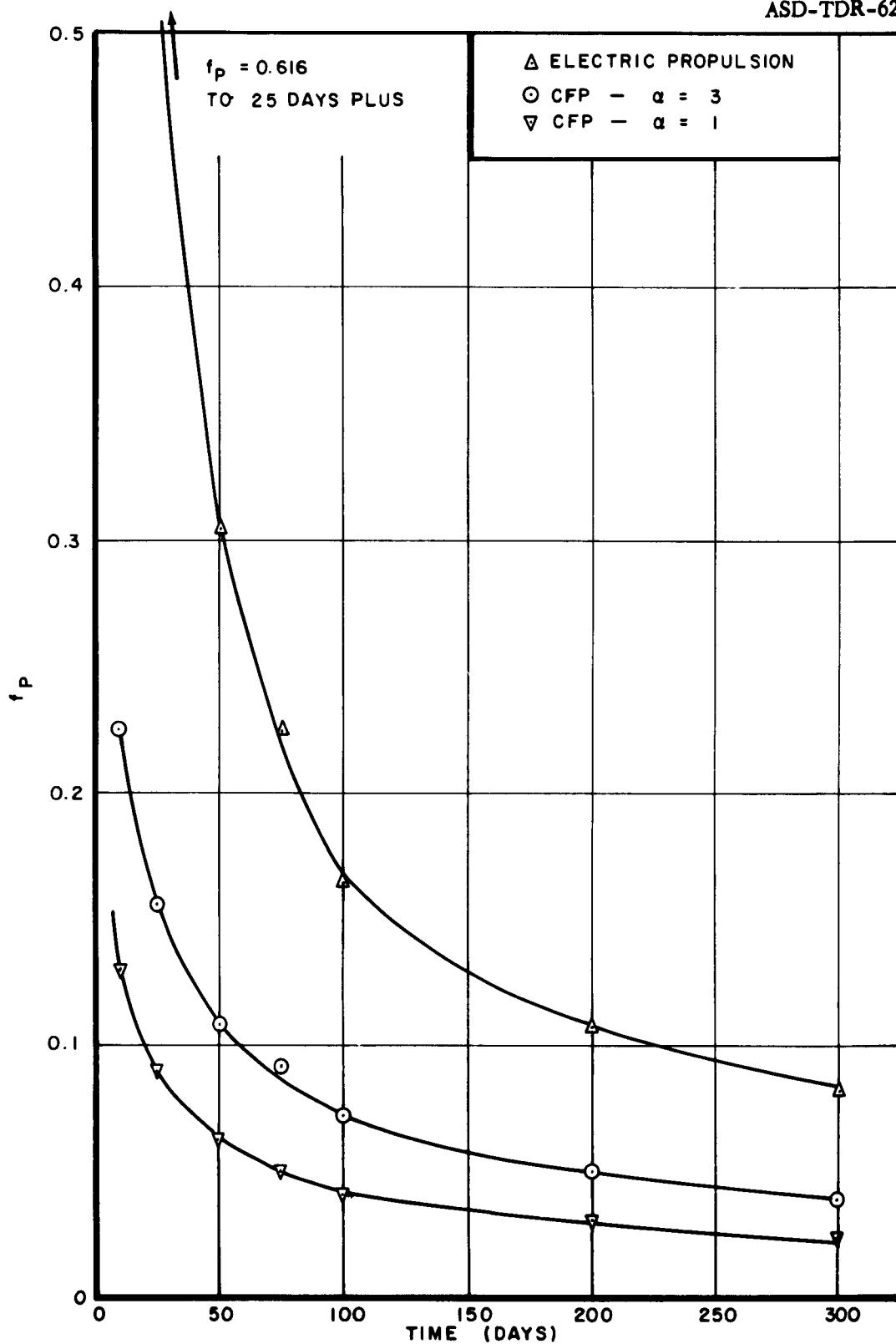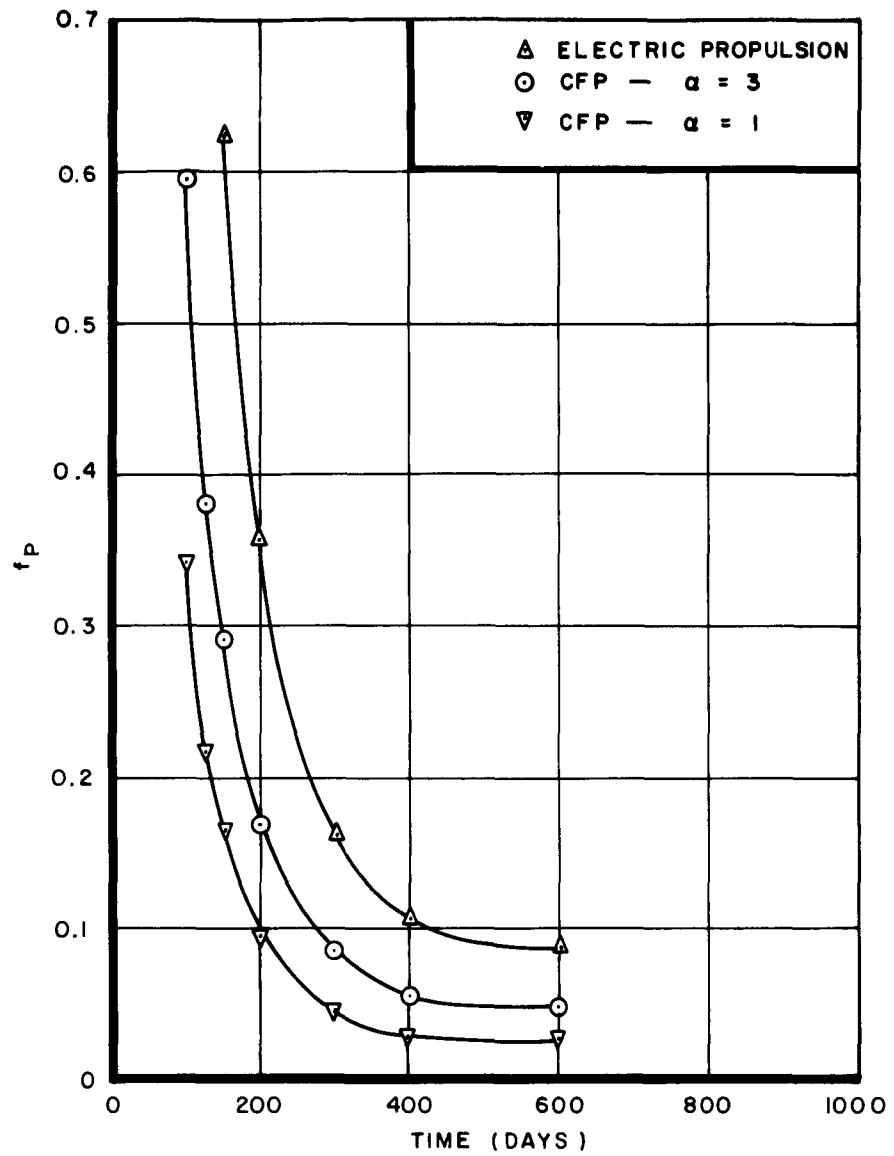Figure 10. Comparison of CFP System with Electric System Based on Usable Payload:
Round Trip to Mars

ASD-TDR-62-696
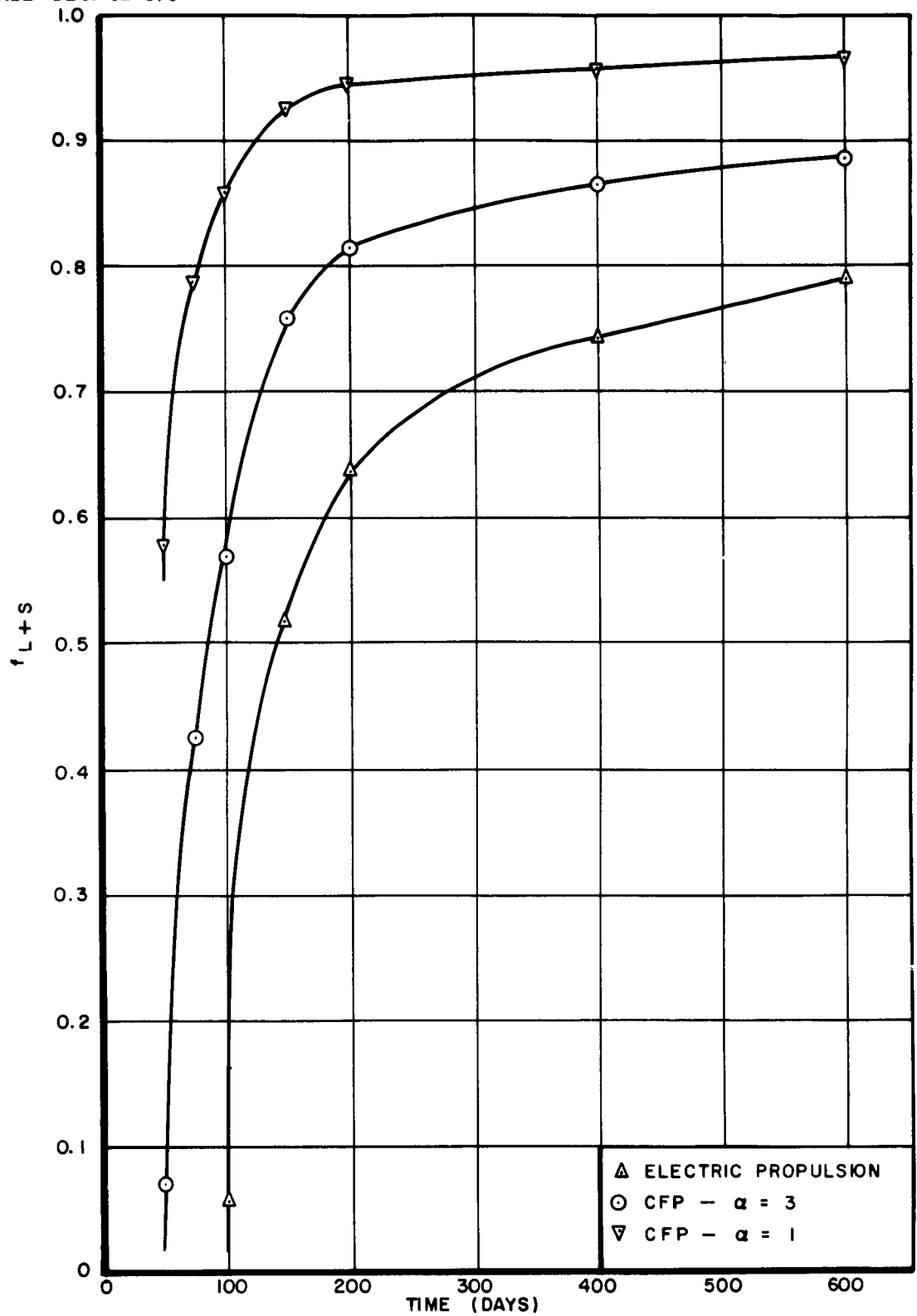
Figure 11. Comparison of CFP System with Electric System Based on Usable Payload:
One-Way Trip to Venus

19
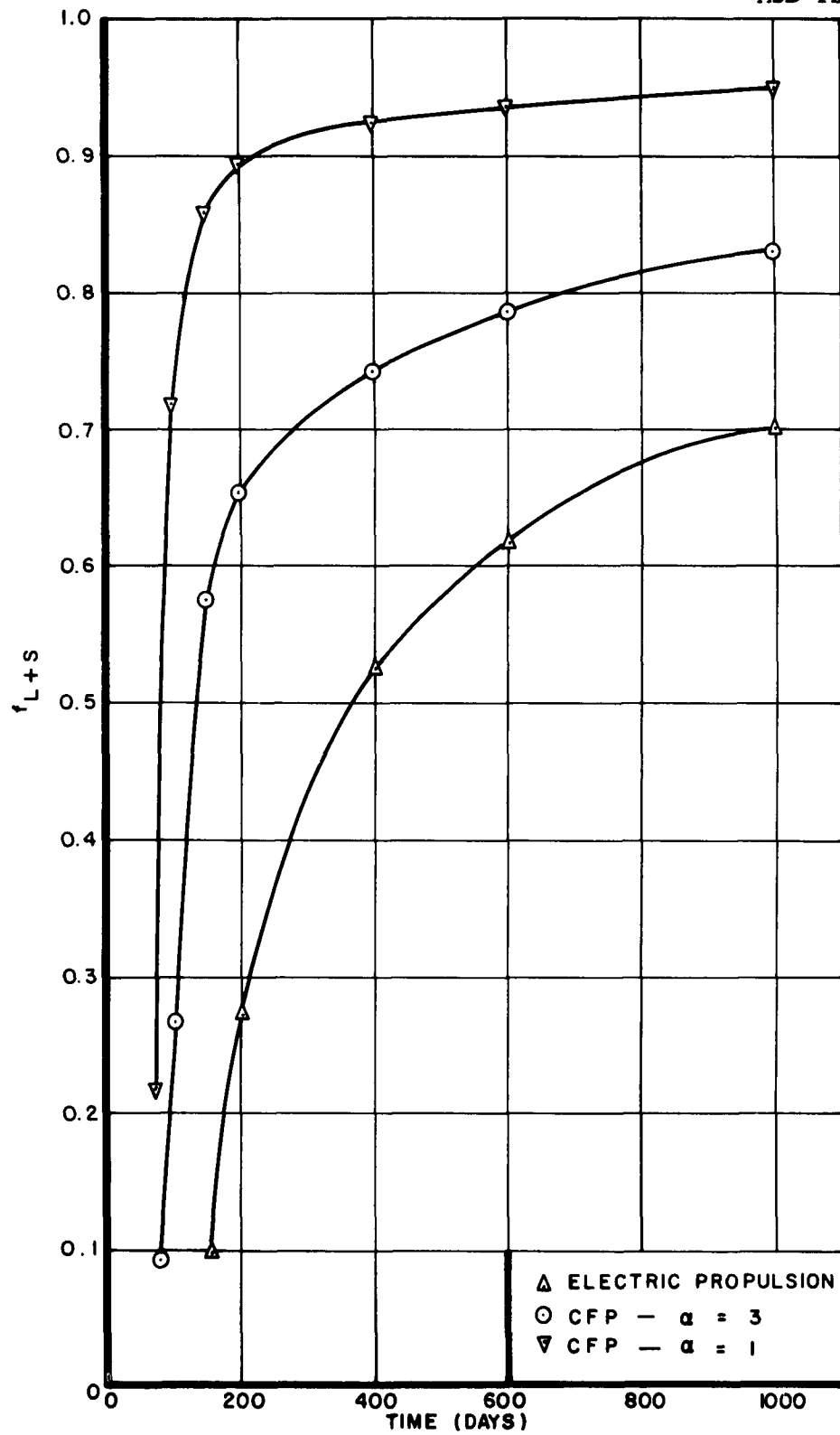
Figure 12. Comparison of CFP System with Electric System Based on Usable Payload:
Round Trip to Venus
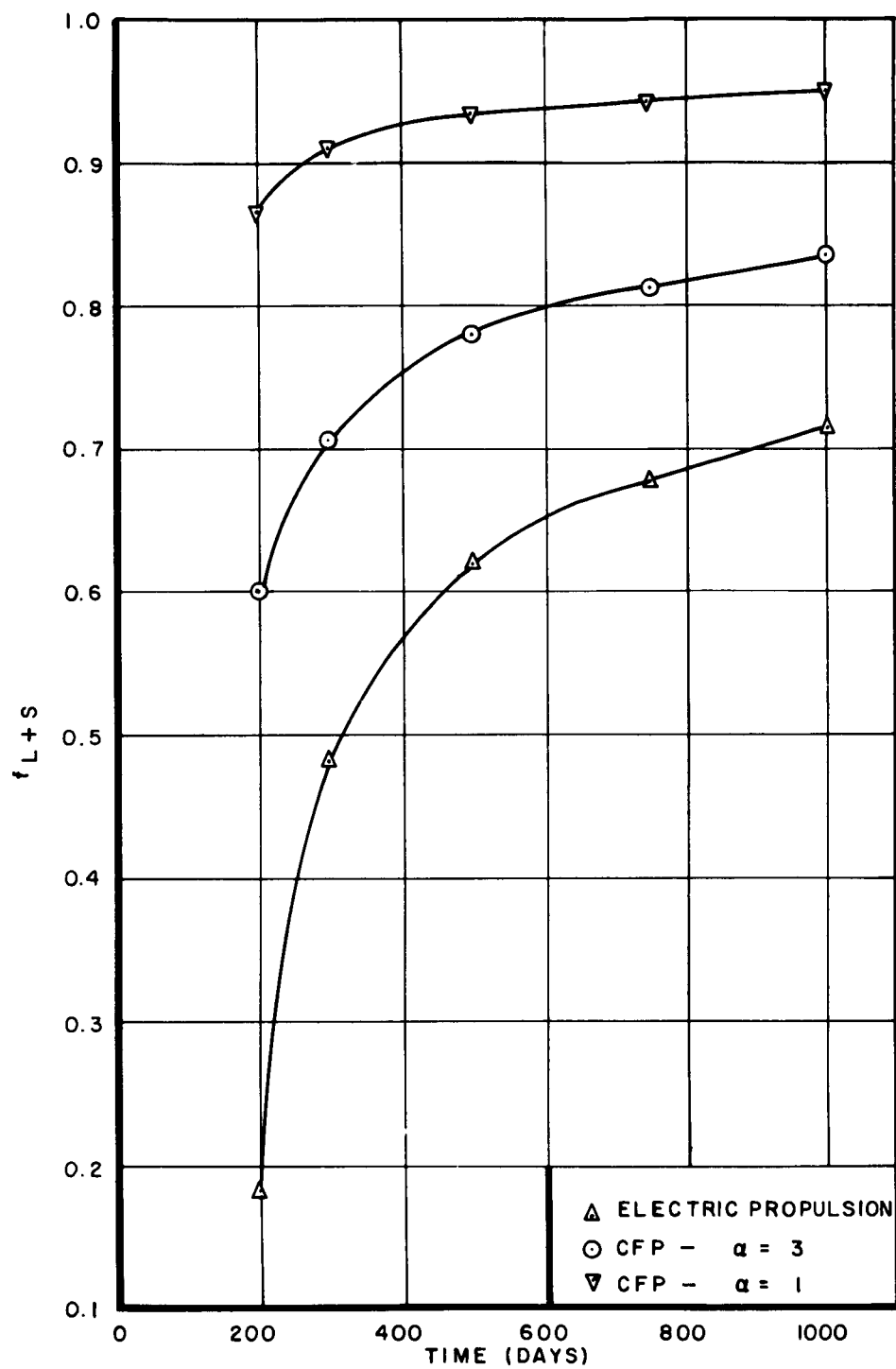
Figure 13. Comparison of CFP System with Electric System Based on Usable Payload:
One-Way Trip to Jupiter
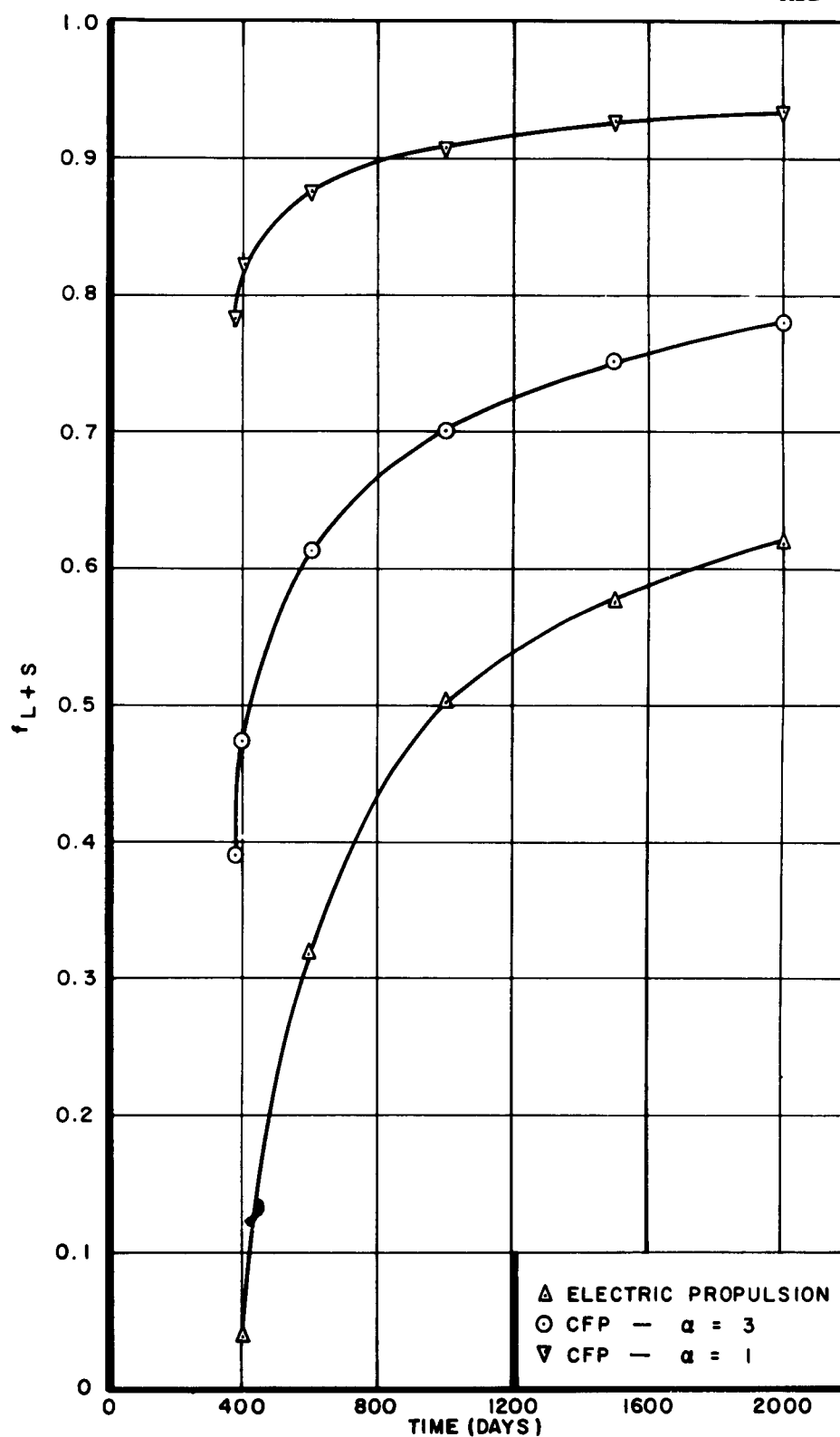
Figure 14. Comparison of CFP System with Electric System Based on Usable Payload:
Round Trip to Jupiter

Figure 15. Comparison of CFP System with Electric System Based on Propellant Requirements: One-Way Trip to Moon

Figure 16. Comparison of CFP System with Electric System Based on Propellant Requirements: Round Trip to Moon

Figure 17. Comparison of CFP System with Electric System Based on Propellant Requirements: One-Way Trip to Mars
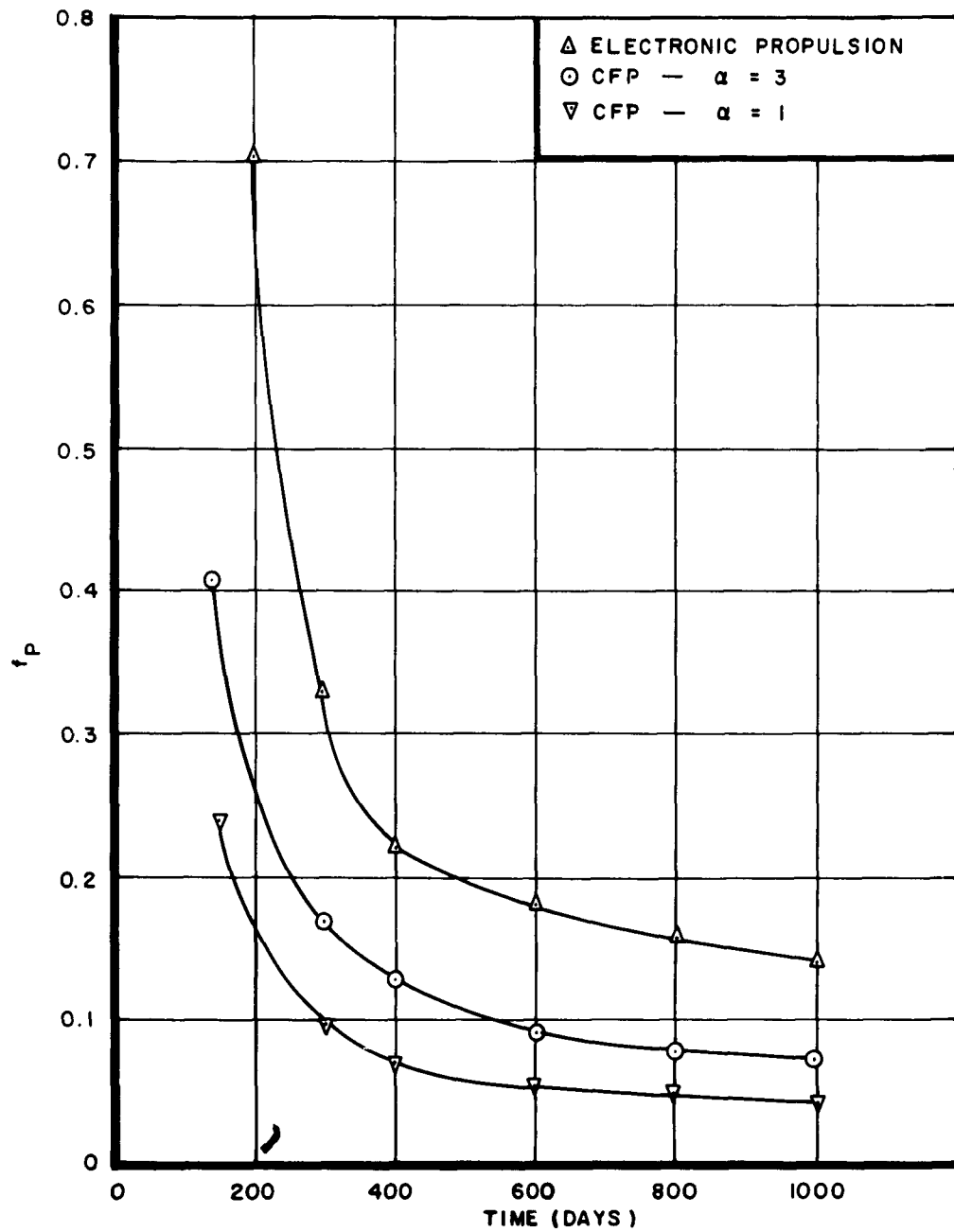
Figure 18. Comparison of CFP System with Electric System Based on Propellant Requirements: Round Trip to Mars
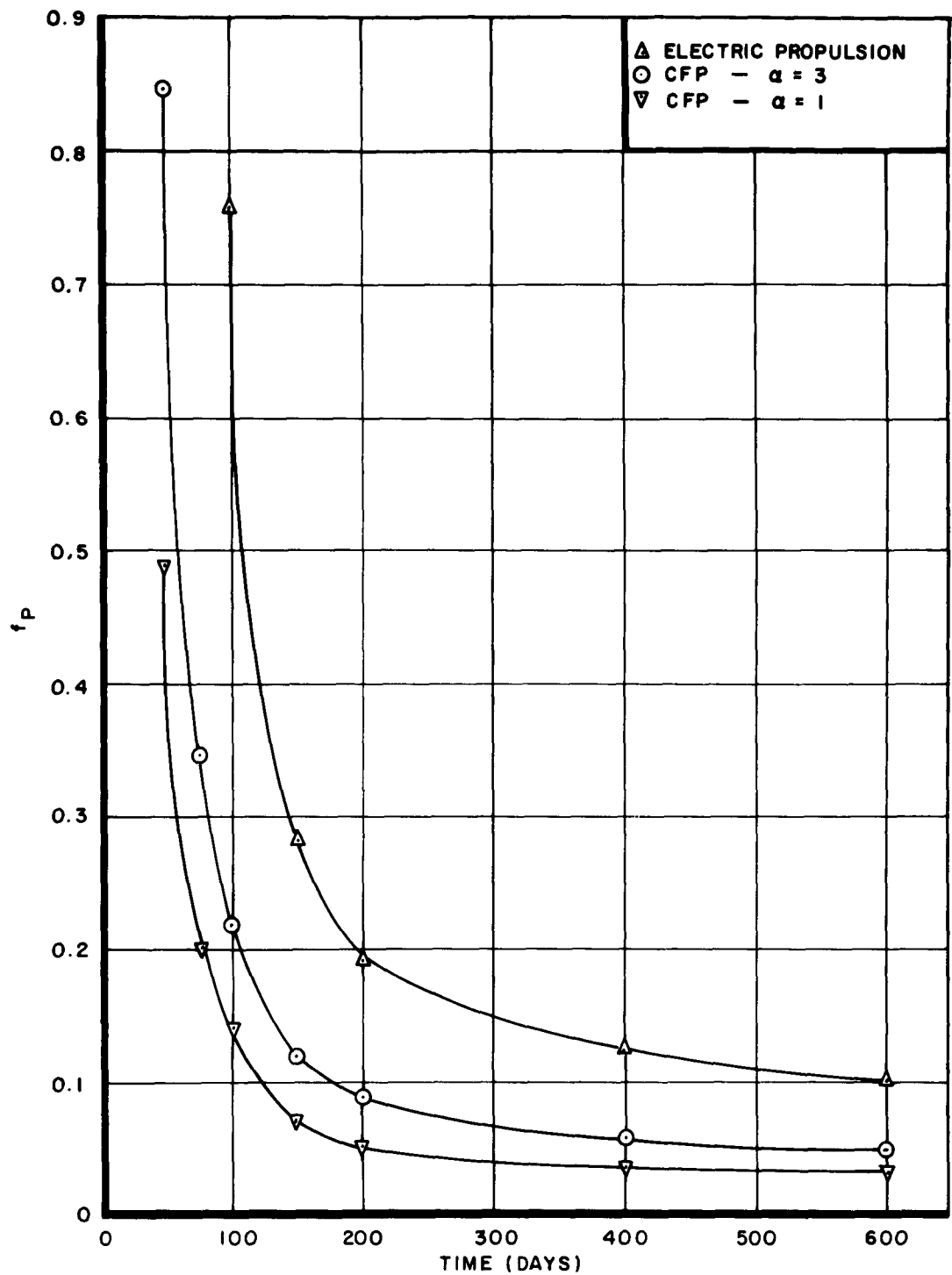
Figure 19. Comparison of CFP System with Electric System Based on Propellant Requirements: One-Way Trip to Venus
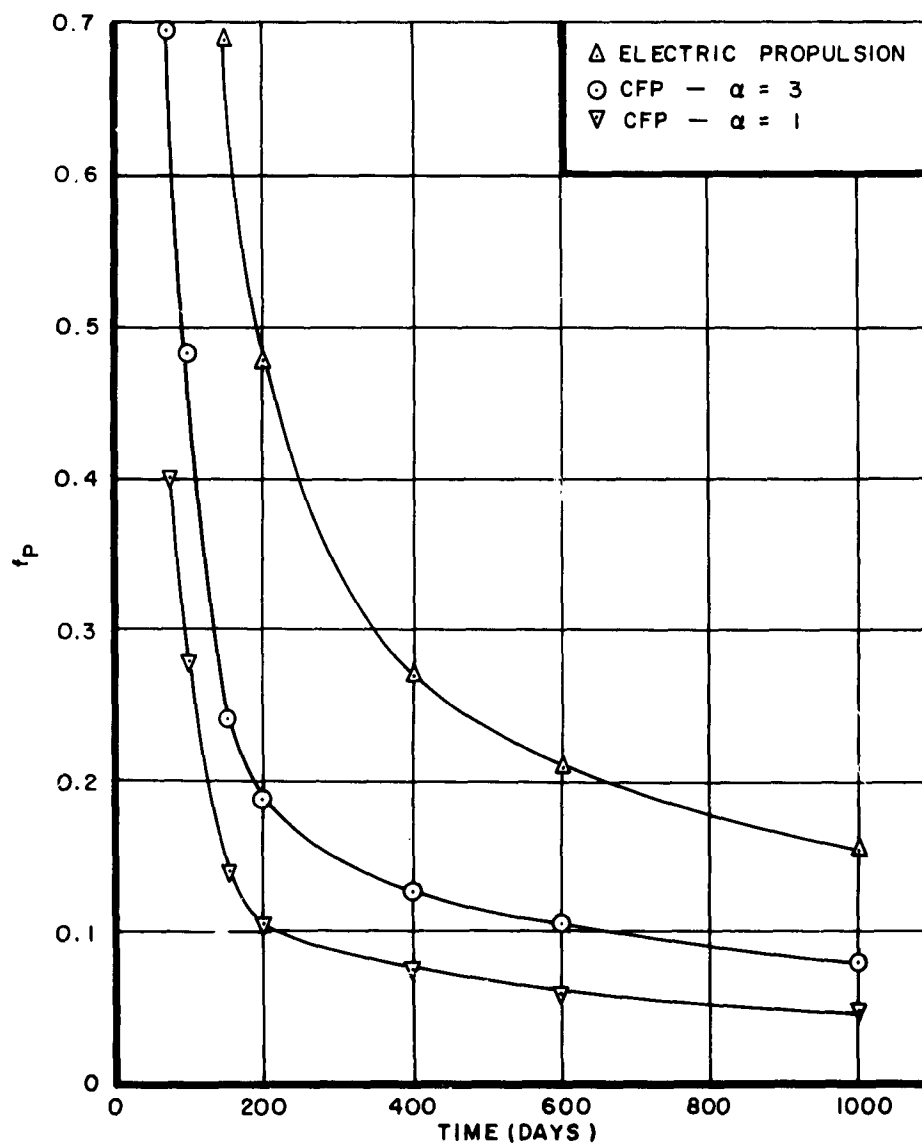
Figure 20. Comparison of CFP System with Electric System Based on Propellant Requirements: Round Trip to Venus
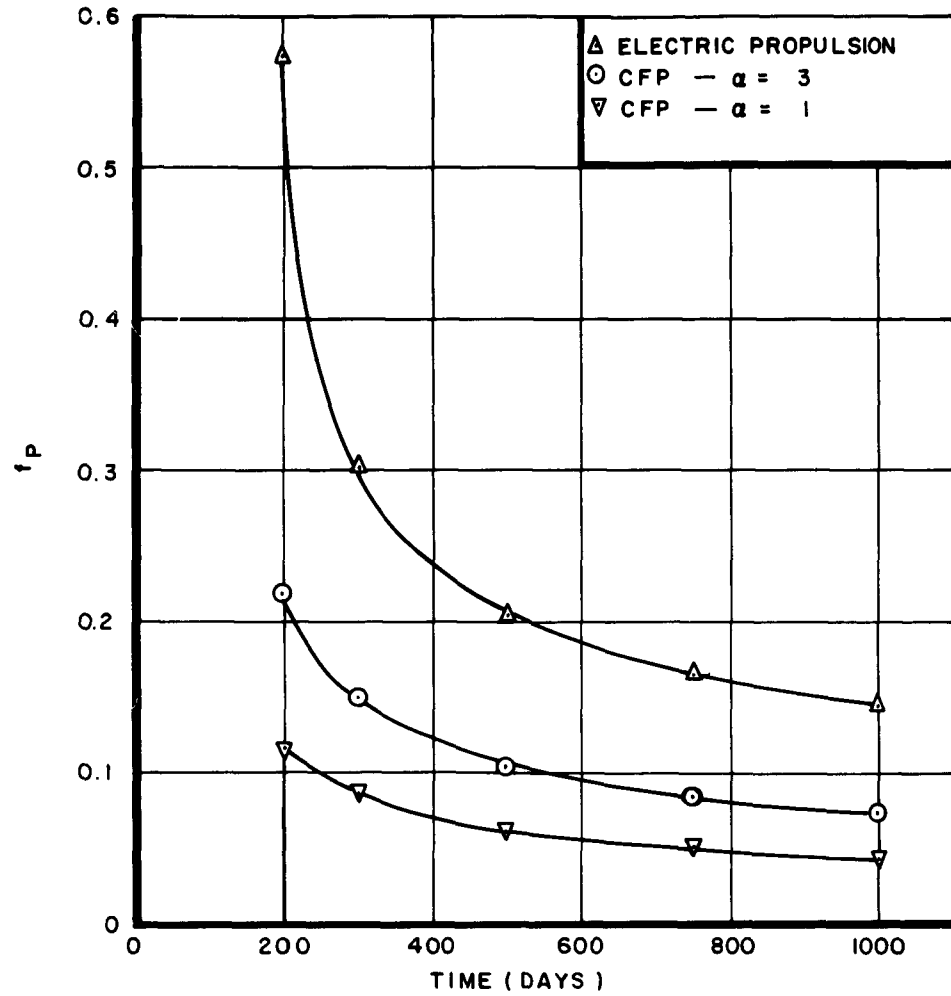
Figure 21. Comparison of CFP System with Electric System Based on Propellant Requirements:
One-Way Trip to Jupiter
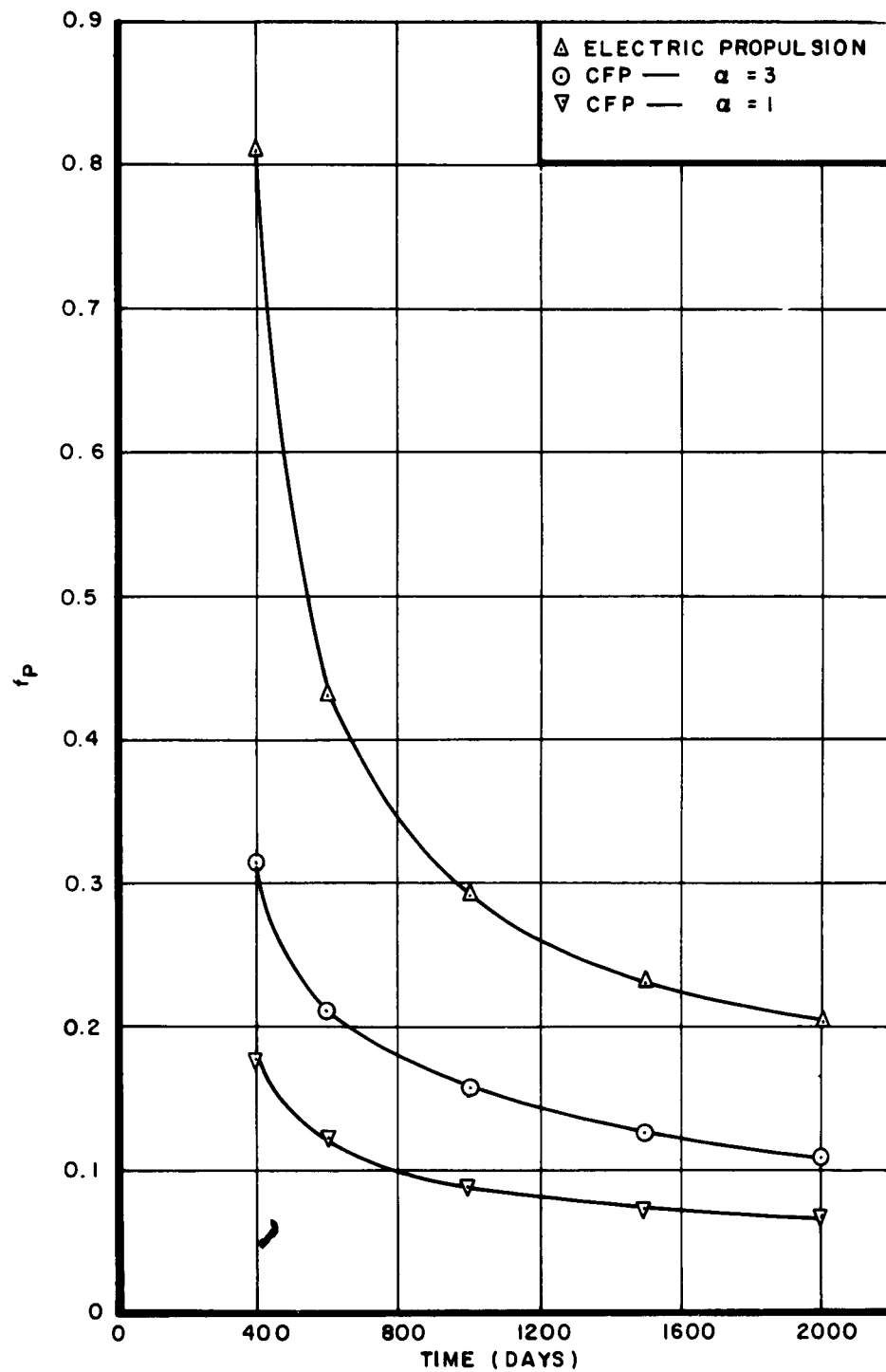
Figure 22. Comparison of CFP System with Electric System Based on Propellant Requirements: Round Trip to Jupiter
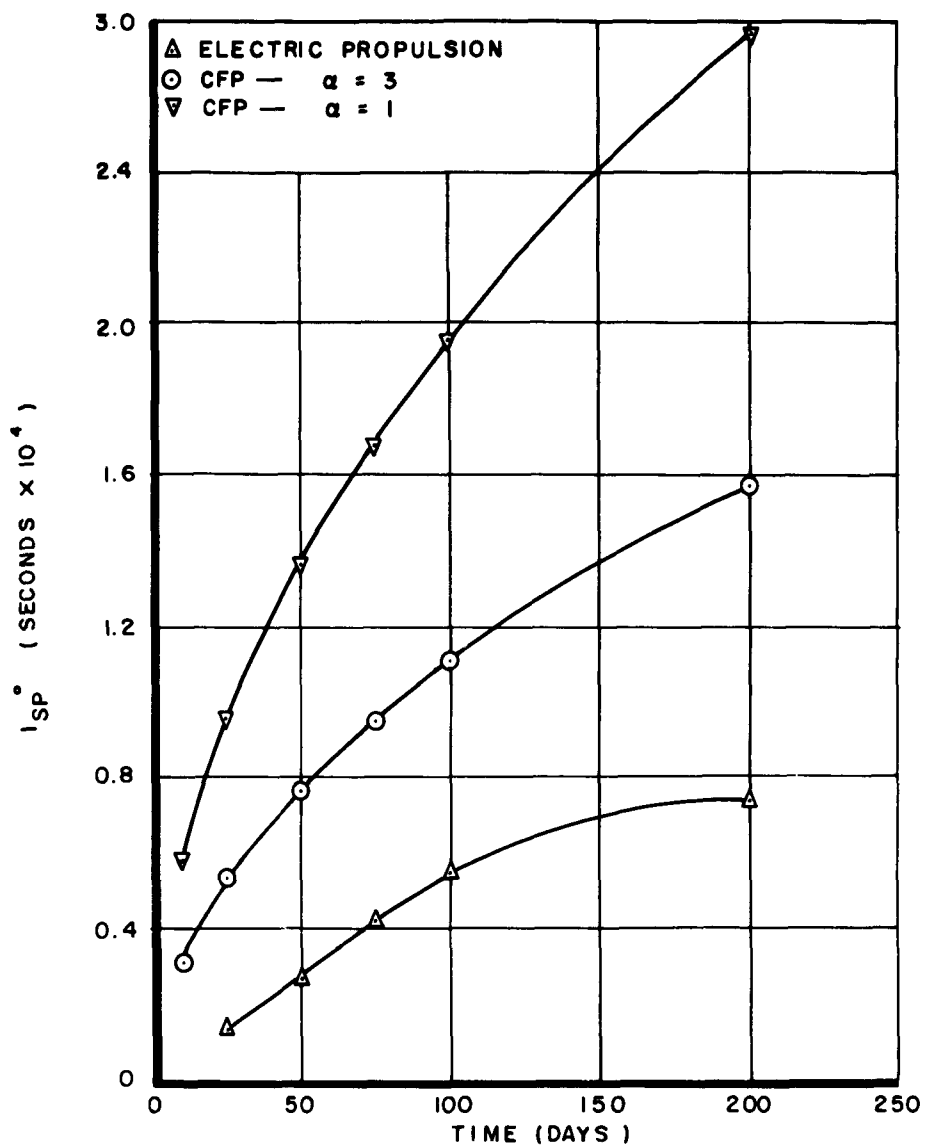
Figure 23. Comparison of CFP System with Electric System Based on Specific Impulse Used Initially at Launch from Orbit: One-Way Trip to Moon
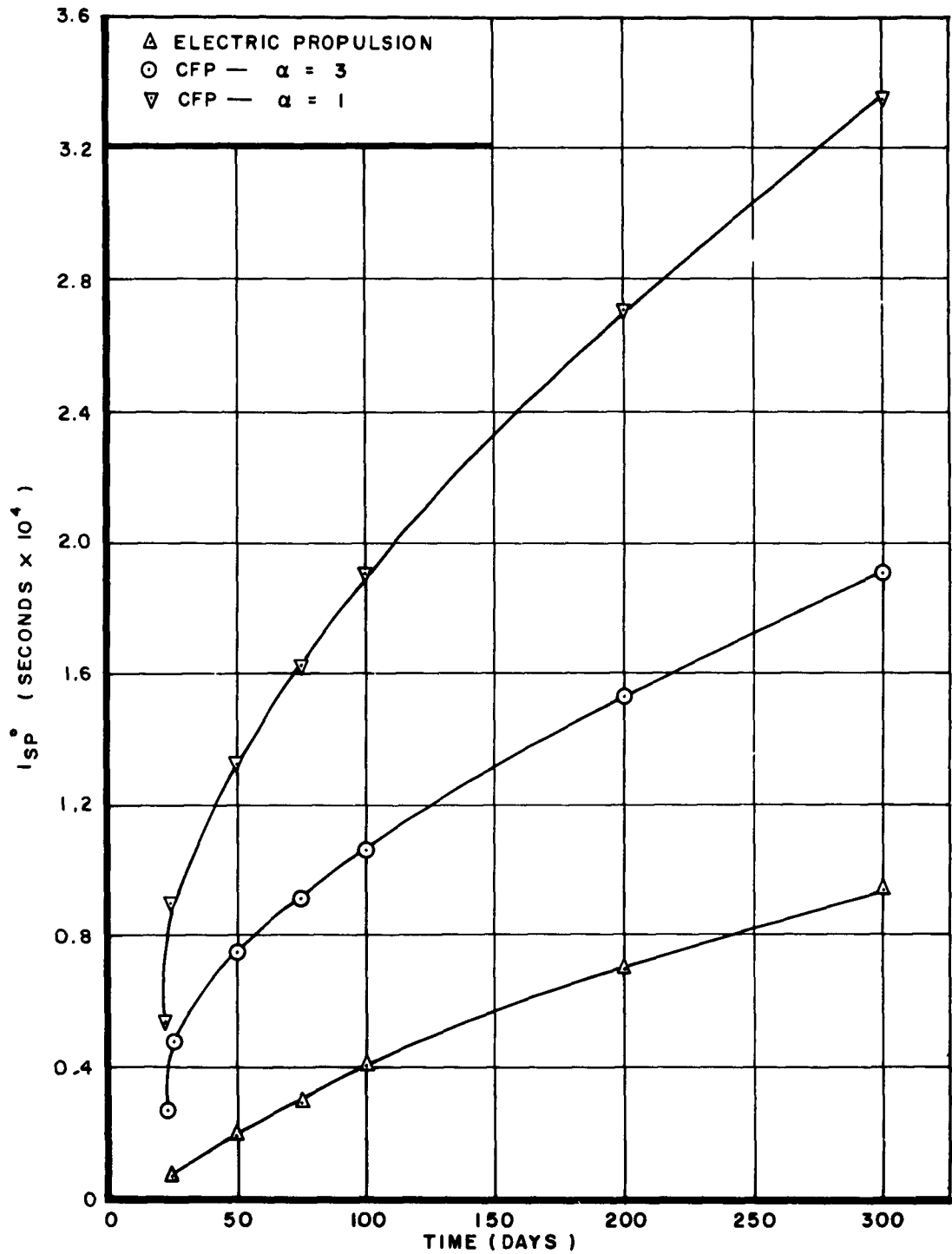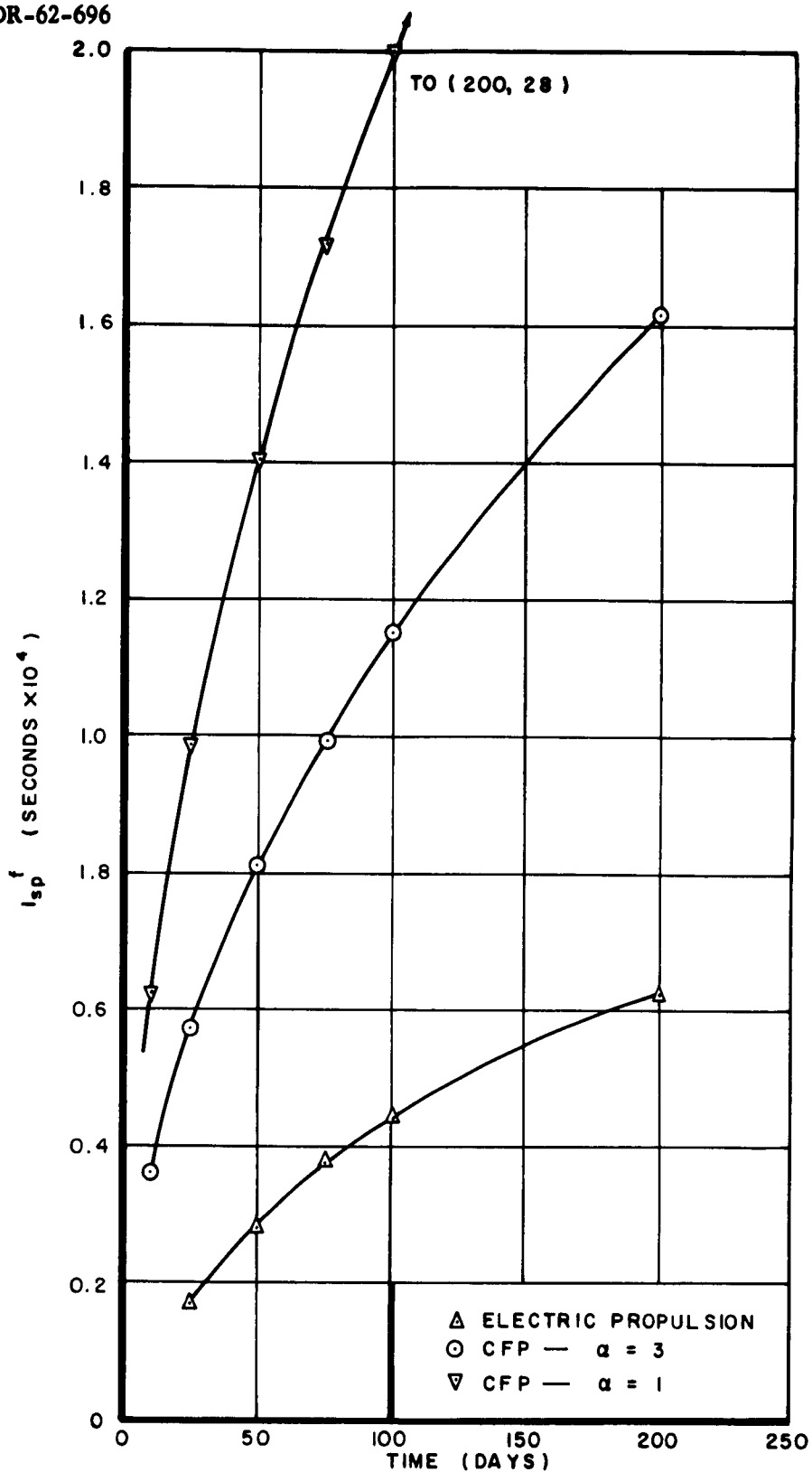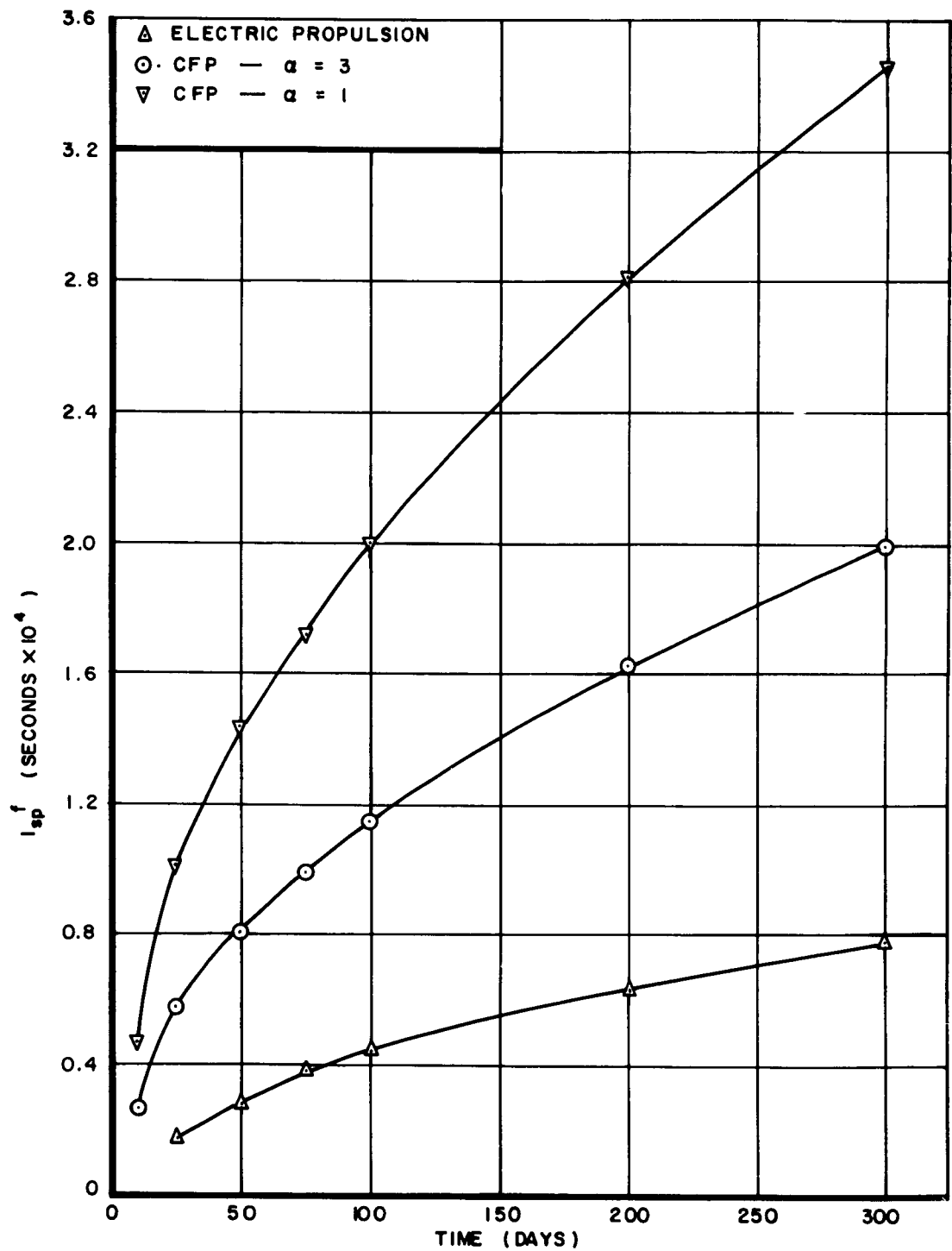
Figure 24. Comparison of CFP System with Electric System Based on Specific Impulse Used
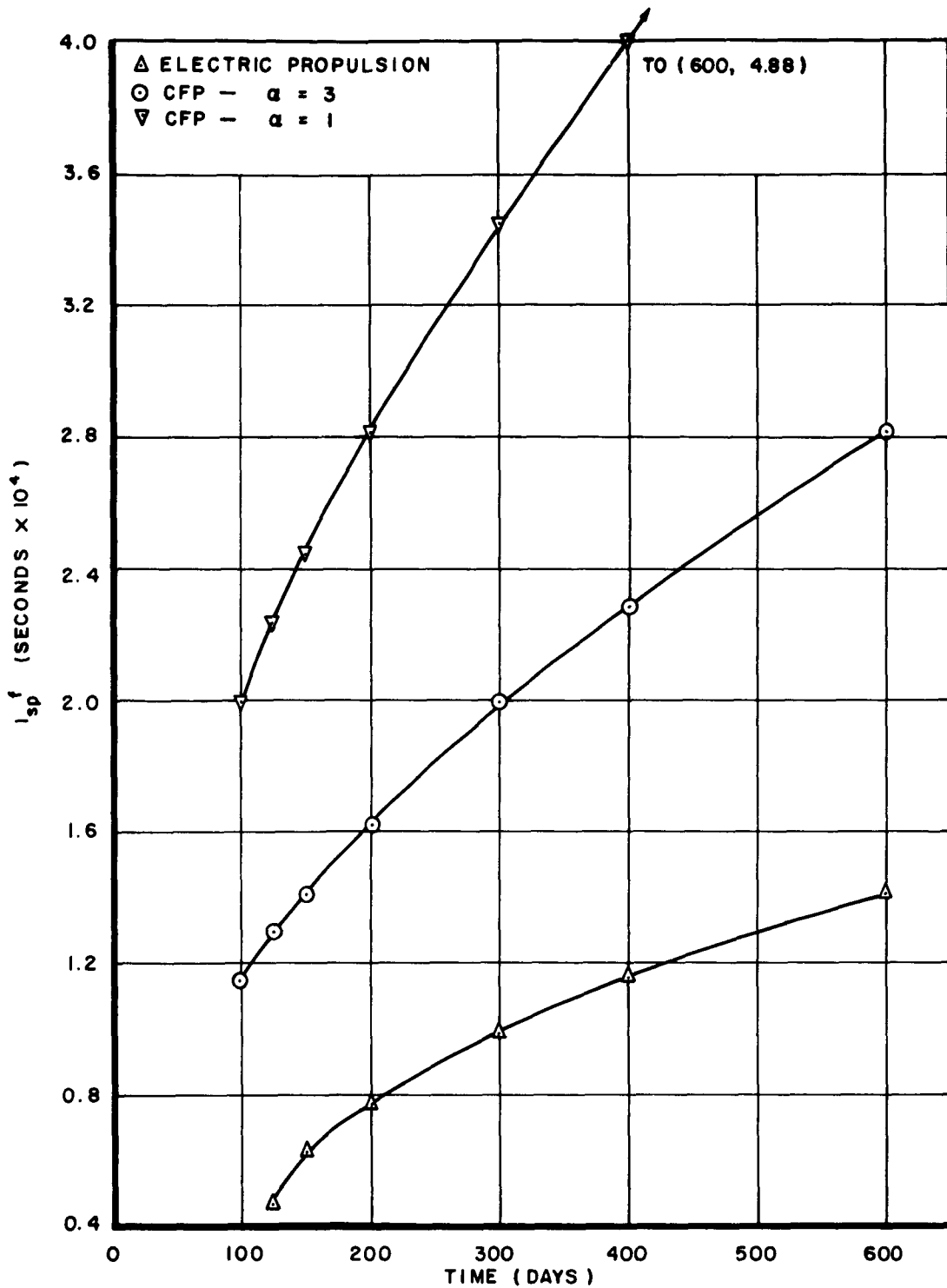Initially at Launch from Orbit: Round Trip to Moon
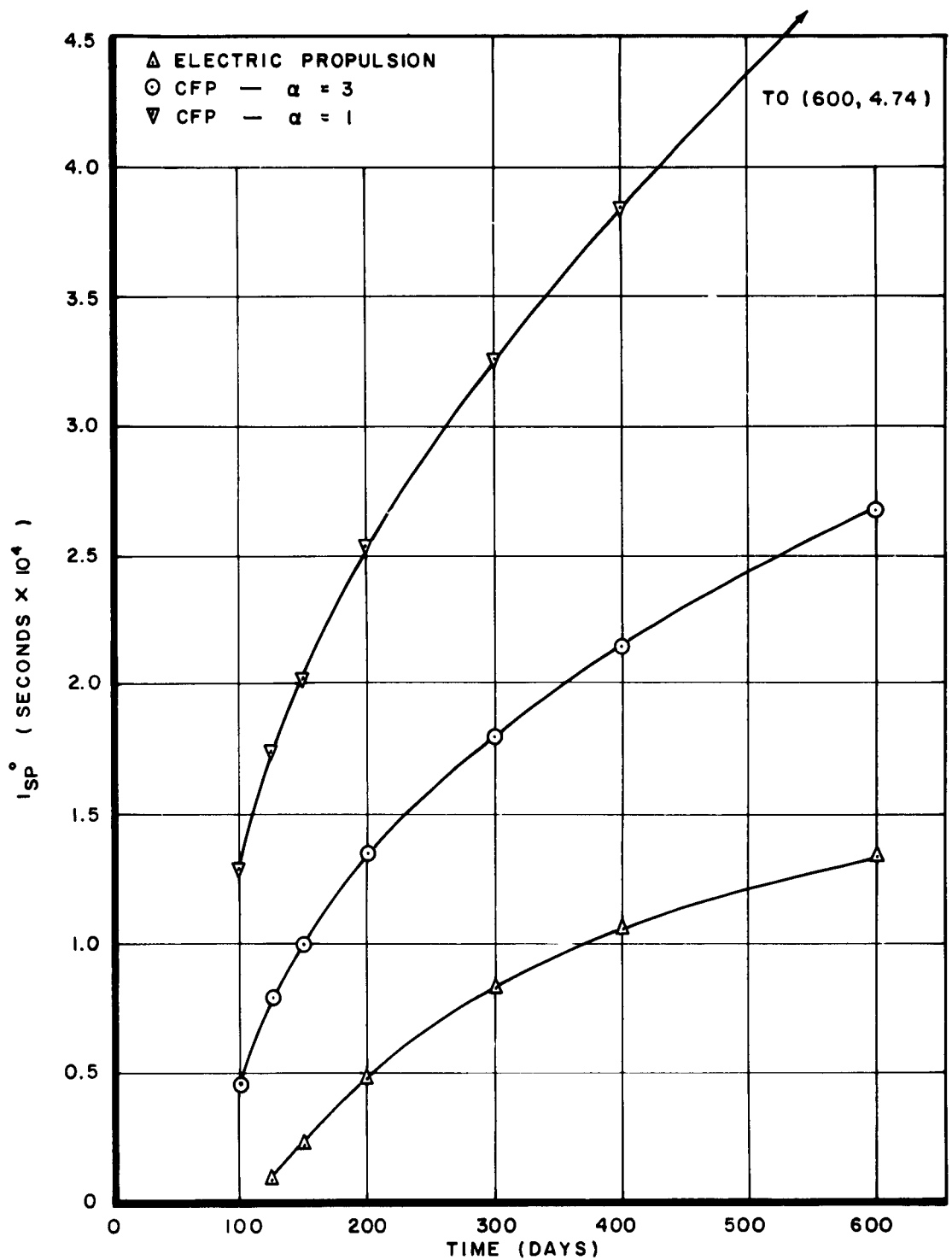
Figure 25. Comparison of CFP System with Electric System Based on Specific Impulse Used
Initially at Launch from Orbit: One-Way Trip to Mars
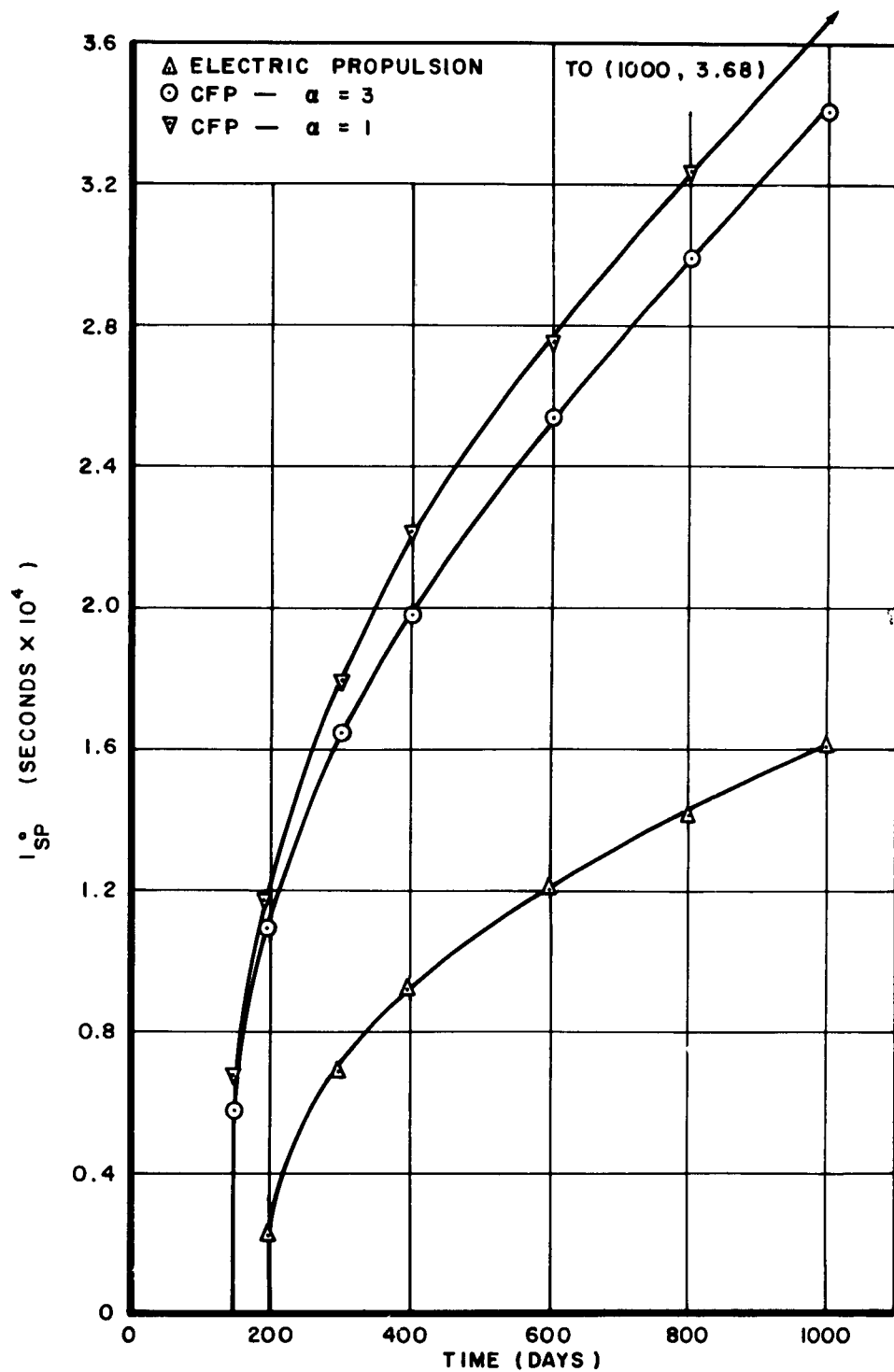
Figure 26. Comparison of CFP System with Electric System Based on Specific Impulse Used
Initially at Launch from Orbit: Round Trip to Mars
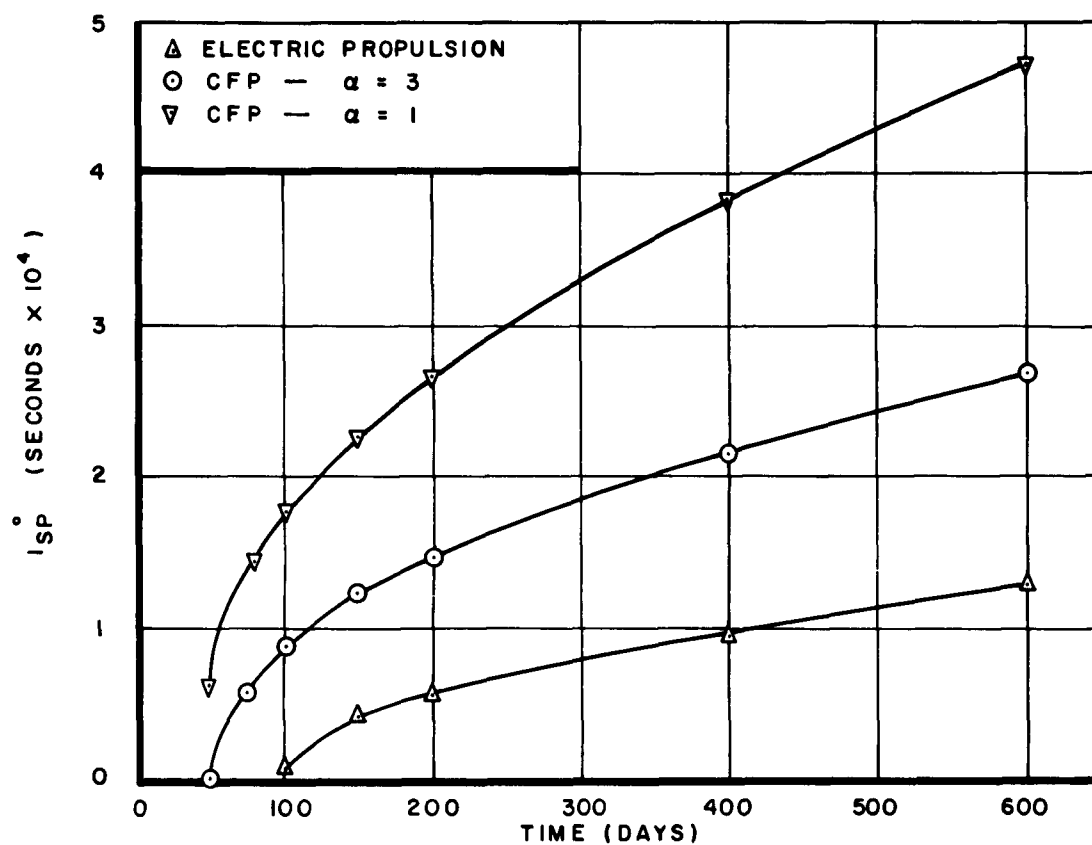
Figure 27. Comparison of CFP System with Electric System Based on Specific Impulse Used Initially at Launch from Orbit: One-Way Trip to Venus
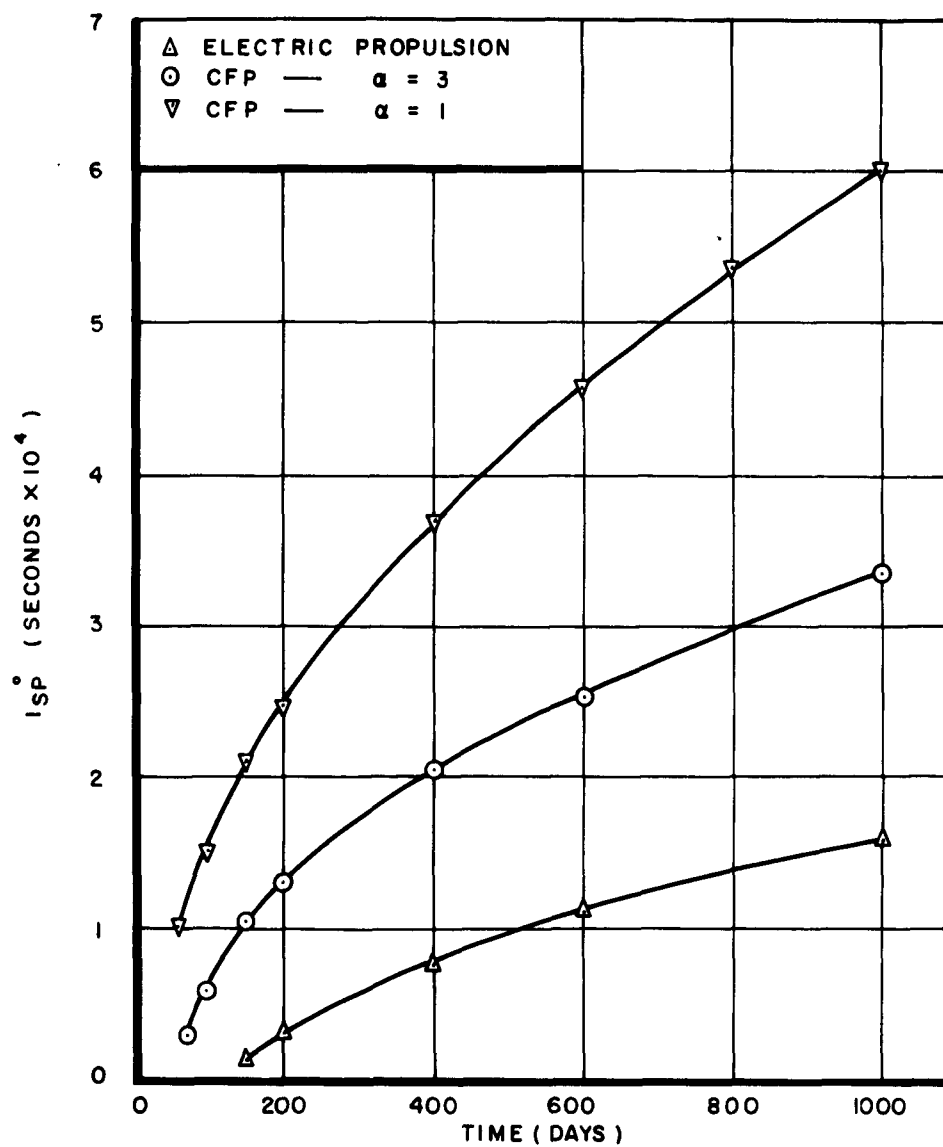
Figure 28. Comparison of CFP System with Electric System Based on Specific Impulse Used
Initially at Launch from Orbit: Round Trip to Venus
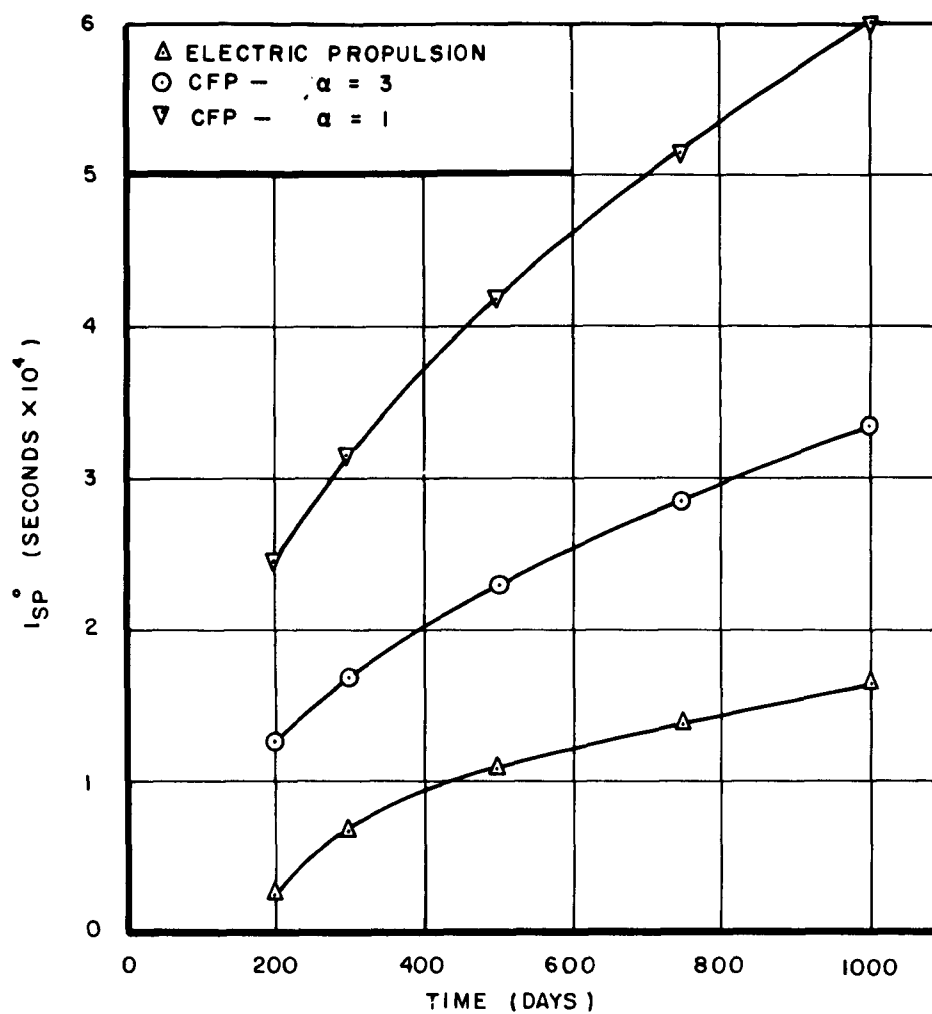
Figure 29. Comparison of CFP System with Electric System Based on Specific Impulse Used
Initially at Launch from Orbit: One-Way Trip to Jupiter
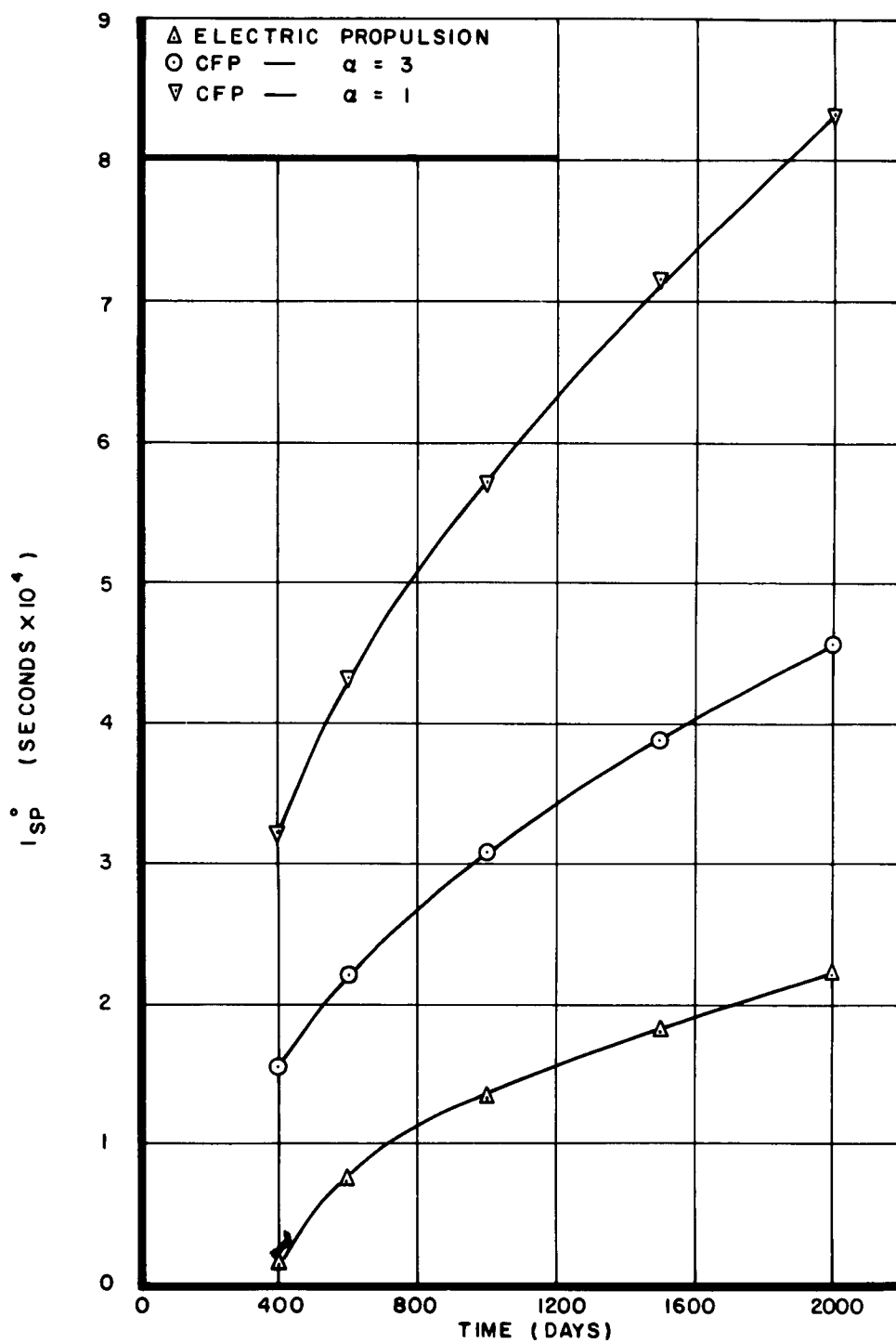
Figure 30. Comparison of CFP System with Electric System Based on Specific Impulse Used
Initially at Launch from Orbit: Round Trip to Jupiter

Figure 31. Comparison of CFP System with Electric System Based on Specific Impulse Used at Completion of Mission: One-Way Trip to Moon
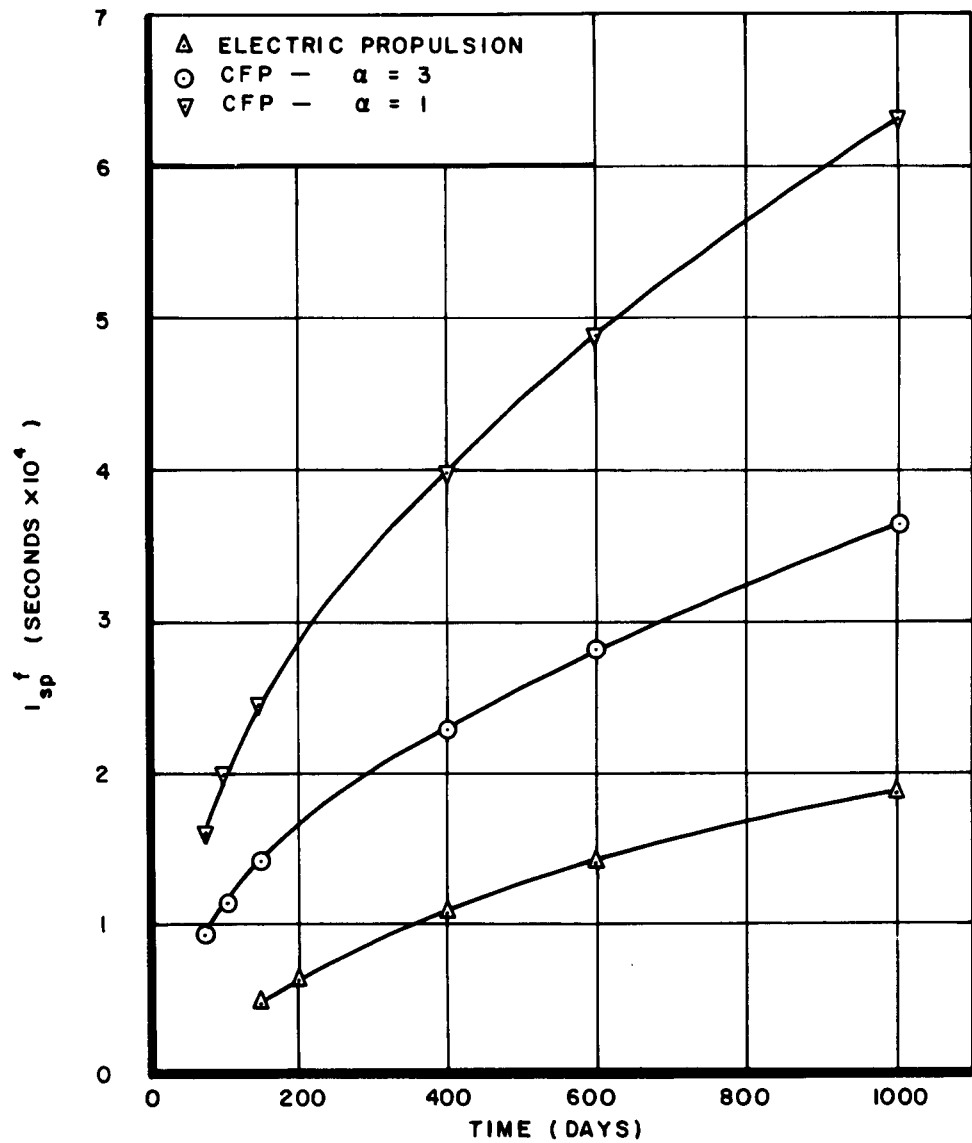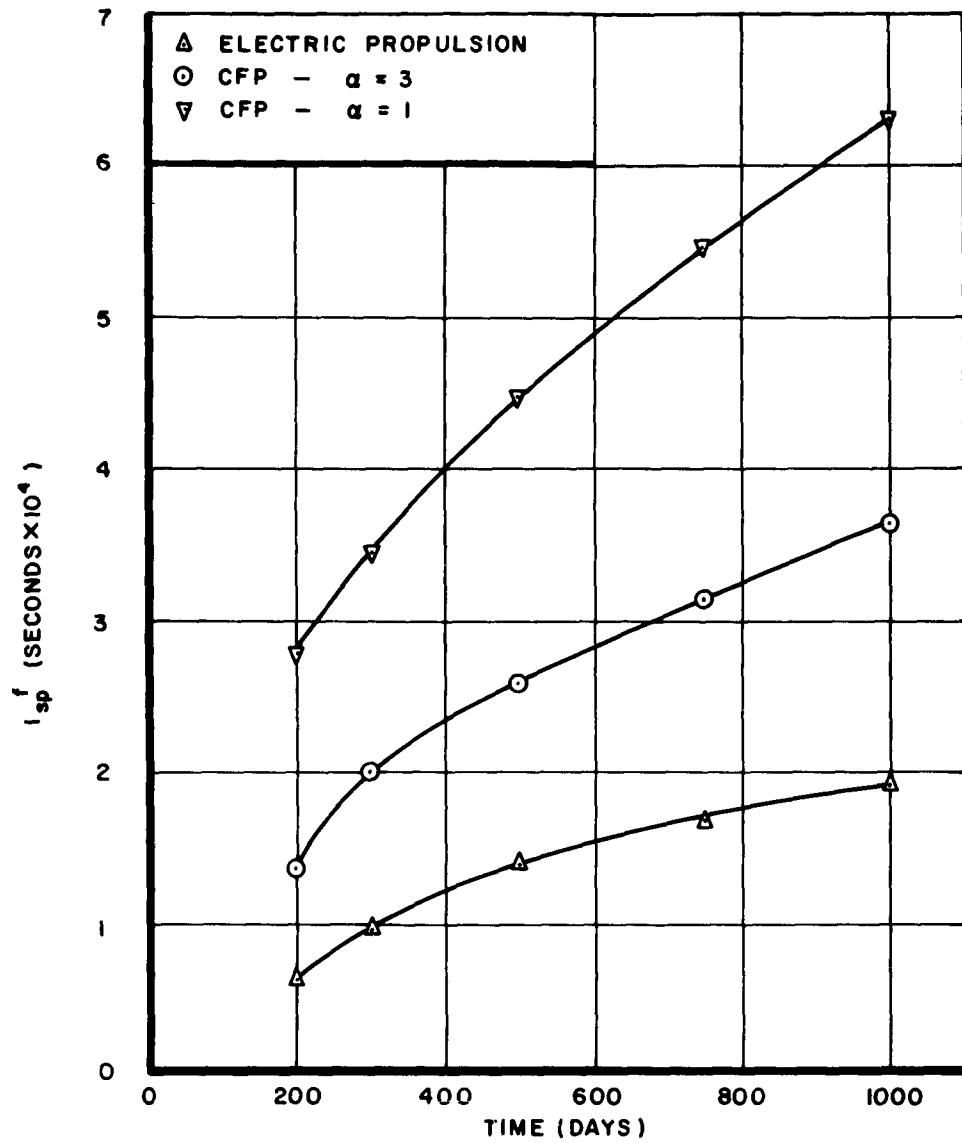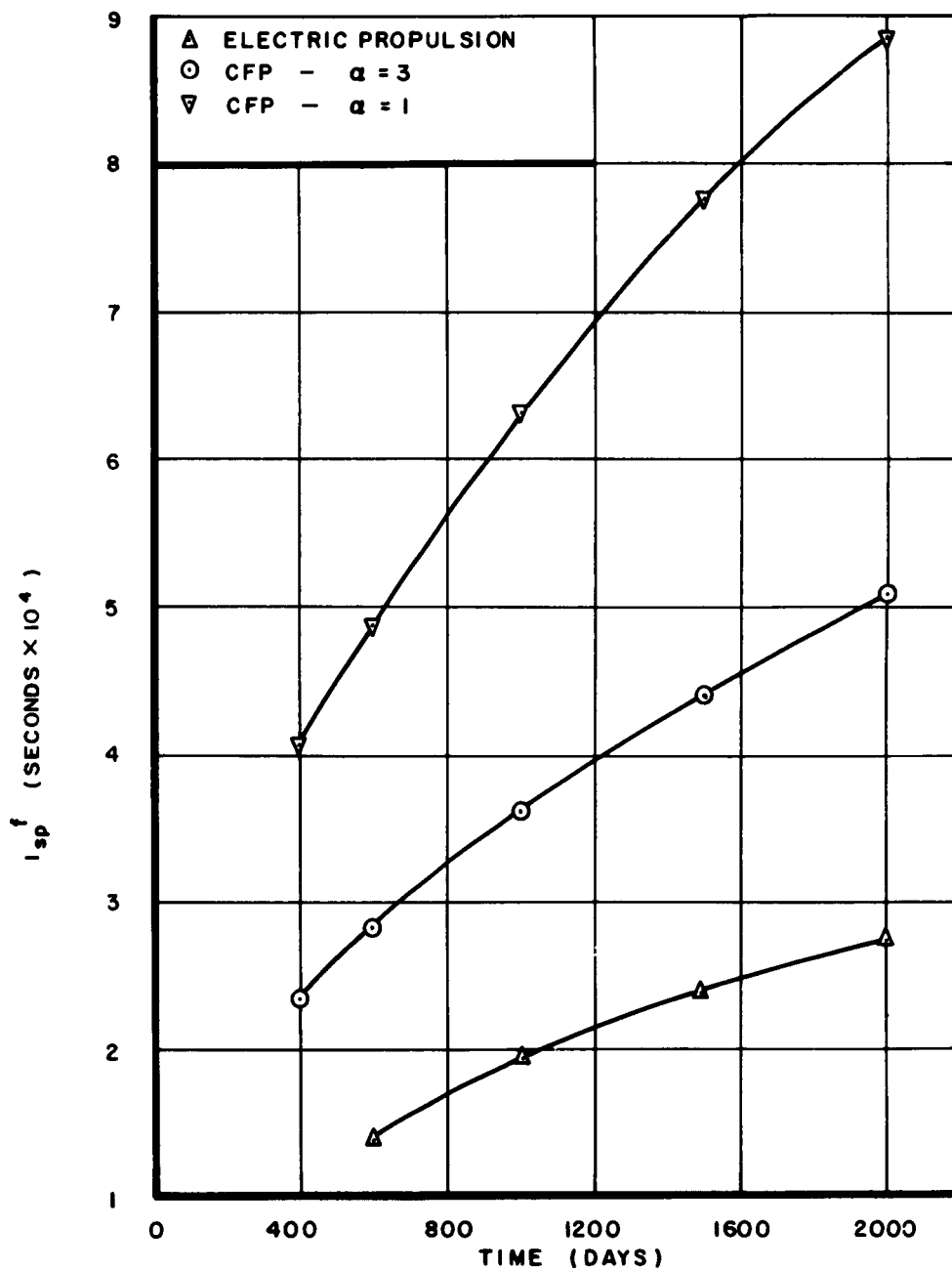
Figure 32. Comparison of CFP System with Electric System Based on Specific Impulse Used
at Completion of Mission; Round Trip to Moon

Figure 33. Comparison of CFP System with Electric System Based on Specific Impulse Used
at Completion of Mission: One-Way Trip to Mars
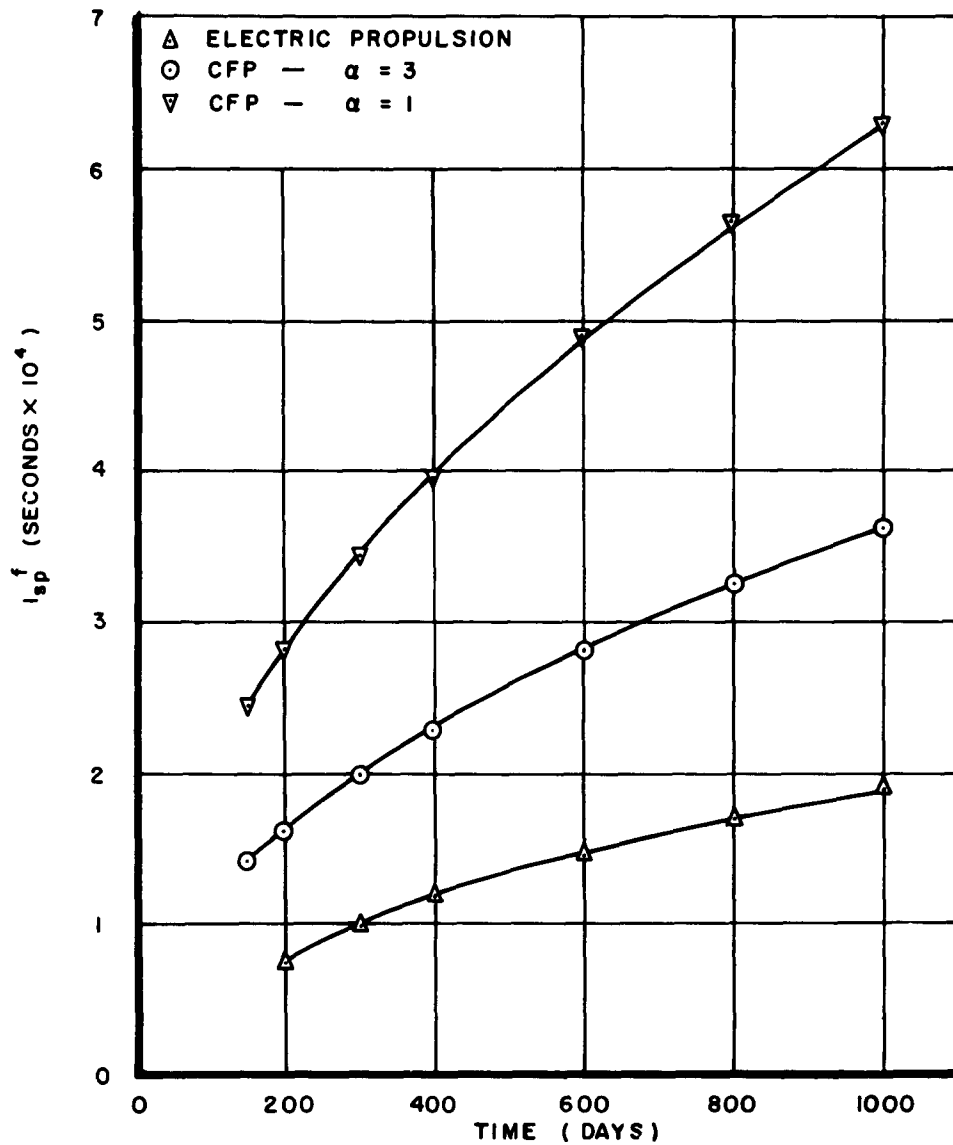
Figure 34. Comparison of CFP System with Electric System Based on Specific Impulse Used at Completion of Mission: Round Trip to Mars
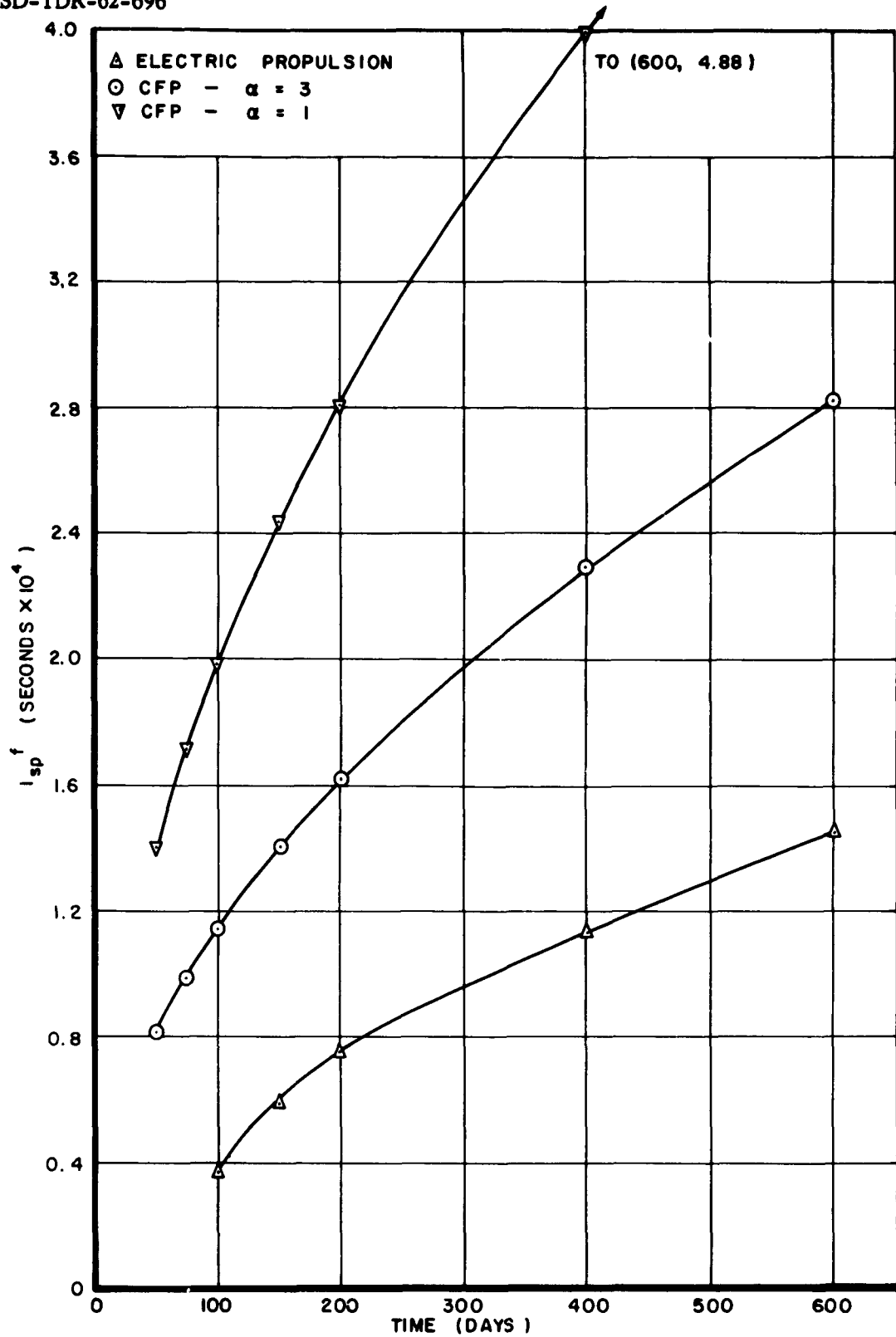
Figure 35. Comparison of CFP System with Electric System Based on Specific Impulse Used
at Completion of Mission: One-Way Trip to Venus

Figure 36. Comparison of CFP System with Electric System Based on Specific Impulse Used at Completion of Mission: Round Trip to Venus

Figure 37. Comparison of CFP System with Electric System Based on Specific Impulse Used at Completion of Mission: One-Way Trip to Jupiter

Figure 38. Comparison of CFP System with Electric System Based on Specific Impulse Used at Completion of Mission: Round Trip to Jupiter

COMPARISONS ON BASES OF IDENTICAL INITIAL WEIGHTS OF VEHICLES AND PAY-
LOADS (UNOPTIMIZED ELECTRIC SYSTEM)

Figures 39 through 46 show the initial weights of the vehicles, and Figures 47 through
54 show the weights of the payloads delivered.

The curves for the weights of payload and vehicle are meaningful only when the two sets
of curves for each mission are used in conjunction with one another (that is Figures 39
and 47 and Figures 40 and 48, etc.)

These payload weights and initial vehicle weights are found by direct analogy to CFP
systems; they are not plotted from equations relating the parameters of the system and
do not correspond to the optimized relationships derived earlier. This section is included
only for purposes of comparison and completeness. As an example in the use of the curves,
consider Figures 39 and 47 for a one-way moon mission. Here only the CFP curves have
been plotted from optimized parameters. For a 40-day mission, a CFP vehicle with $\alpha = 3$
would weigh $\sim 460,000$ pounds (Figure 39) and would carry slightly less than 400,000 pounds
payload and associated structure (Figure 47). To deliver an identical payload in the same
length of time, the electric system with $\alpha = 10$ would weigh $\sim 565,000$ pounds (Figure 39).
Conversely, an electric system with an initial vehicle weight equal to that of the CFP
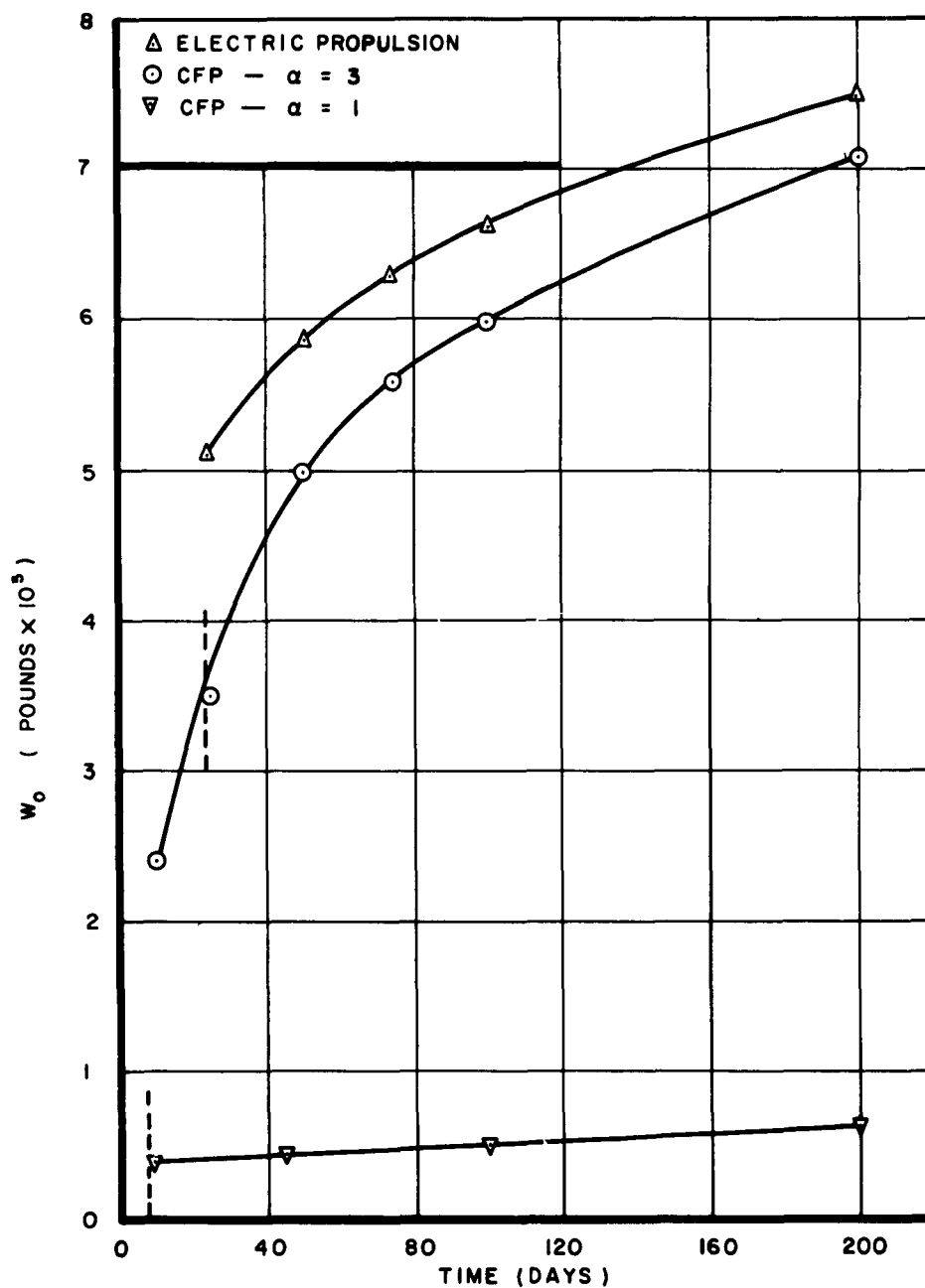system ($\sim 460,000$ pounds) would be able to deliver $\sim 330,000$ pounds payload.

Figure 39. Comparison of CFP System with Electric System Based on Identical Initial Weights of Vehicle and Payload (Unoptimized Electric System): Vehicle Weight - One-Way Trip to Moon
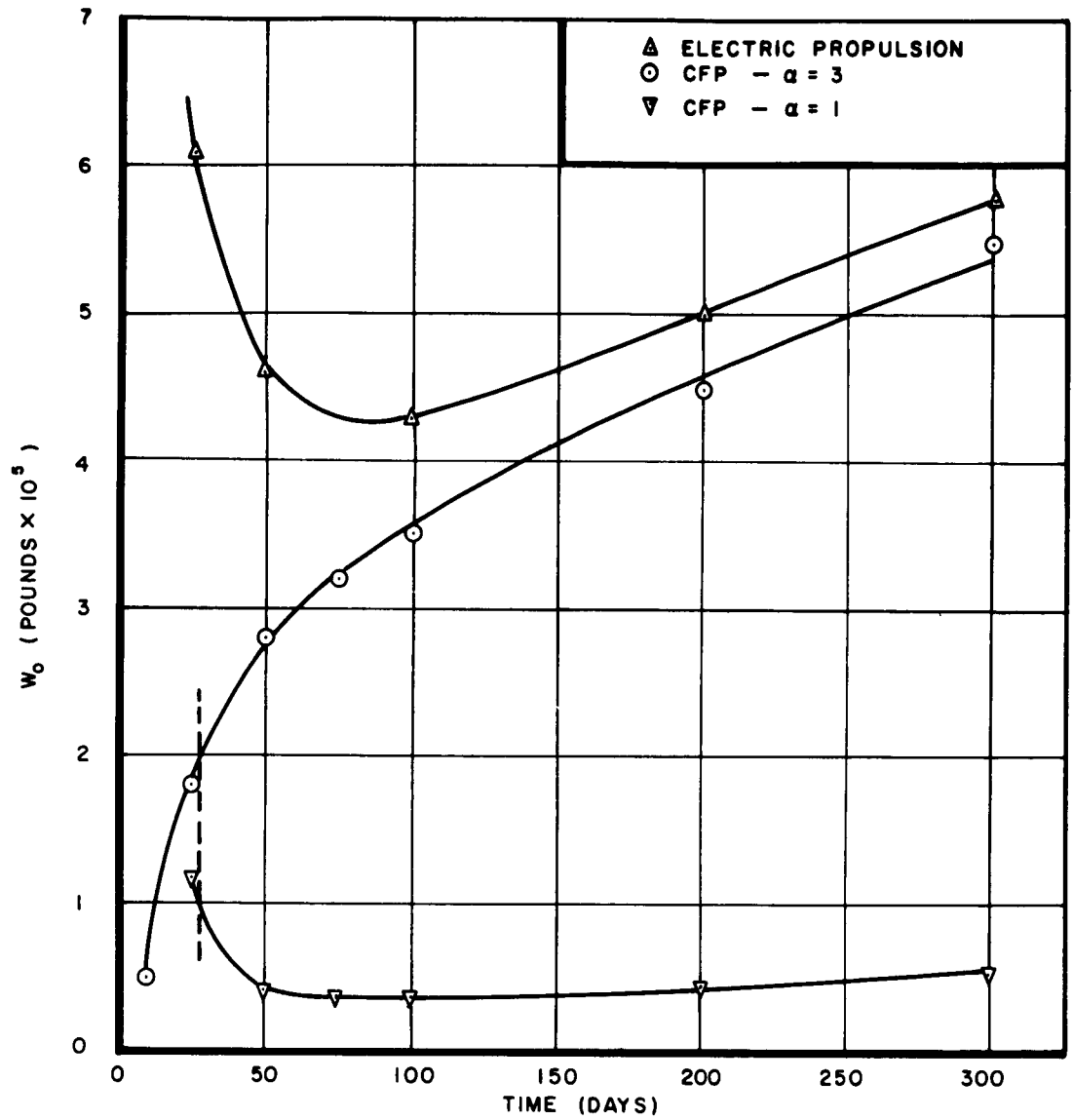
Figure 40. Comparison of CFP System with Electric System Based on Identical Initial Weights of Vehicle and Payload (Unoptimized Electric System): Vehicle Weight - Round Trip to Moon
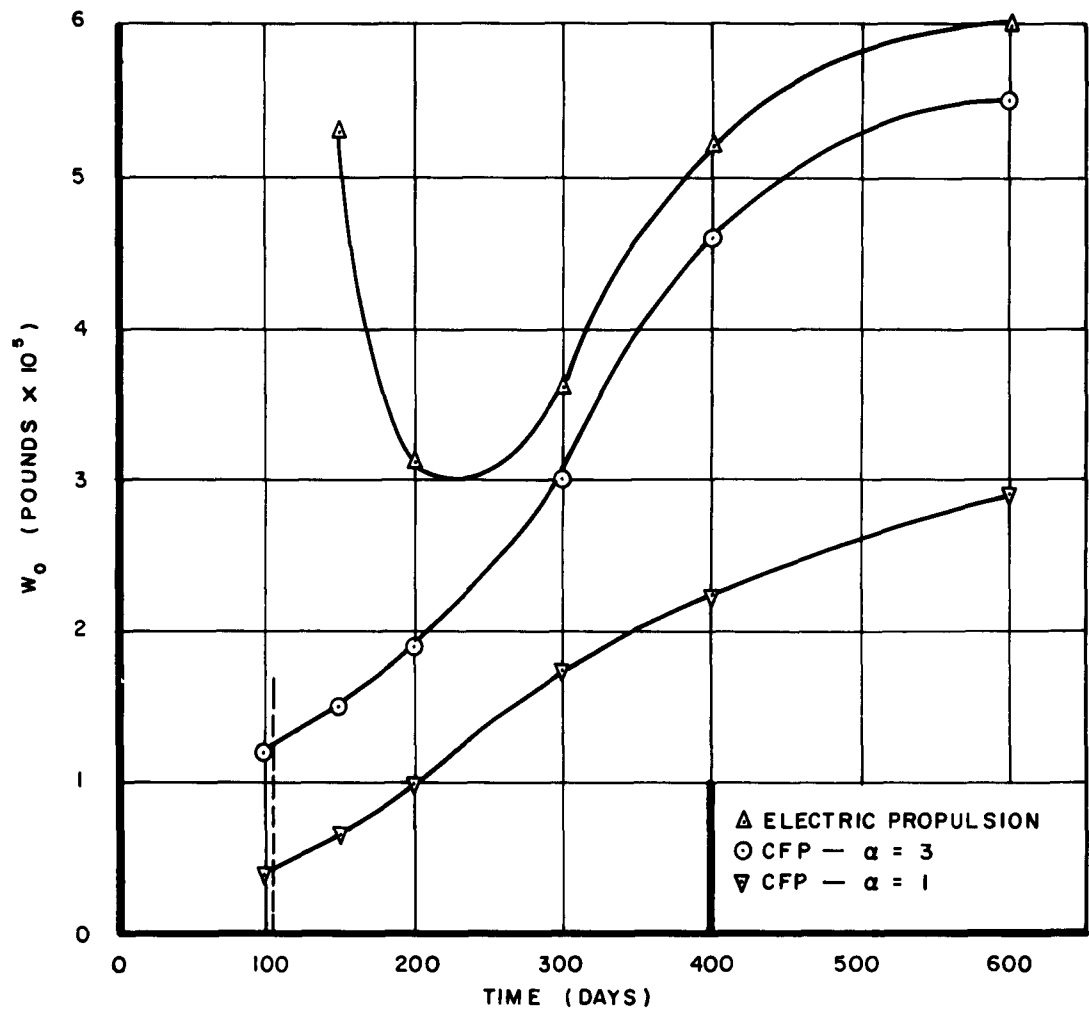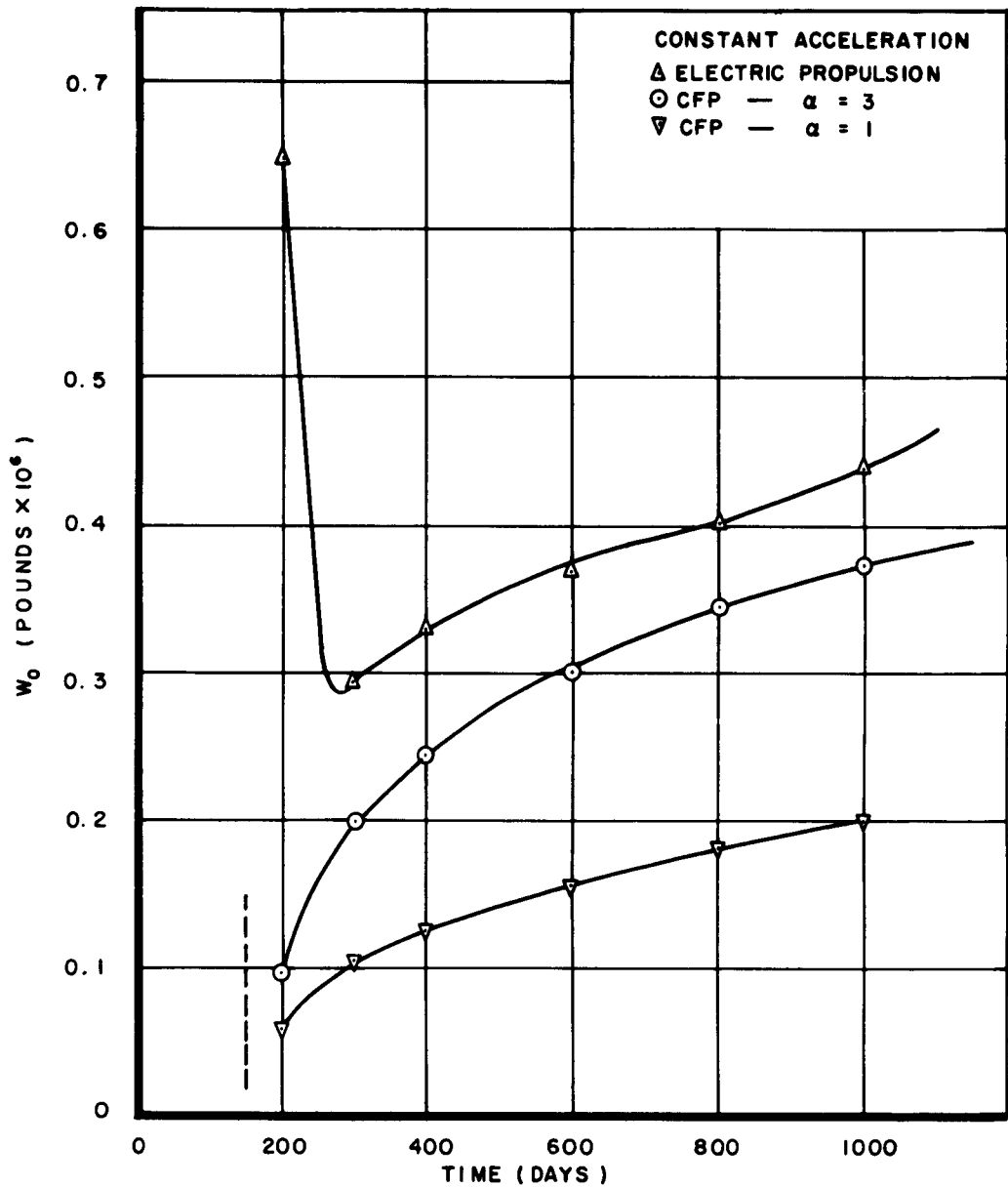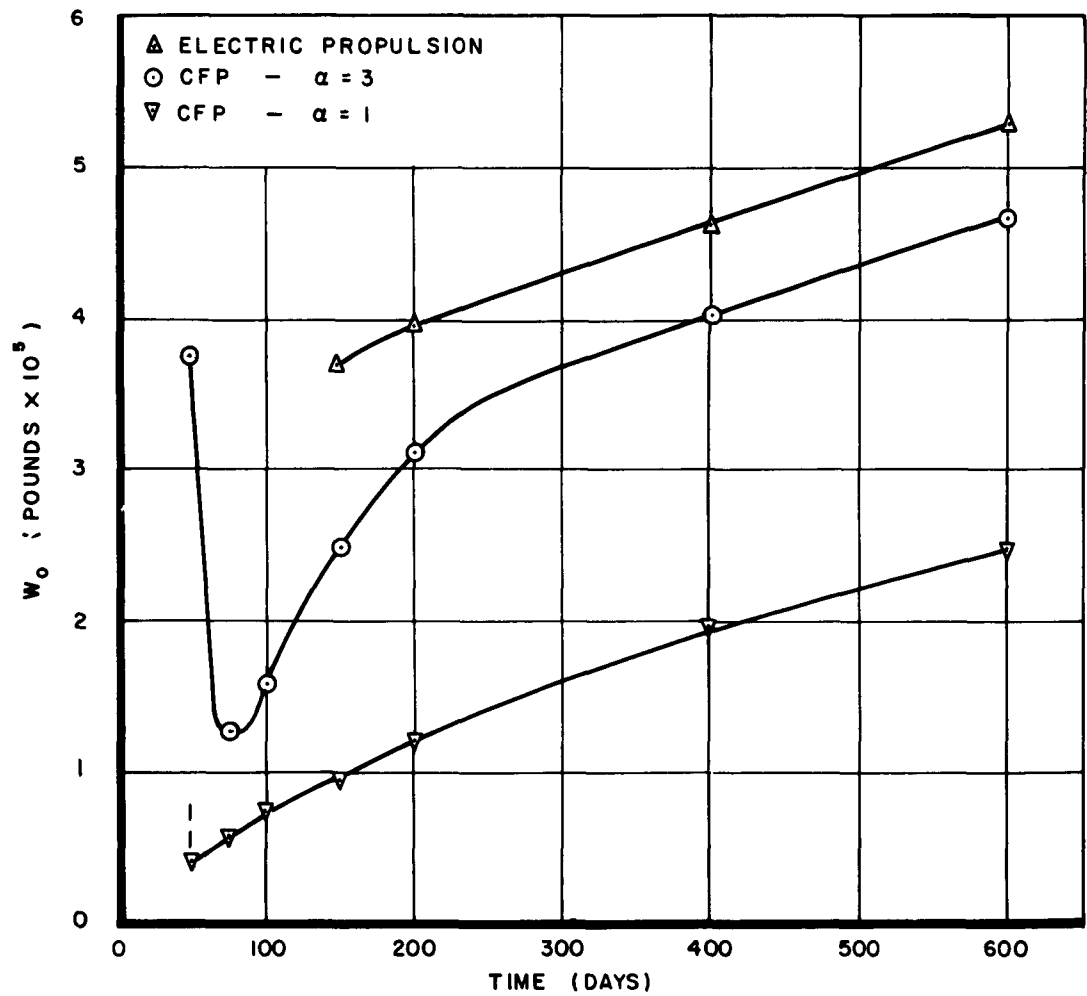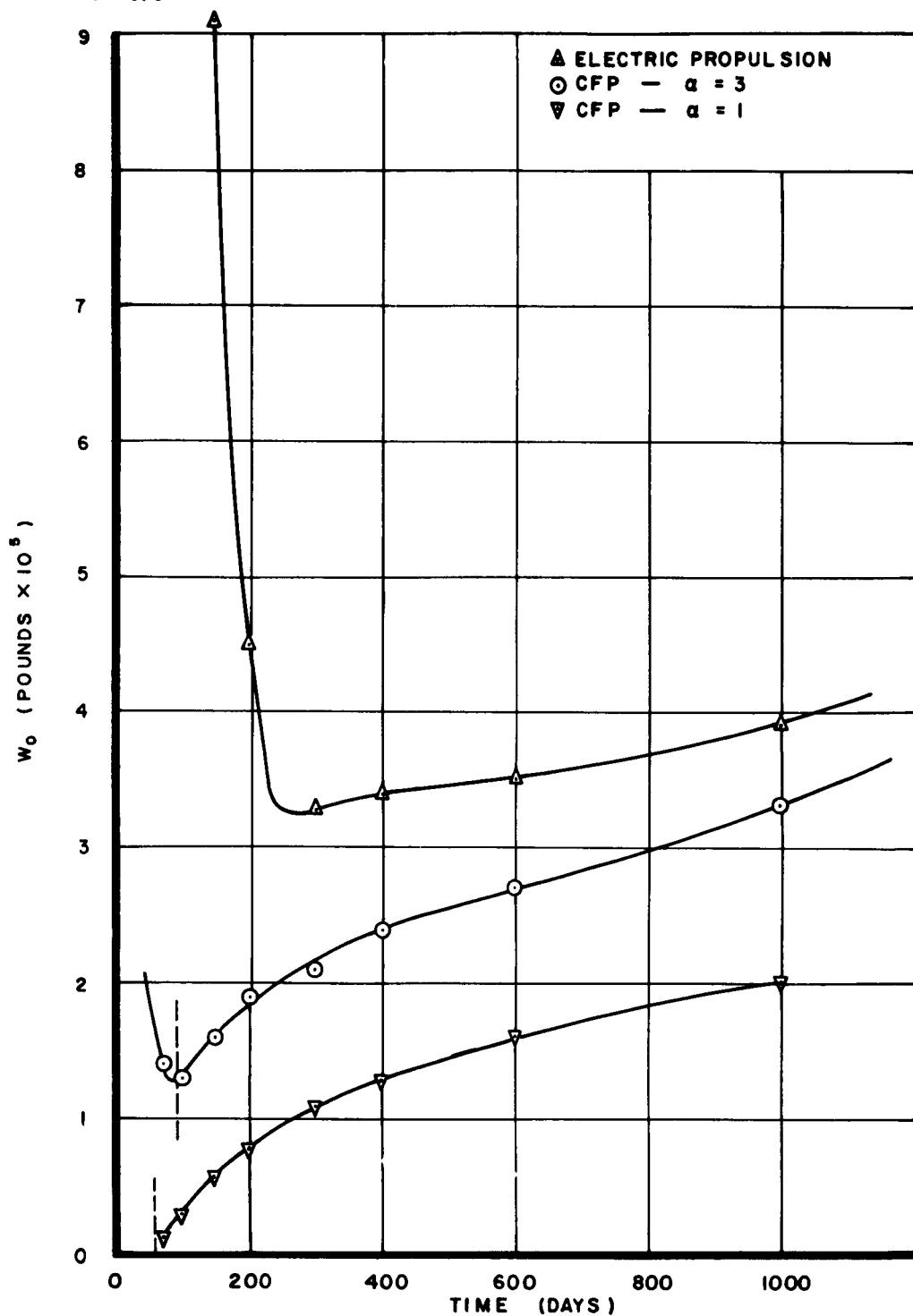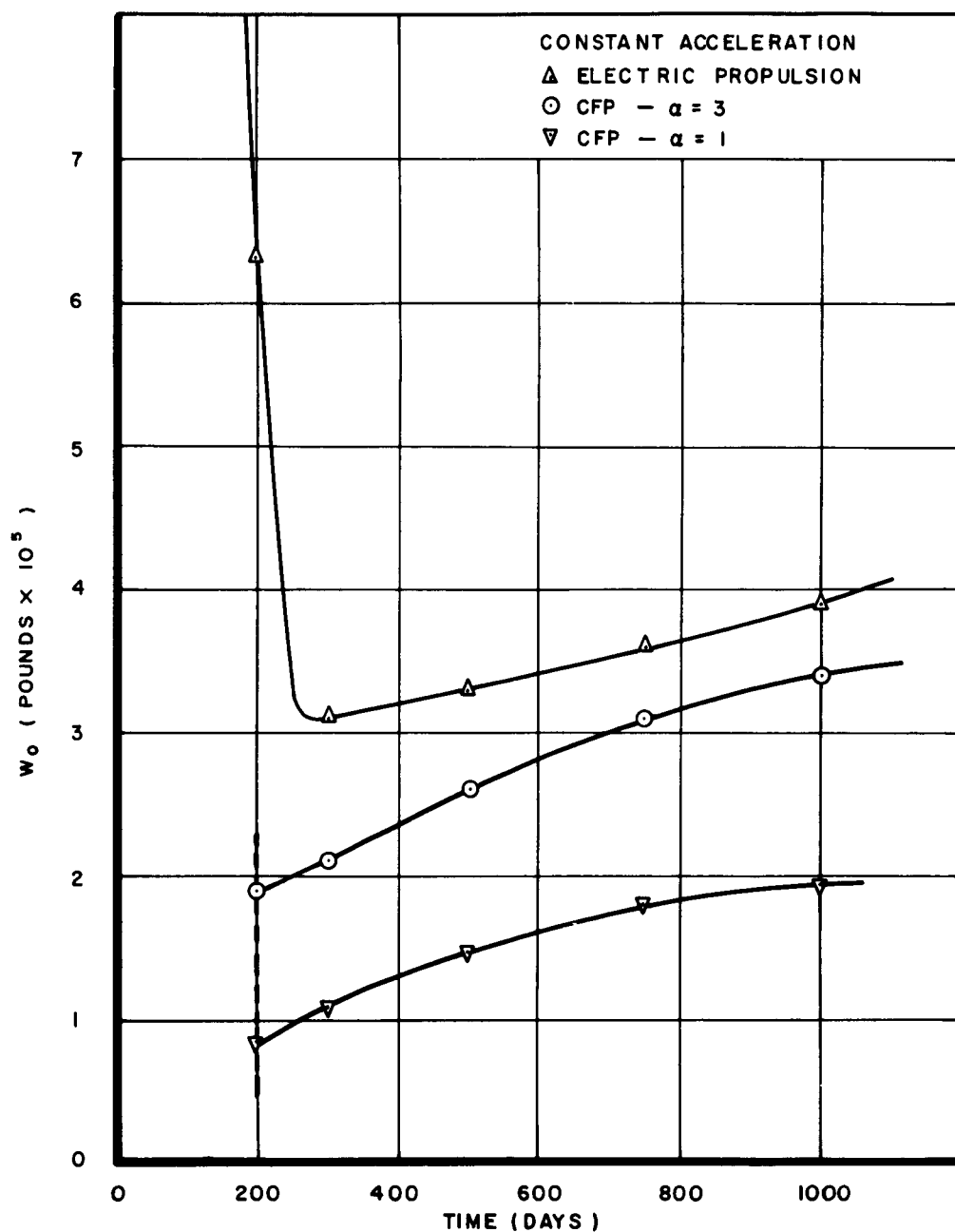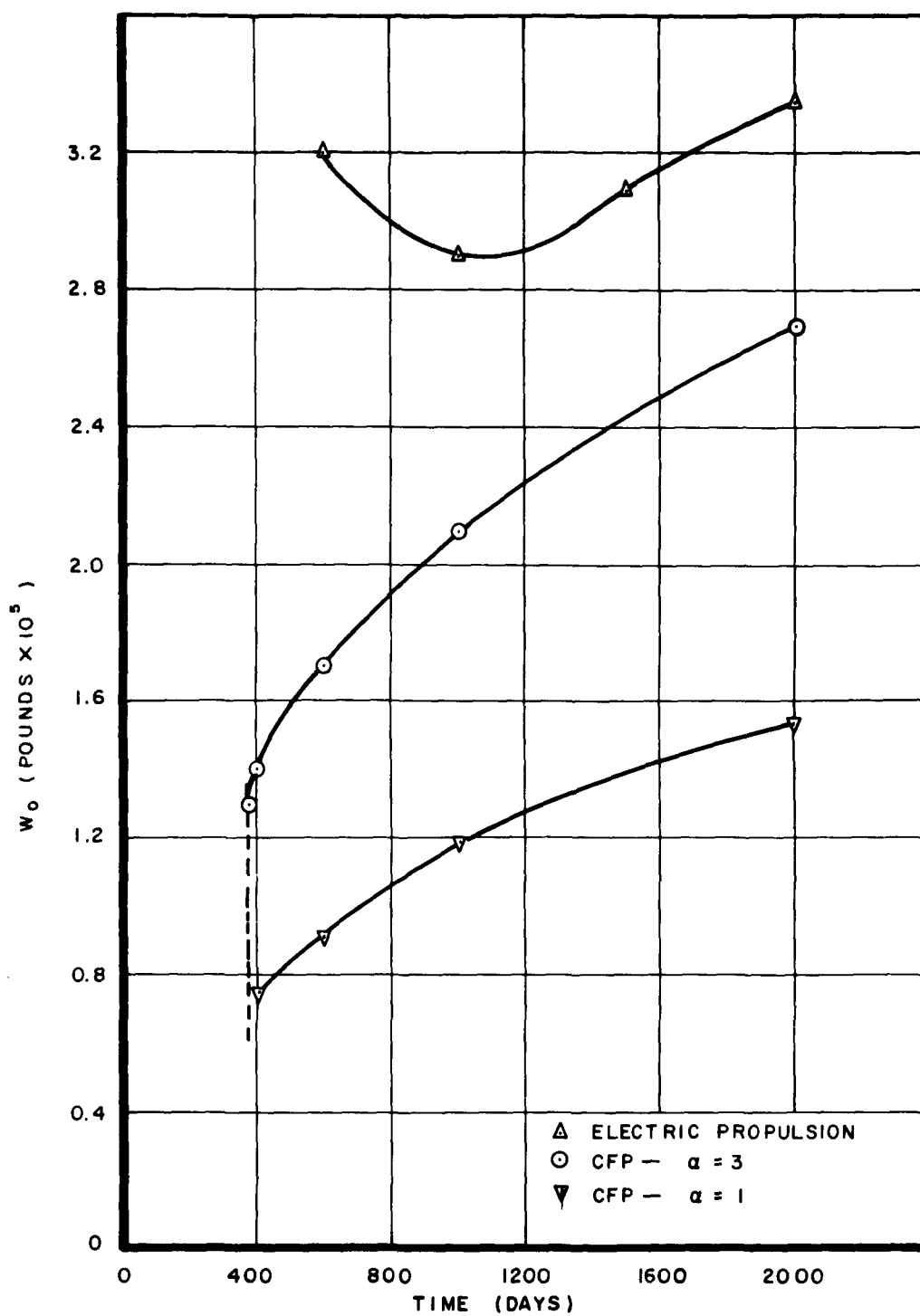
Figure 41. Comparison of CFP System with Electric System Based on Identical Initial Weights of Vehicle and Payload (Unoptimized Electric System): Vehicle Weight - One-Way Trip to Mars

Figure 42. Comparison of CFP System with Electric System Based on Identical Initial Weights of Vehicle and Payload (Unoptimized Electric System): Vehicle Weight – Round Trip to Mars
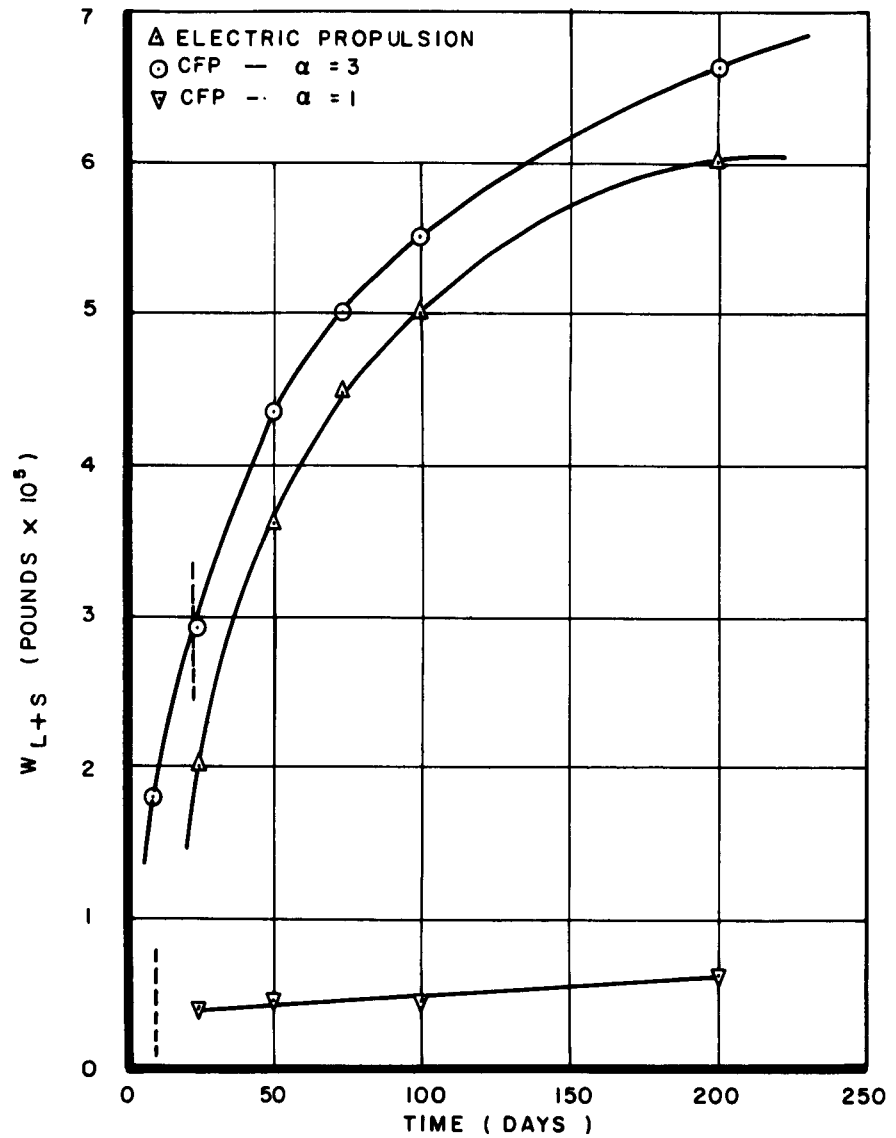
Figure 43. Comparison of CFP System with Electric System Based on Identical Initial Weights of Vehicle and Payload (Unoptimized Electric System): Vehicle Weight – One-Way Trip to Venus
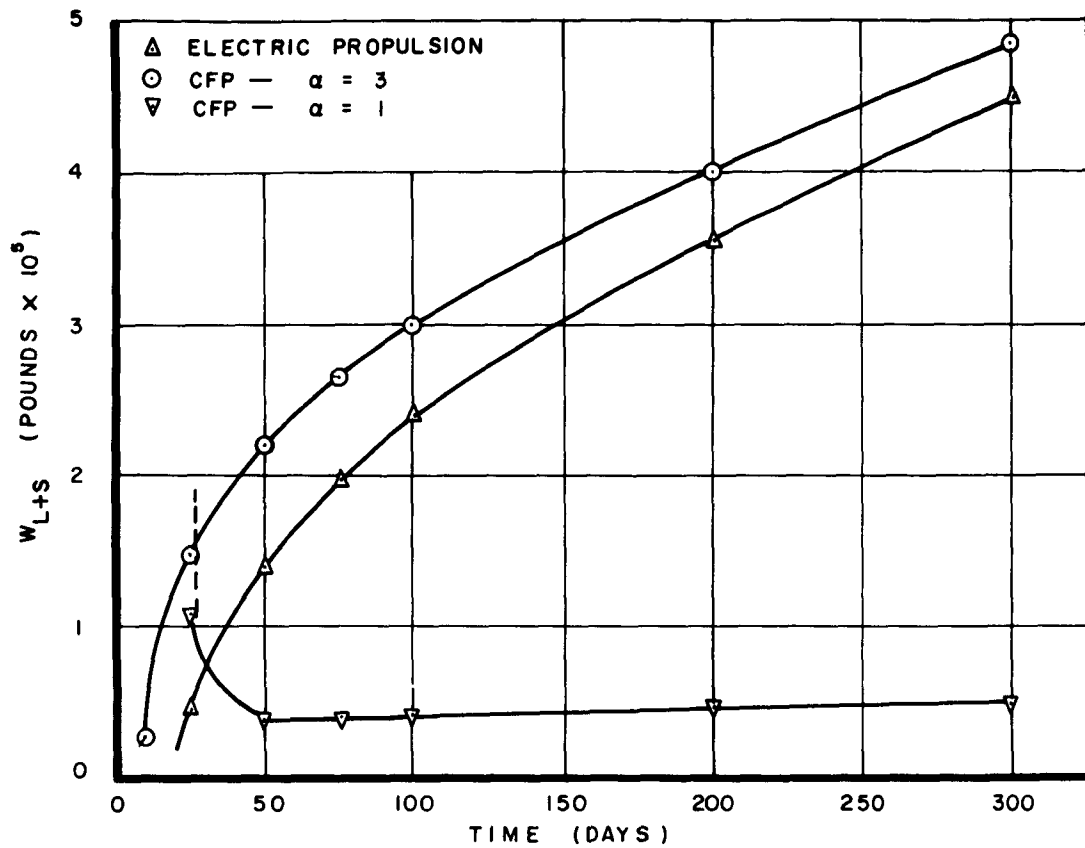
Figure 44. Comparison of CFP System with Electric System Based on Identical Initial Weights of Vehicle and Payload (Unoptimized Electric System): Vehicle Weight - Round Trip to Venus
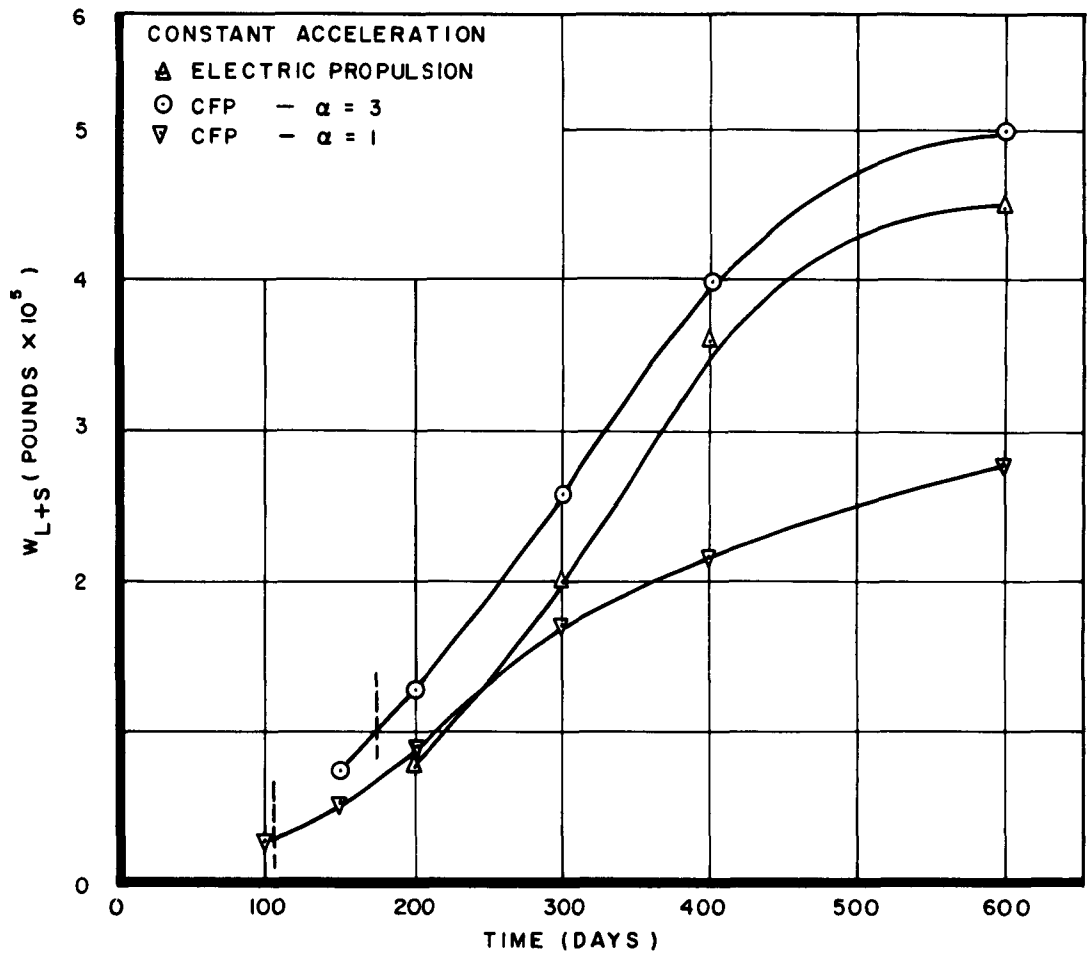
Figure 45. Comparison of CFP System with Electric System Based on Identical Initial Weights of Vehicle and Payload (Unoptimized Electric System): Vehicle Weight - One-Way Trip to Jupiter

Figure 46. Comparison of CFP System with Electric System Based on Identical Initial Weights of Vehicle and Payload (Unoptimized Electric System): Vehicle Weight -Round Trip to Jupiter

Figure 47. Comparison of CFP System with Electric System Based on Identical Initial Weights of Vehicle and Payload (Unoptimized Electric System): Payload Weight - One-Way Trip to Moon
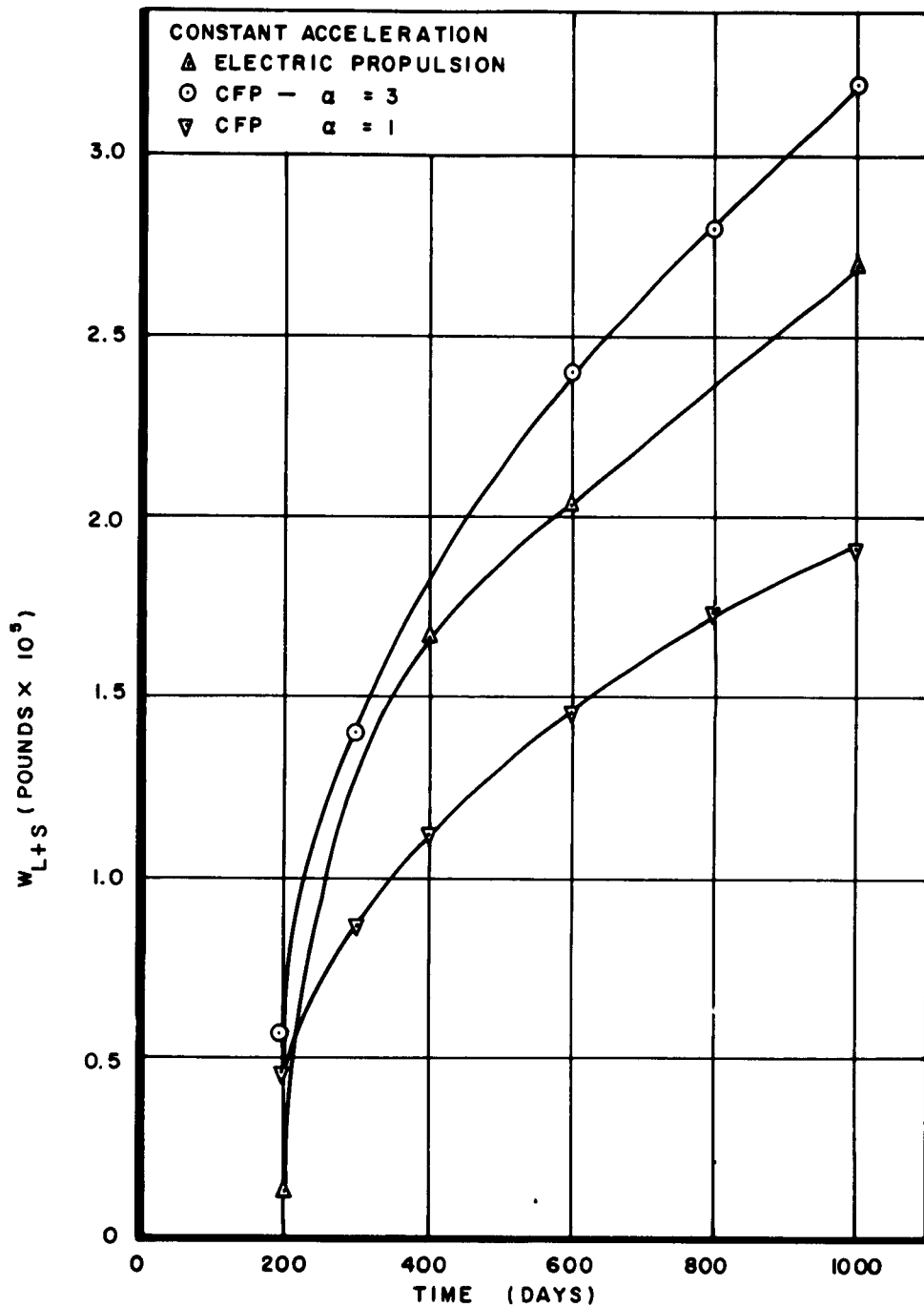
Figure 48. Comparison of CFP System with Electric System Based on Identical Initial Weights of Vehicle and Payload (Unoptimized Electric System): Payload Weight - Round Trip to Moon
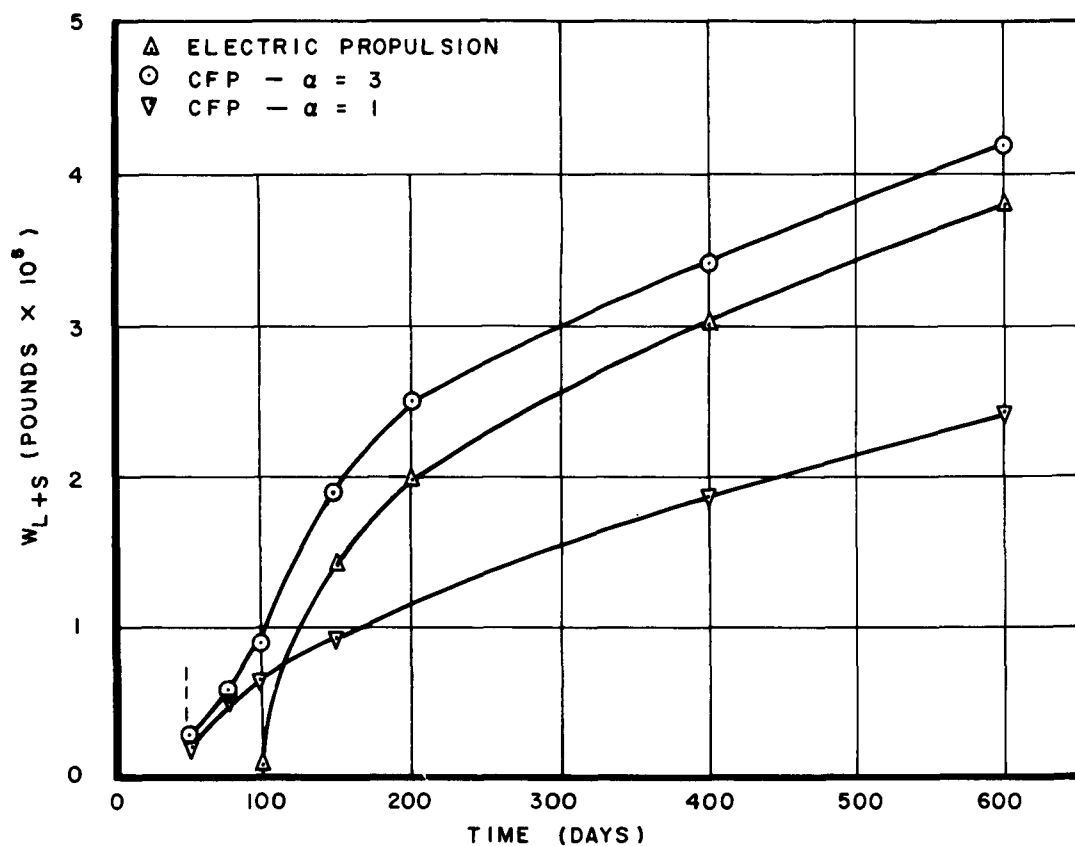
Figure 49. Comparison of CFP System with Electric System Based on Identical Initial Weights of Vehicle and Payload (Unoptimized Electric System): Payload Weight - One-Way Trip to Mars
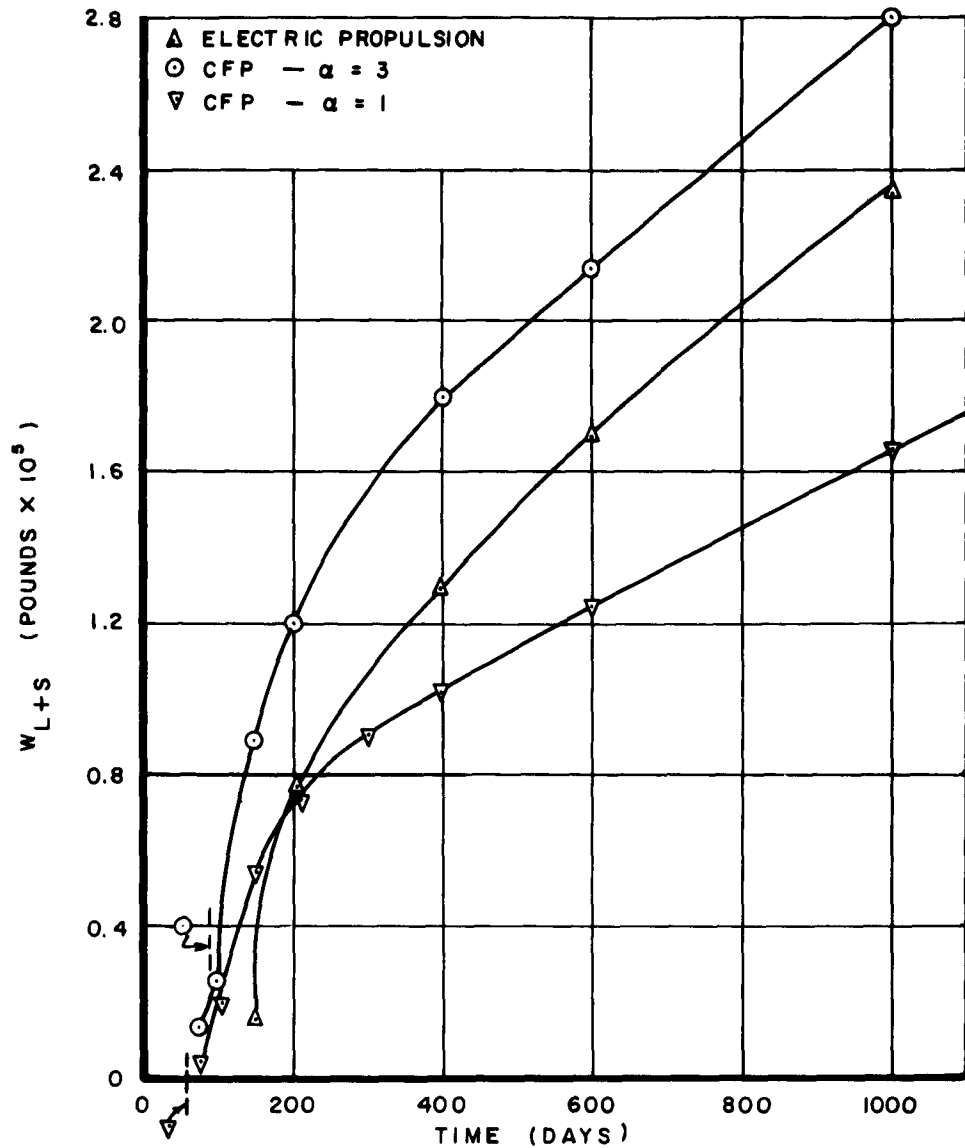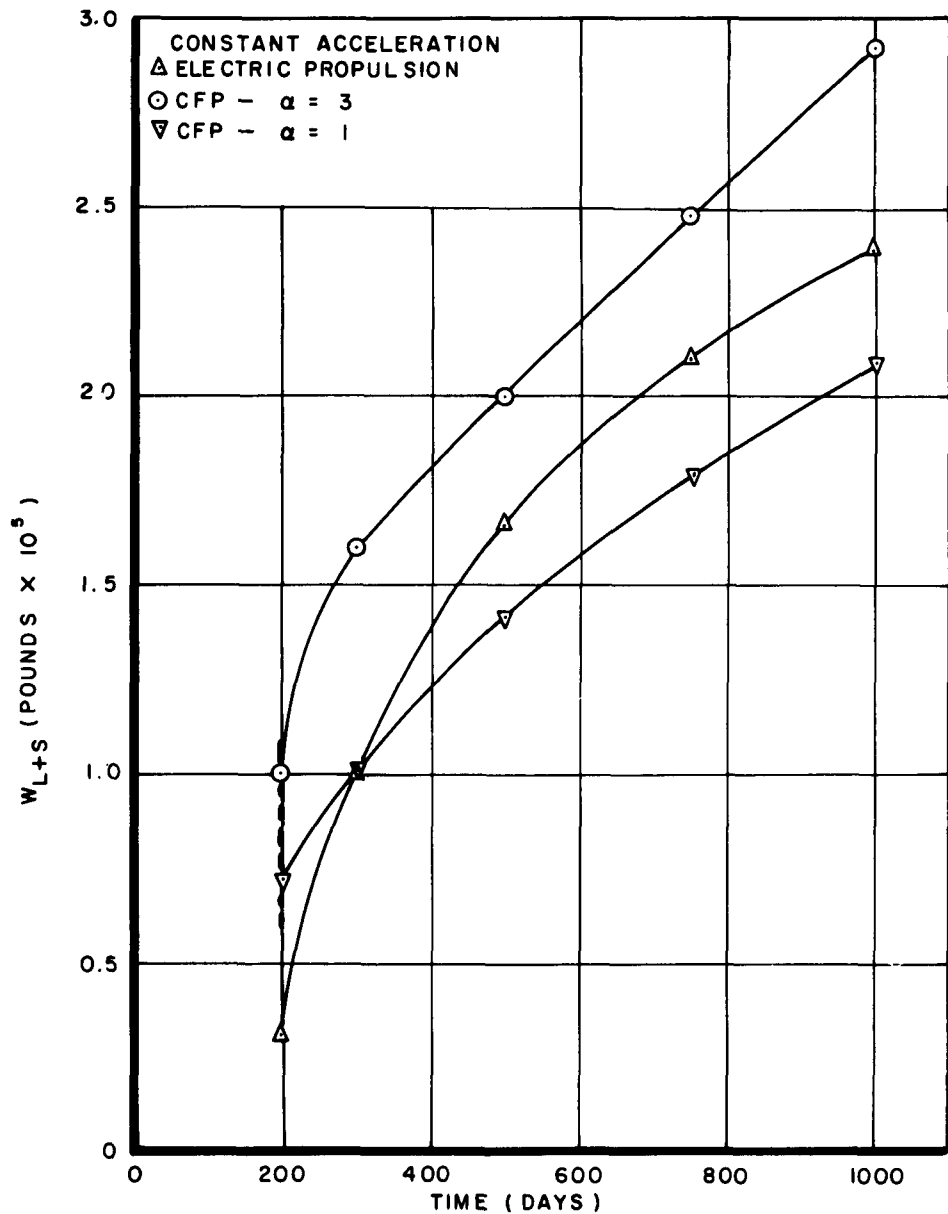
Figure 50. Comparison of CFP System with Electric System Based on Identical Initial Weights of Vehicle and Payload (Unoptimized Electric System): Payload Weight – Round Trip to Mars

Figure 51. Comparison of CFP System with Electric System Based on Identical Initial Weights of Vehicle and Payload (Unoptimized Electric System): Payload Weight - One-Way Trip to Venus
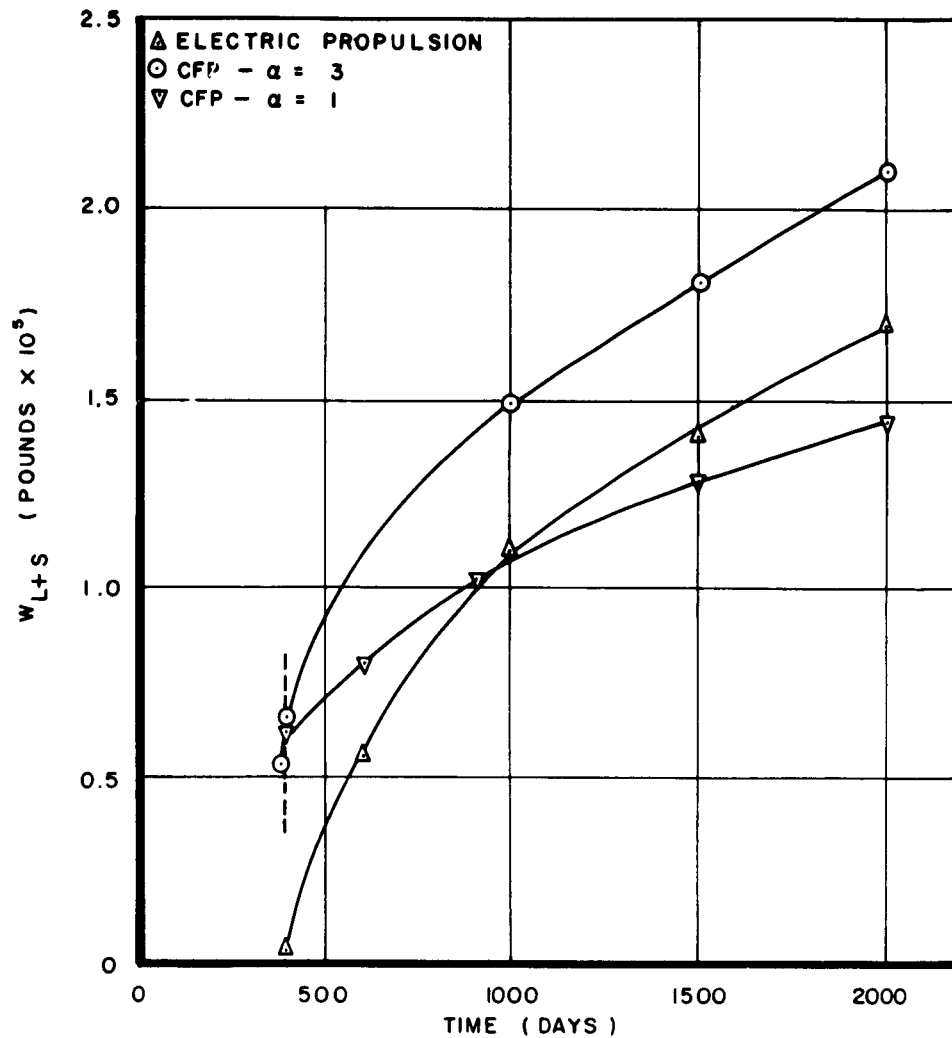
Figure 52. Comparison of CFP System with Electric System Based on Identical Initial Weights of Vehicle and Payload (Unoptimized Electric System): Payload Weight - Round Trip to Venus

Figure 53. Comparison of CFP System with Electric System Based on Identical Initial Weights of Vehicle and Payload (Unoptimized Electric System): Payload Weight - One-Way Trip to Jupiter

Figure 54. Comparison of CFP System with Electric System Based on Identical Initial Weights of Vehicle and Payload (Unoptimized Electric System): Payload Weight - Round Trip to Jupiter

COMPARISONS ON BASES OF WEIGHTS OF VEHICLES AND PAYLOADS (OPTIMIZED SYSTEMS)

Figures 55 through 62 show the initial weights of the vehicles, and Figures 63 through 70 show the weights of payloads delivered.

For these figures, both the curves for the CFP and the electric systems are plotted directly from calculated parameters of the vehicle and represent optimum values. This optimum size is then an increasing function of α.

Since $W_o = \dfrac{W_G}{f_G}$ and W_G increases linearly with α (and P), the total weight of the vehicle (W_o) must be large if W_G is to remain a reasonably small fraction of W_o. The numerical values of W_o and W_{L+S} are computed for 10-megawatt systems and assume the "normalization" discussed previously in the Section titled Analytical Approach.
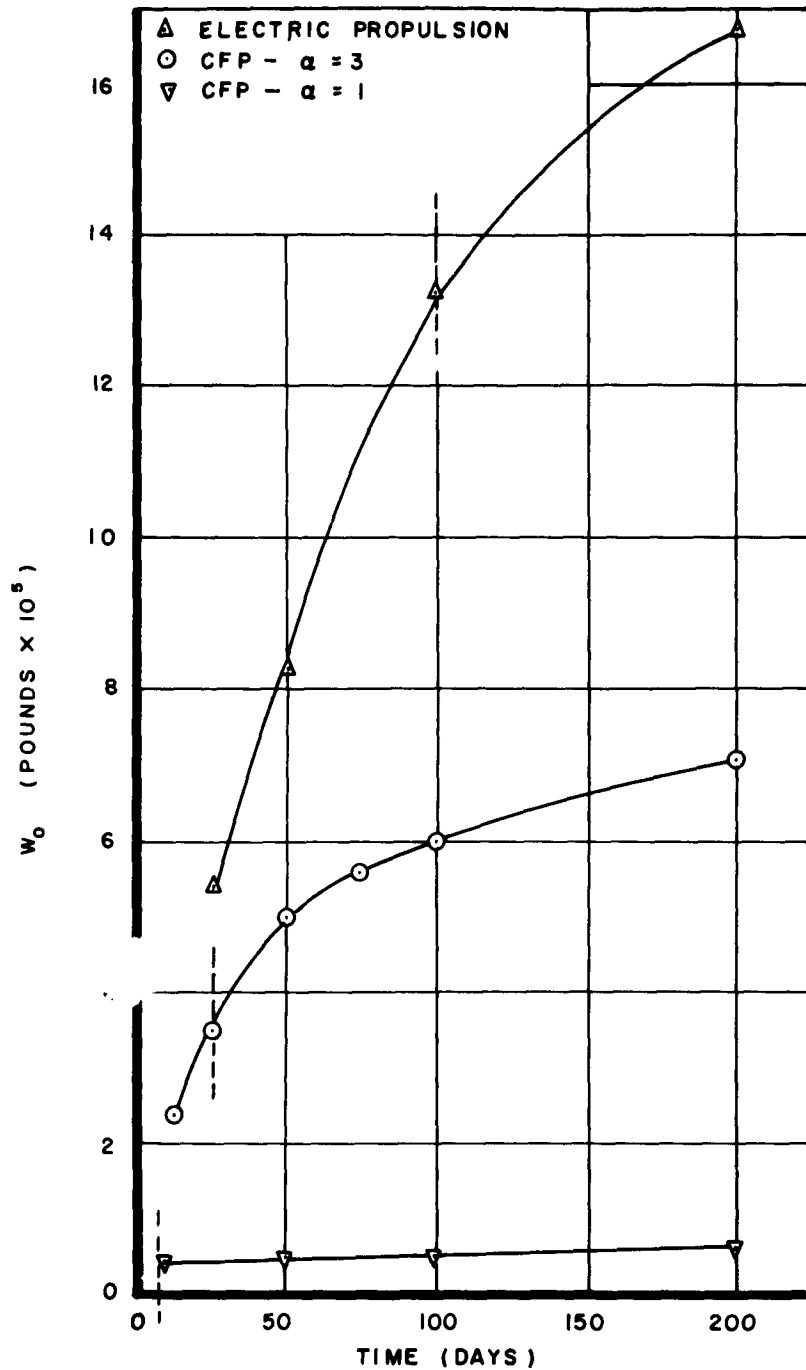
Figure 55. Comparison of CFP System with Electric System Based on Weights of Vehicle and Payload (Optimized Systems): Vehicle Weight - One-Way Trip to Moon
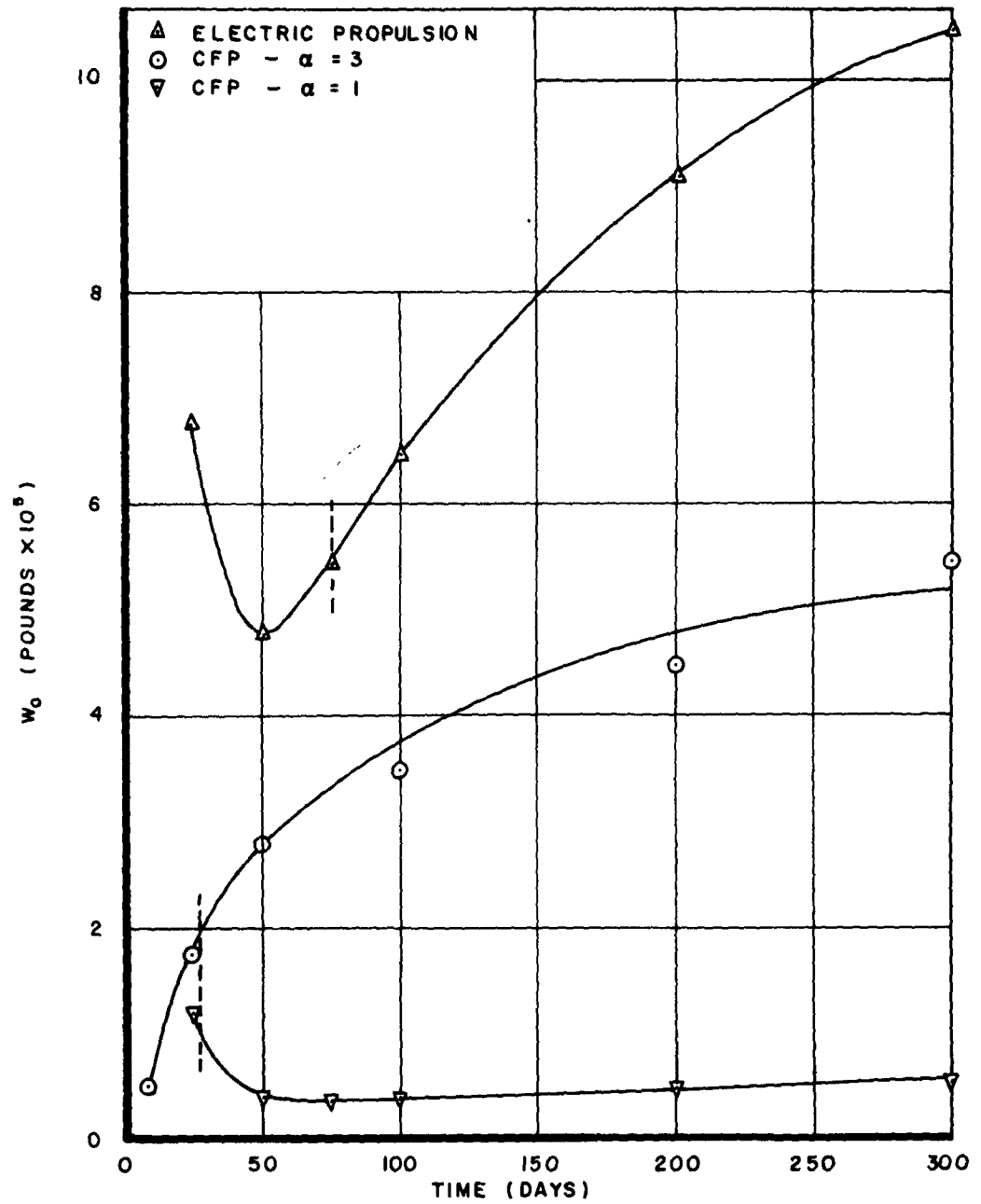
Figure 56. Comparison of CFP System with Electric System Based on Weights of
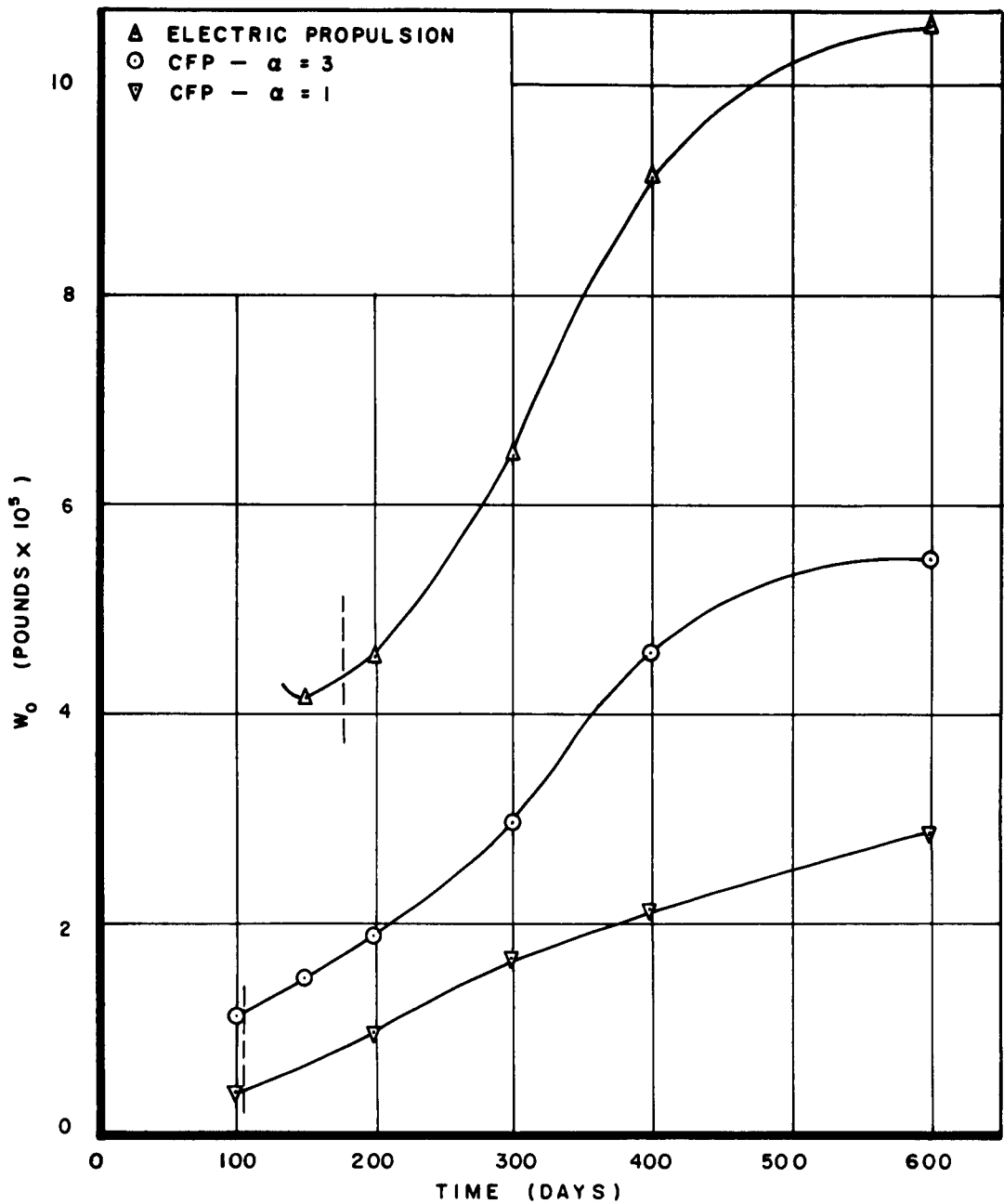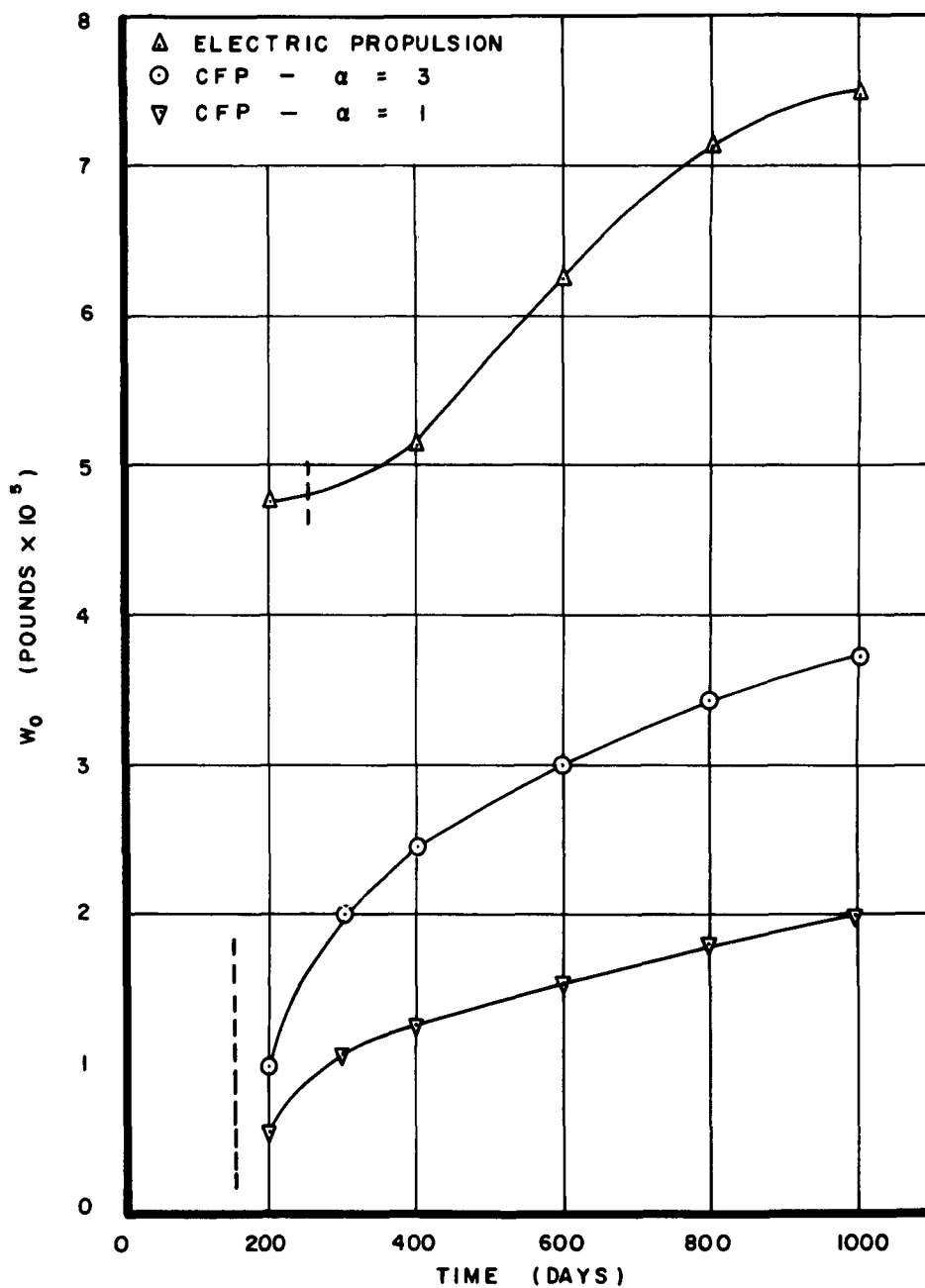Vehicle and Payload (Optimized Systems): Vehicle Weight - Round
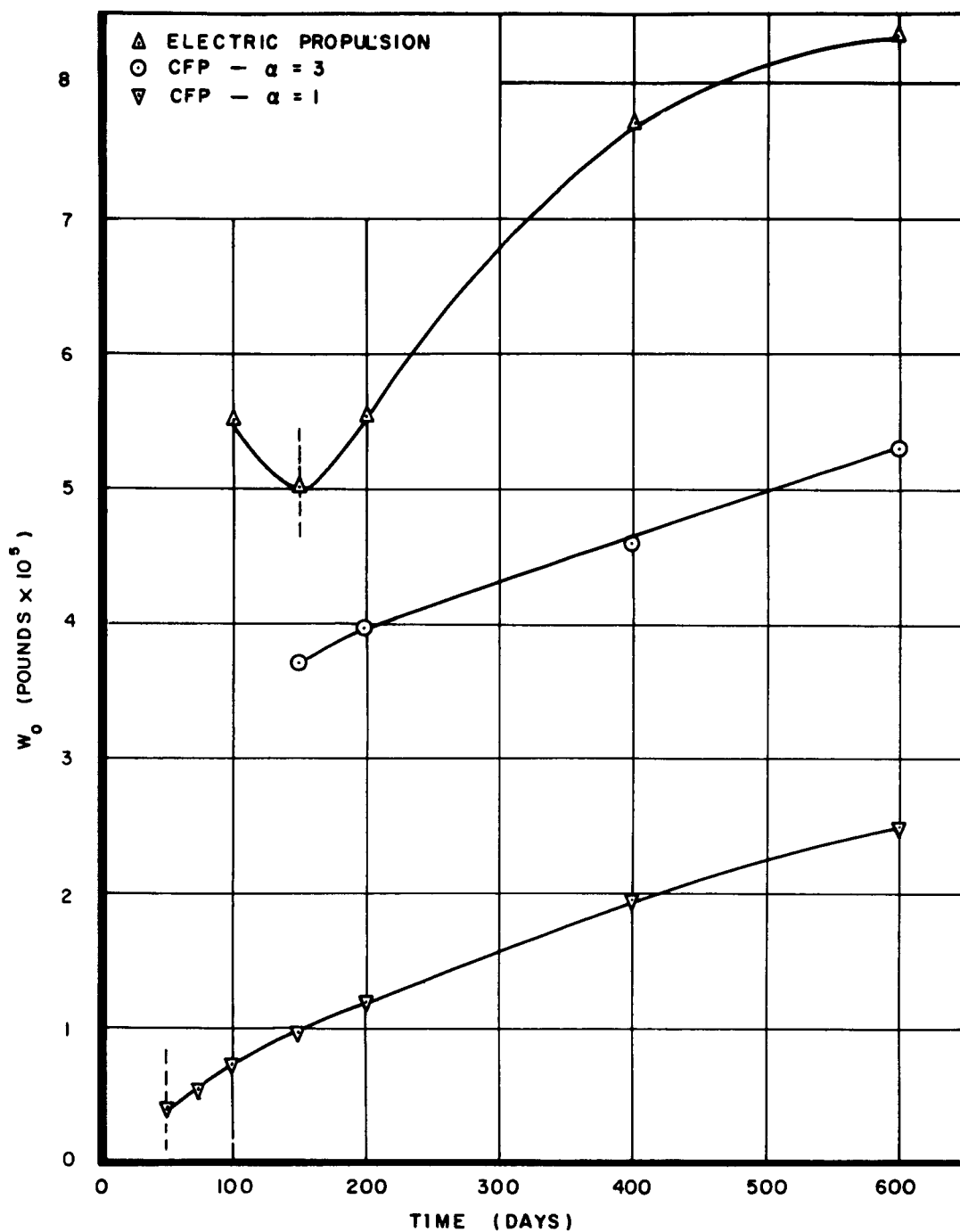Trip to Moon

Figure 57. Comparison of CFP System with Electric System Based on Weights of Vehicle and Payload (Optimized Systems): Vehicle Weight - One-Way Trip to Mars

Figure 58. Comparison of CFP System with Electric System Based on Weights of Vehicle and Payload (Optimized Systems): Vehicle Weight - Round Trip to Mars

Figure 59. Comparison of CFP System with Electric System Based on Weights of
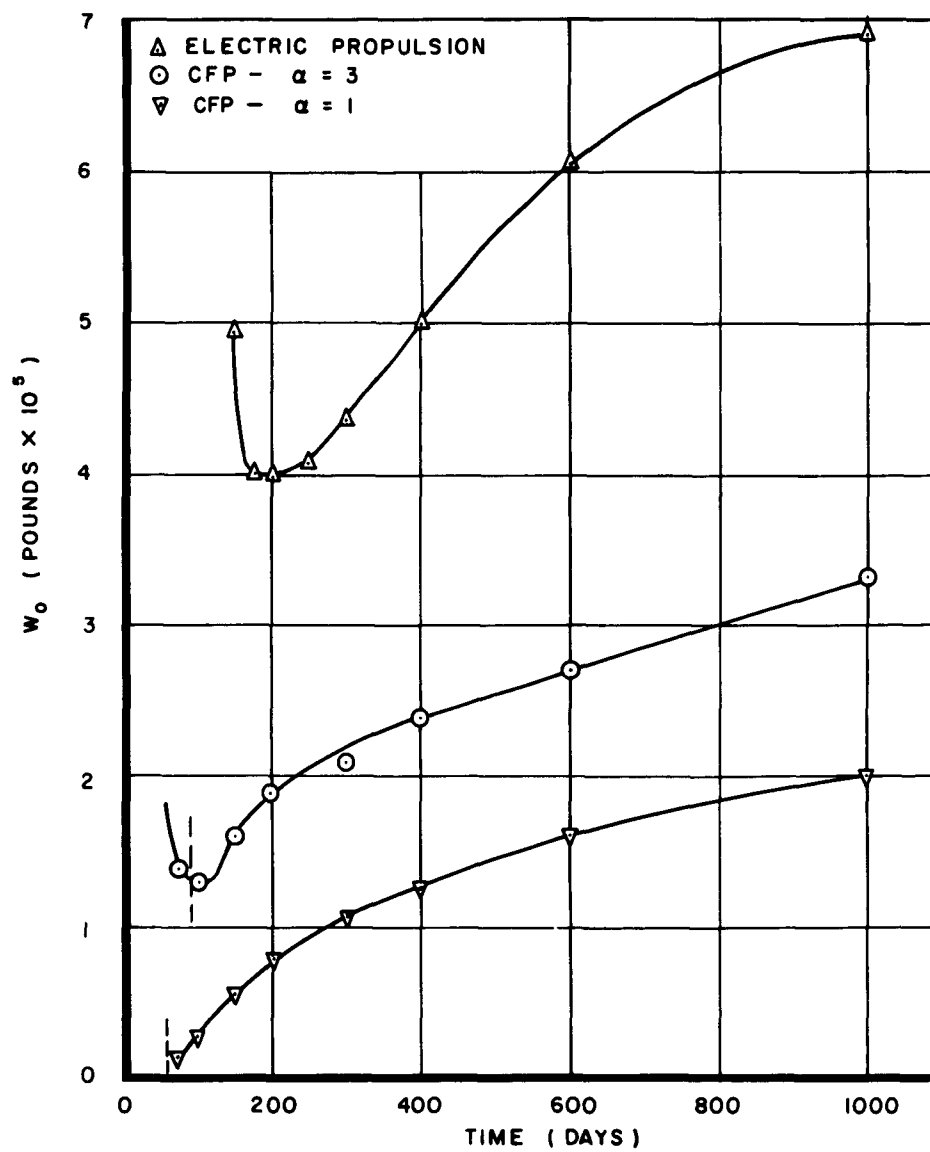Vehicle and Payload (Optimized Systems): Vehicle Weight - One-Way
Trip to Venus

Figure 60. Comparison of CFP System with Electric System Based on Weights of Vehicle and Payload (Optimized Systems): Vehicle Weight - Round Trip to Venus
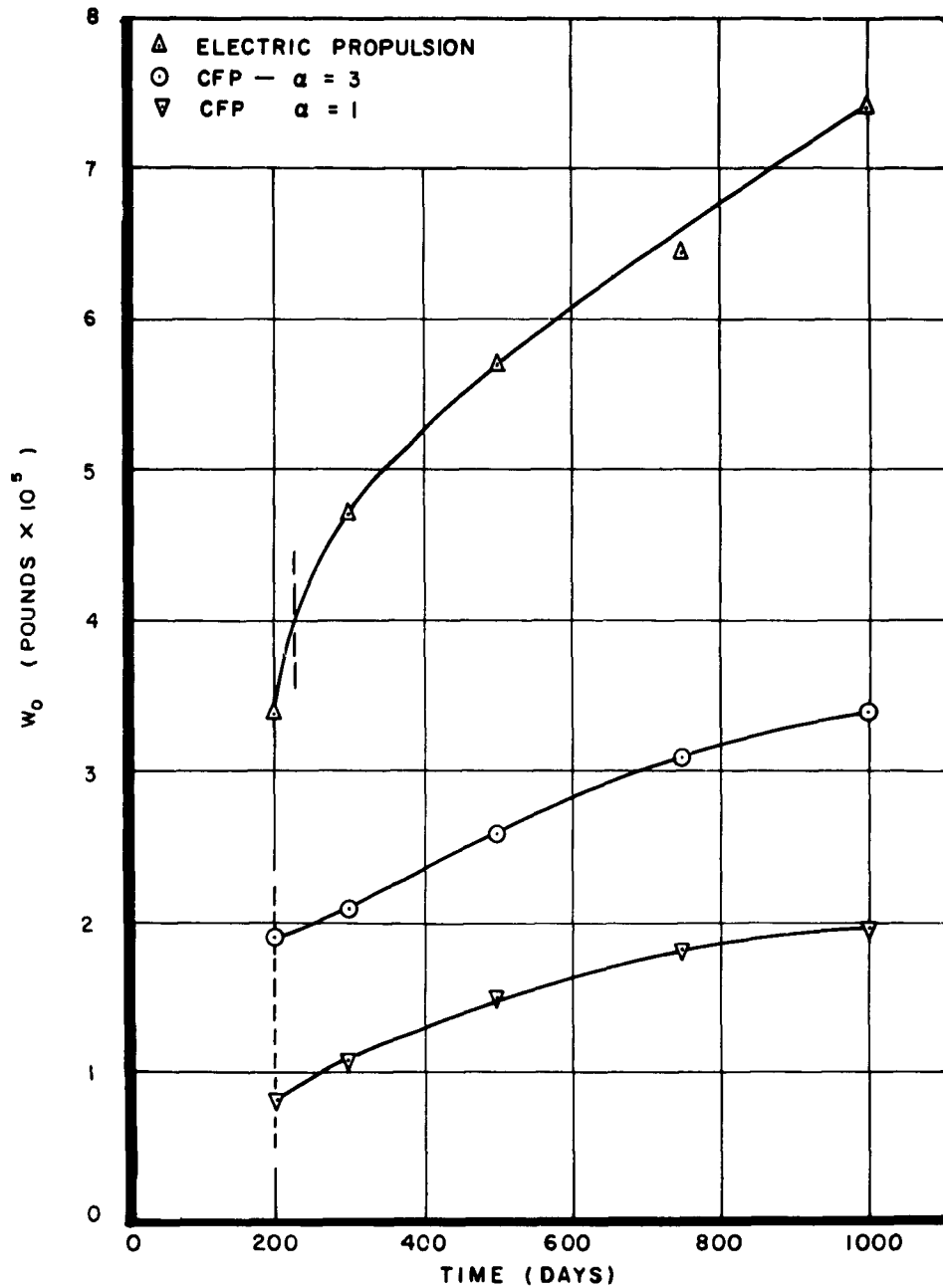
Figure 61. Comparison of CFP System with Electric System Based on Weights of
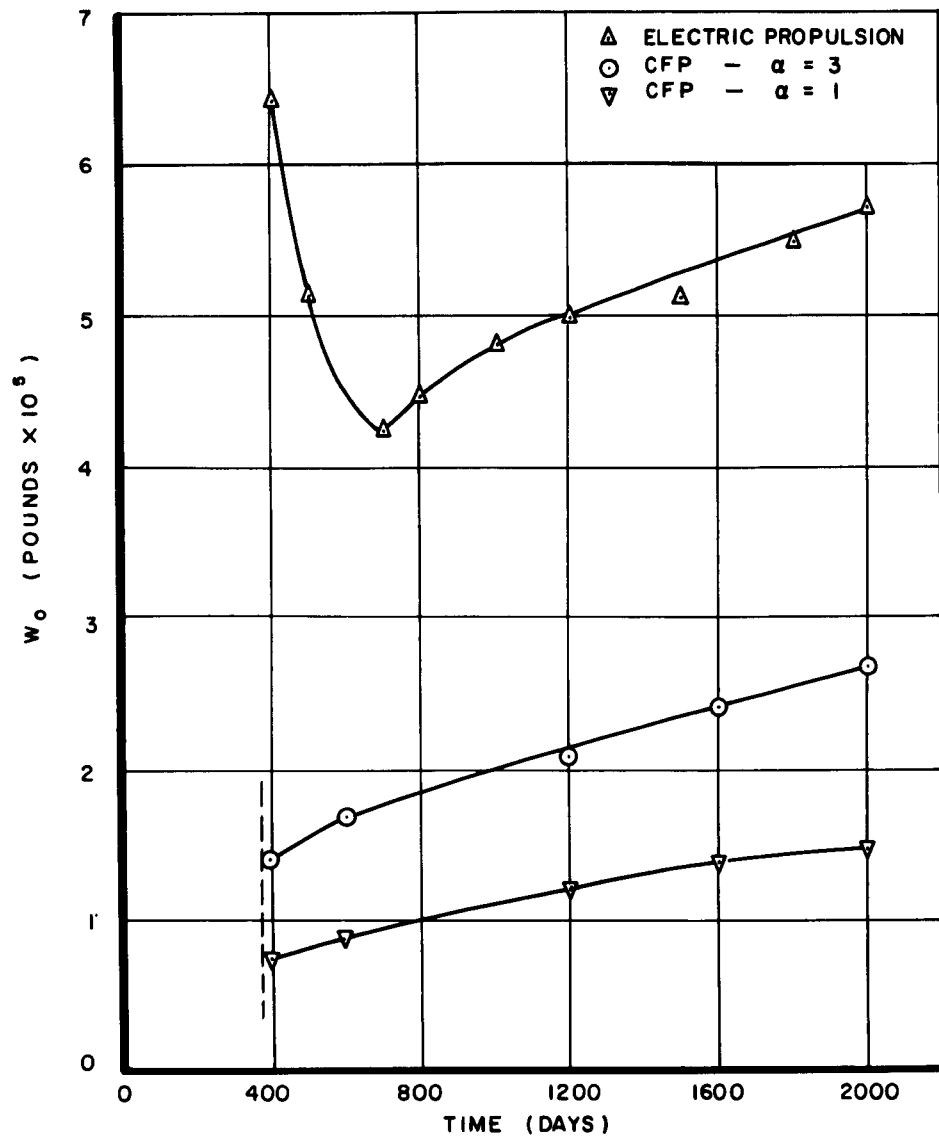Vehicle and Payload (Optimized Systems): Vehicle Weight - One-Way
Trip to Jupiter

Figure 62. Comparison of CFP System with Electric System Based on Weights of
Vehicle and Payload (Optimized Systems): Vehicle Weight - Round
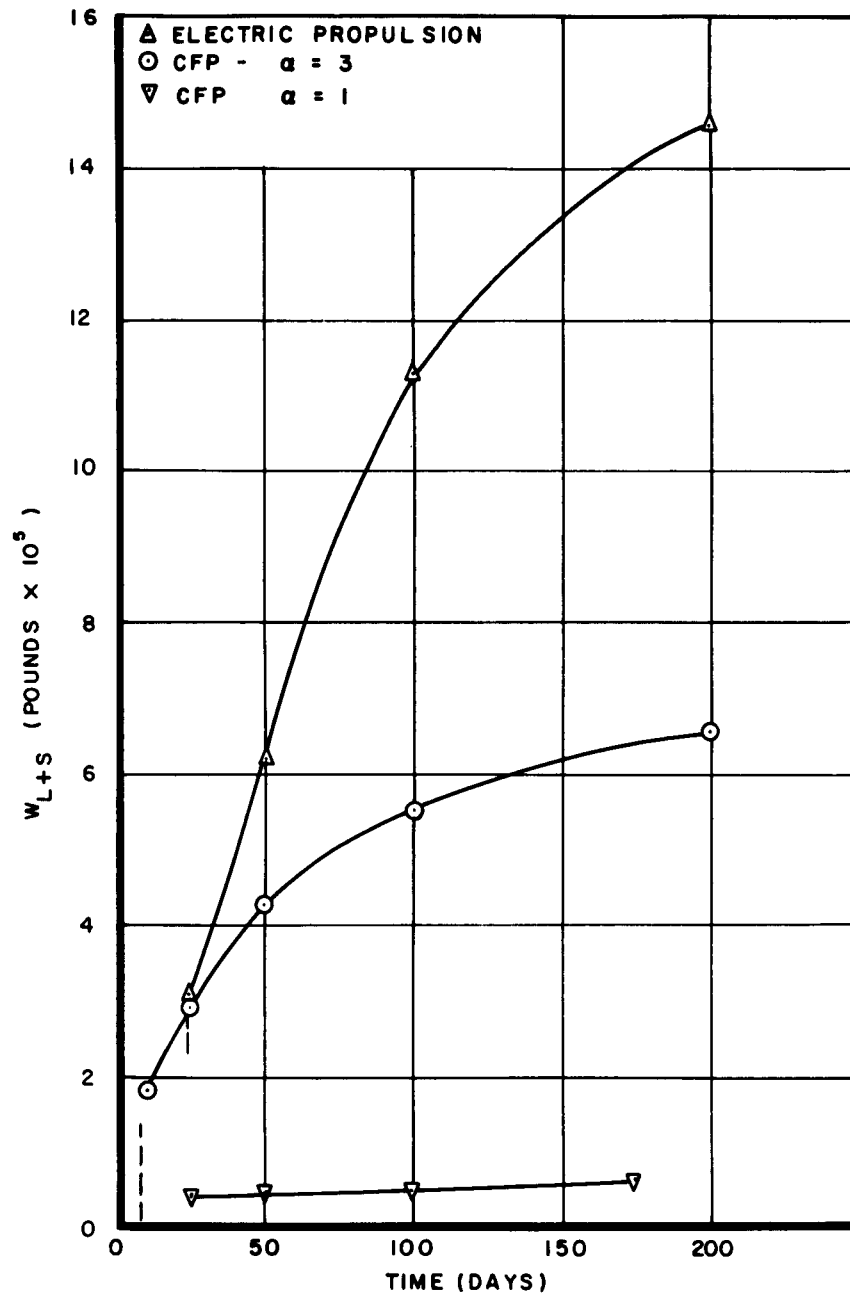Trip to Jupiter

Figure 63. Comparison of CFP System with Electric System Based on Weights of Vehicle and Payload (Optimized Systems): Payload Weight - One-Way Trip to Moon
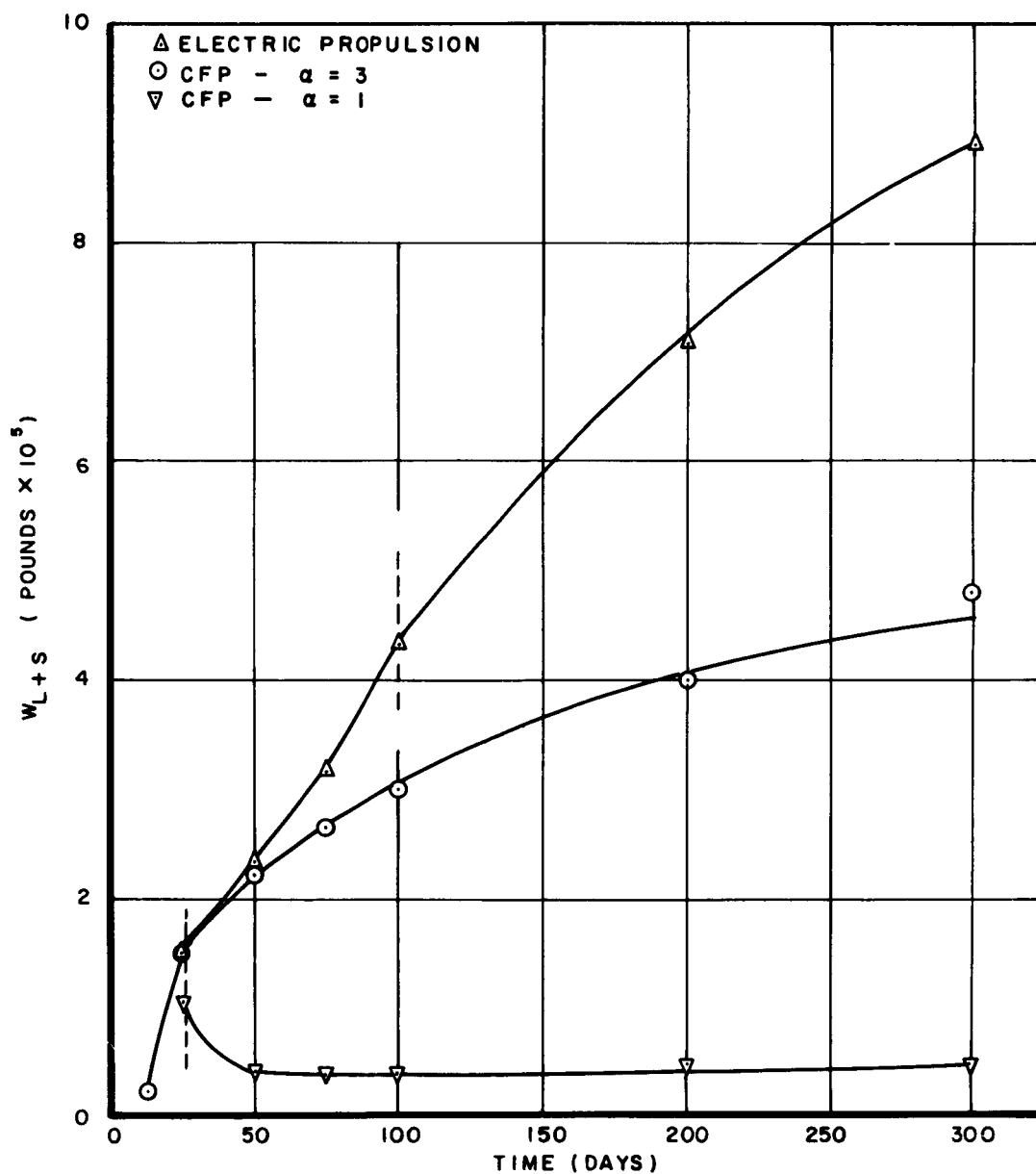
Figure 64. Comparison of CFP System with Electric System Based on Weights of
Vehicle and Payload (Optimized Systems): Payload Weight - Round
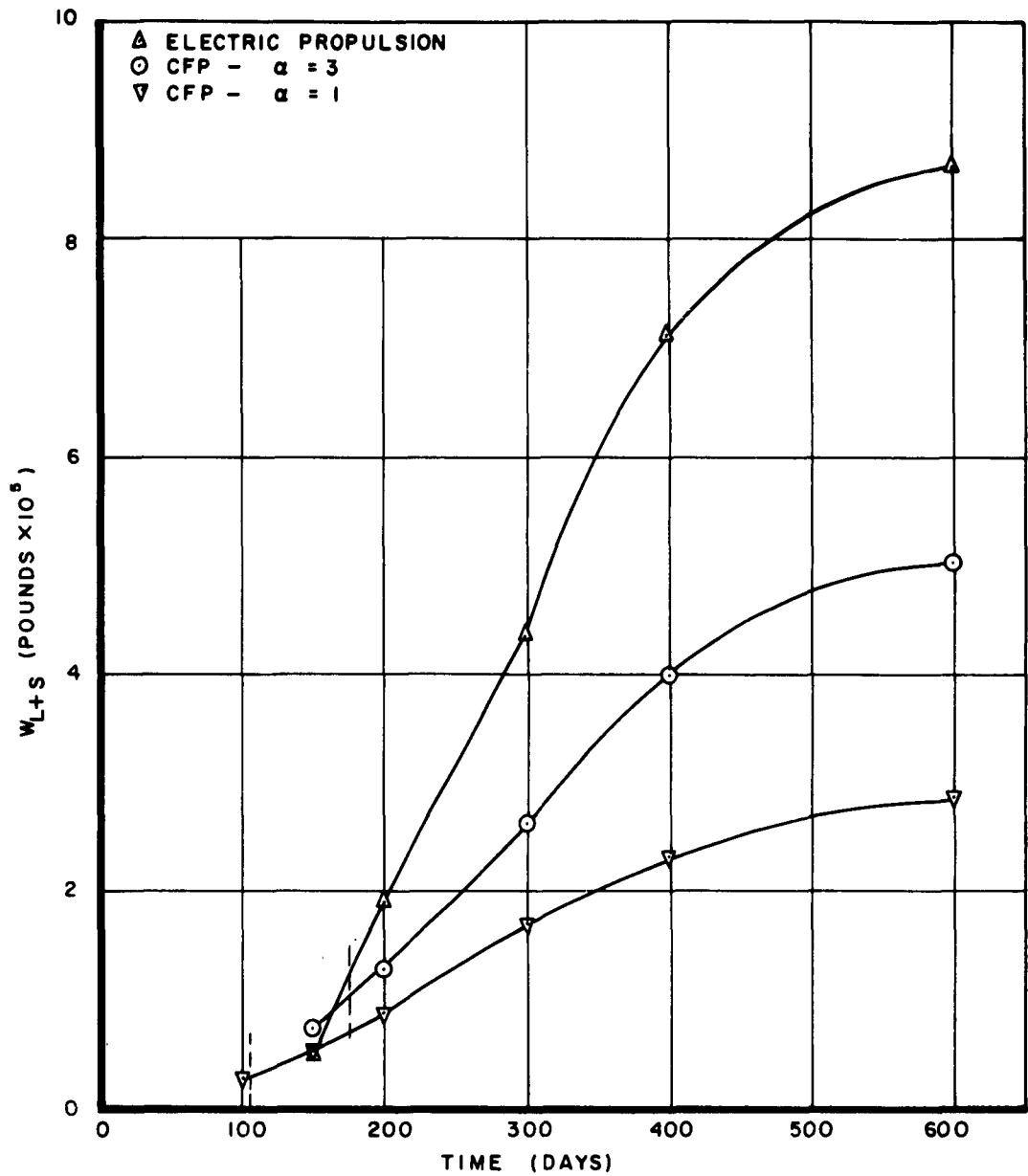Trip to Moon

Figure 65. Comparison of CFP System with Electric System Based on Weights of Vehicle and Payload (Optimized Systems): Payload Weight - One-Way Trip to Mars
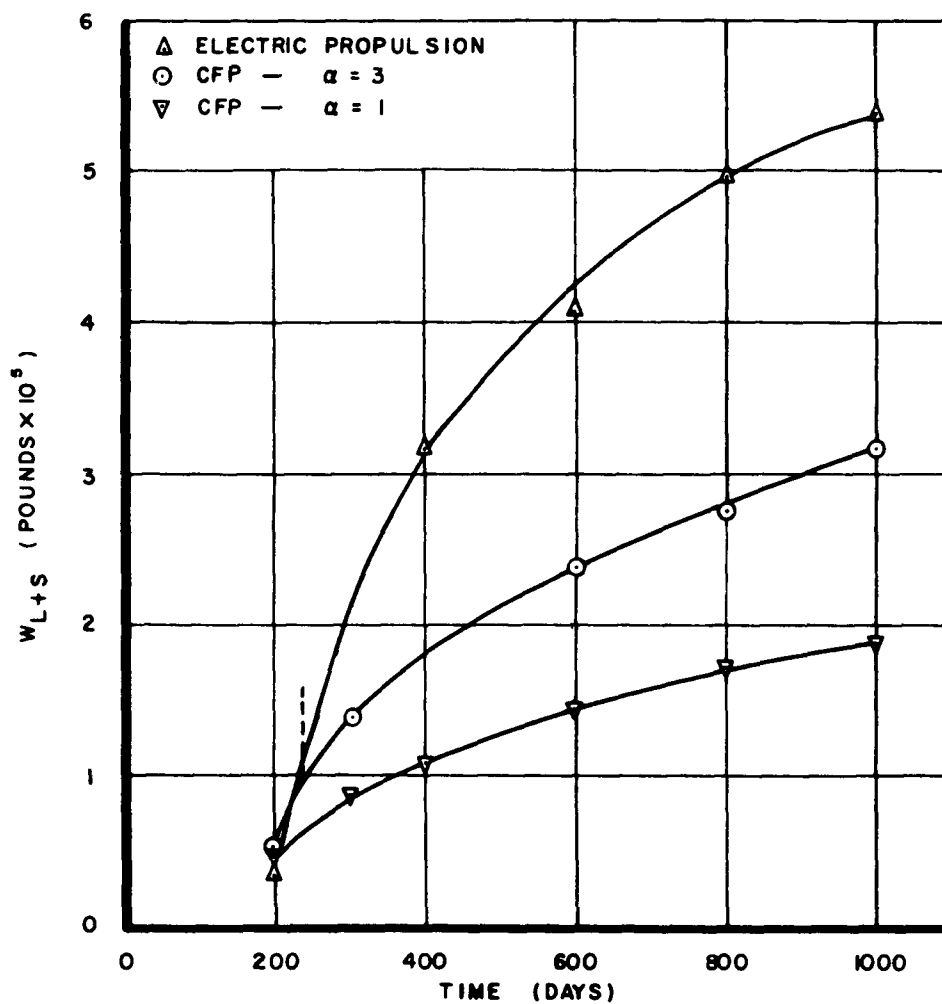
Figure 66. Comparison of CFP System with Electric System Based on Weights of
Vehicle and Payload (Optimized Systems): Payload Weight - Round
Trip to Mars

Figure 67. Comparison of CFP System with Electric System Based on Weights of Vehicle and Payload (Optimized Systems): Payload Weight - One-Way Trip to Venus

Figure 68. Comparison of CFP System with Electric System Based on Weights of
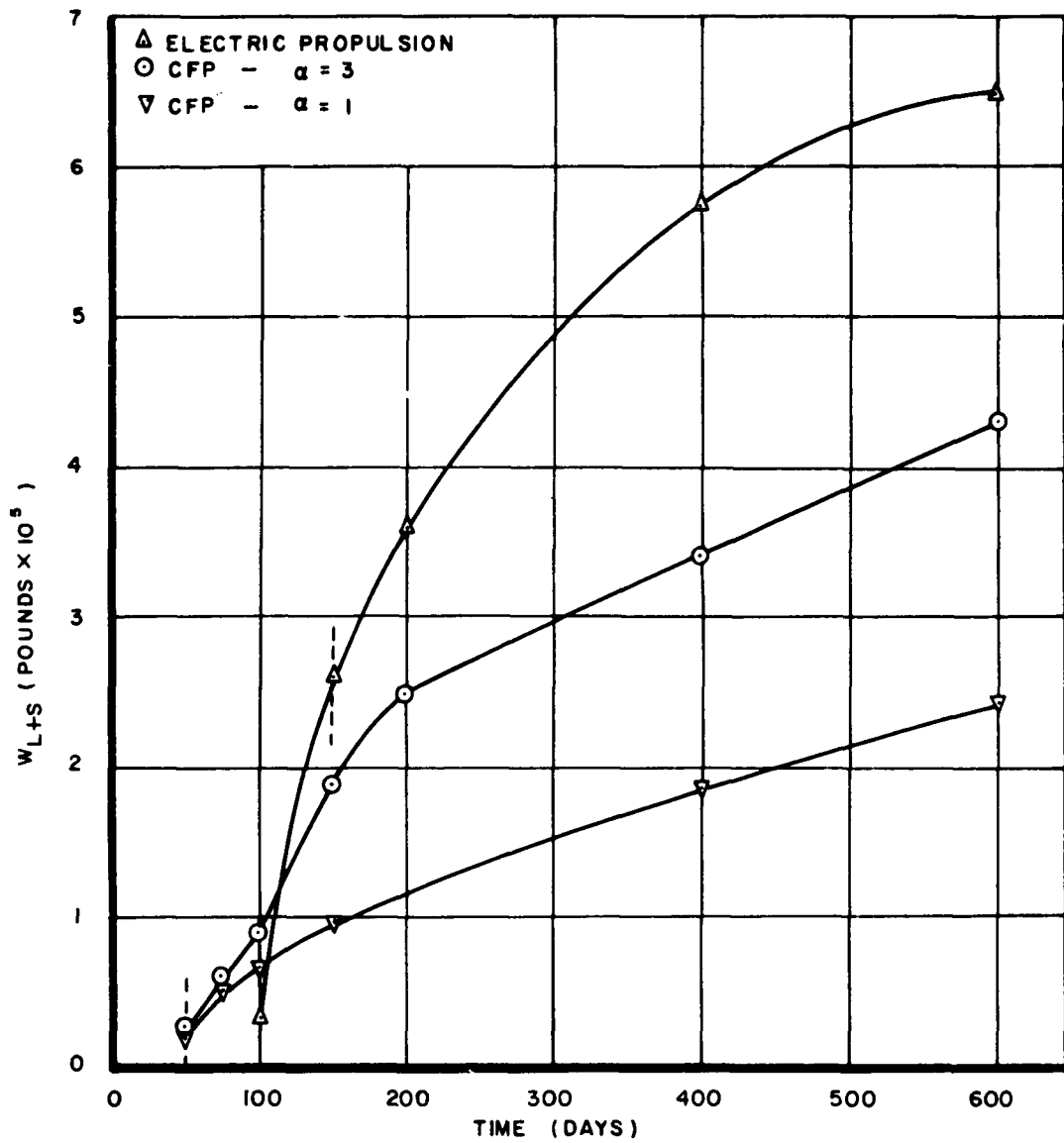Vehicle and Payload (Optimized Systems): Payload Weight - Round
Trip to Venus

Figure 69. Comparison of CFP System with Electric System Based on Weights of Vehicle and Payload (Optimized Systems): Payload Weight - One-Way Trip to Jupiter
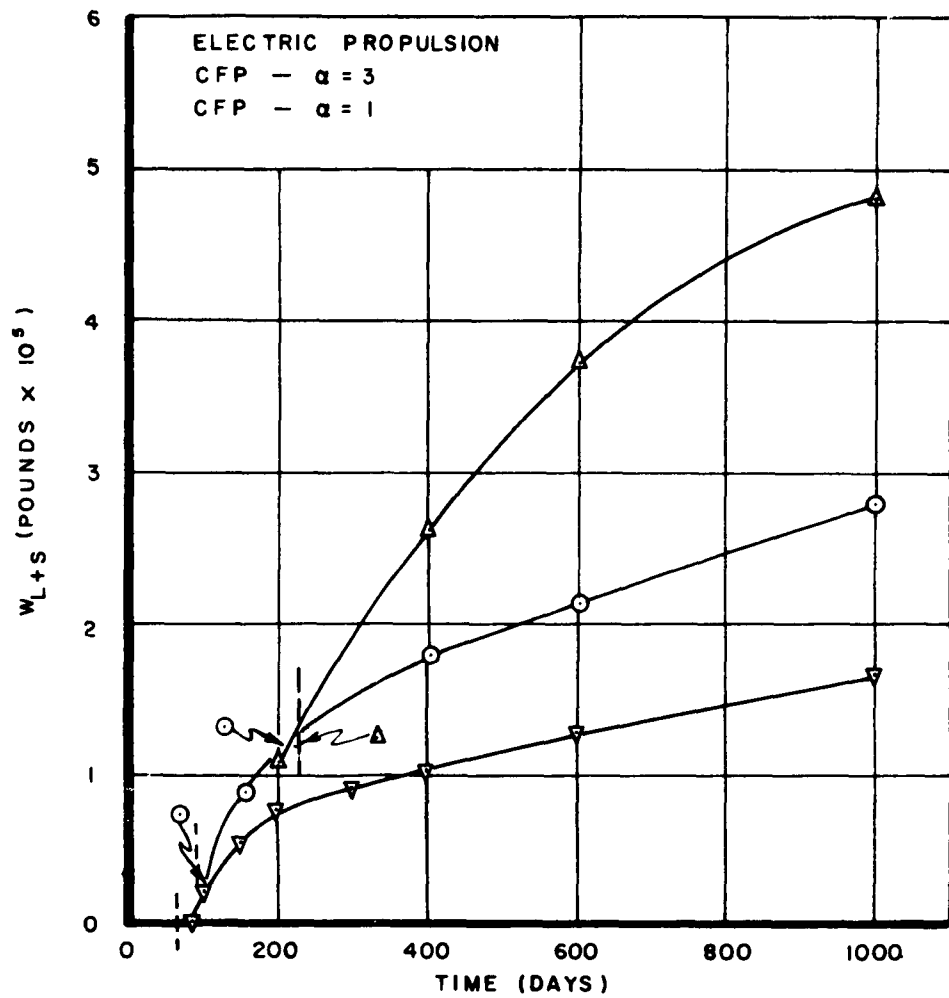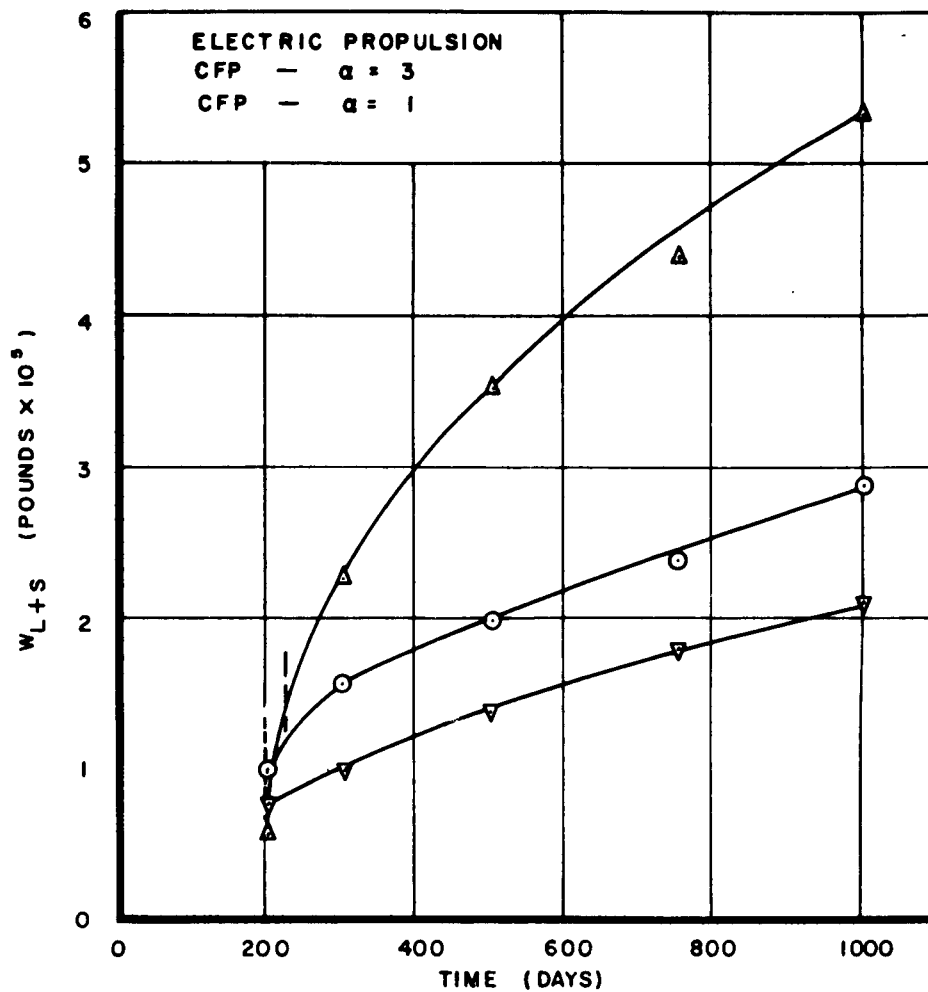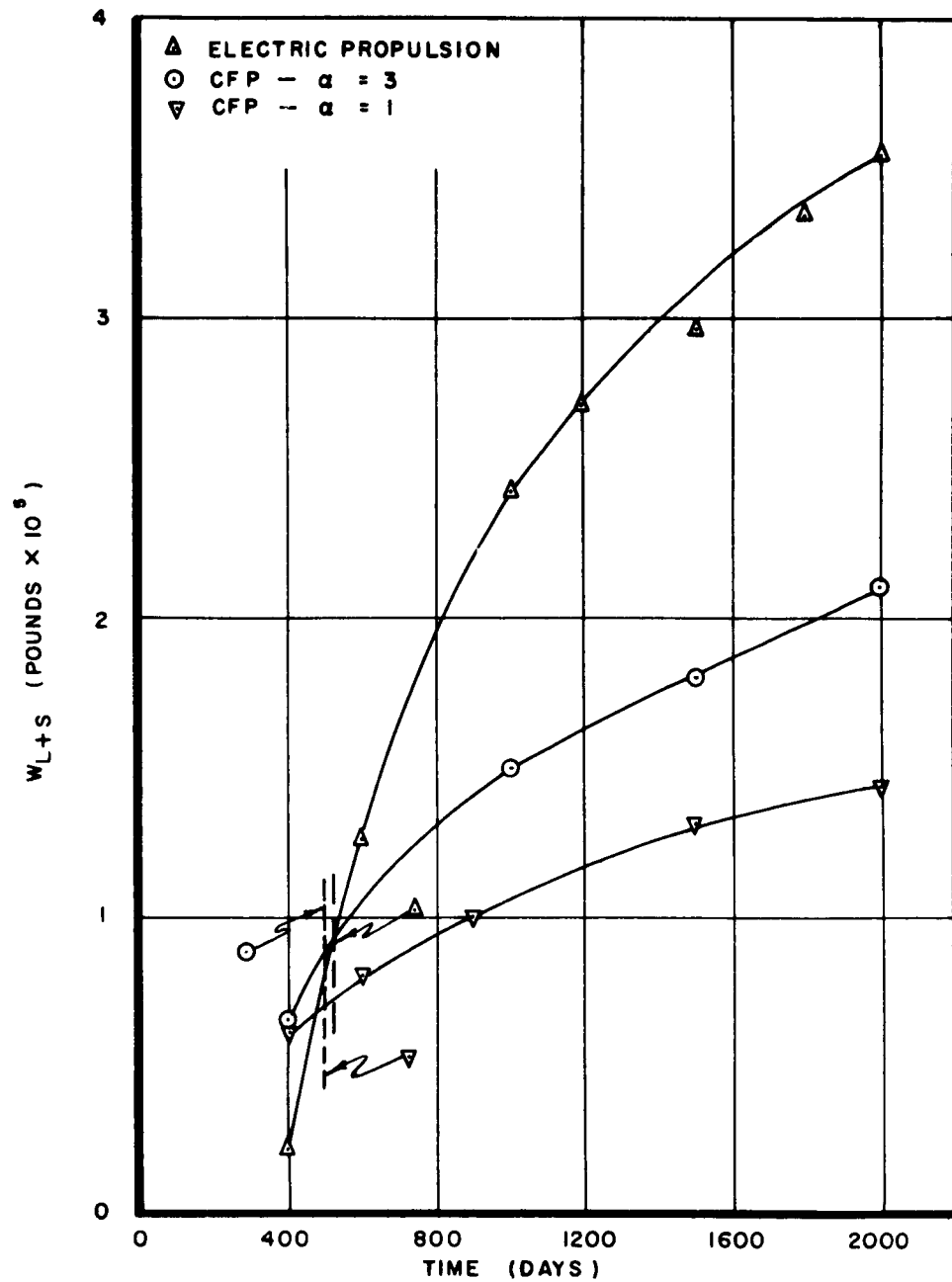
Figure 70. Comparison of CFP System with Electric System Based on Weights of Vehicle and Payload (Optimized Systems): Payload Weight - Round Trip to Jupiter

CONCLUSIONS

Justification for applied research on a new or advanced propulsion concept must logically follow two criteria. First, the basic research and supporting analytical studies must demonstrate that the propulsion concept is both feasible and potentially competitive with contemporary schemes. Secondly, the advantages of this concept over those presently available or in development must be shown. Comparison on the basis of thrust-to-weight ratio, payload fraction, specific impulse, operating lifetime, fuel consumption, and secondary power and auxiliary system requirements shows the CFP system to be competitive with, and in some cases superior to, other contemporary propulsion devices for ultra high ΔV missions.

The ultimate usefulness of a propulsion system is measured in terms of its applicability to various missions. Obviously, the variable thrust and specific impulse available from a fusion engine will render a vehicle that is powered by this system highly versatile in its applications. Some of the more obvious applications to which thermonuclear propulsion appears particularly well adapted are orbit-to-orbit transfer of extremely heavy loads, orbital or other maneuvers requiring a high total ΔV, and deep space penetration.

LIST OF REFERENCES

1. Shiel, Vincent, 1/Lt, USAF, <u>Ion Propulsion Mission Requirements and Their Effect on Ion Engine Design</u>, WADC Technical Note 59-156, Wright Air Development Center, Wright-Patterson AFB, Ohio, March 1959.

2. <u>The Ion Rocket Engine</u>, Report No. R 645P, Rocketdyne Division, North American Aviation, Inc., 1957.

3. <u>Comparison of Chemical & Electrical Propulsion Systems for Interplanetary Travel</u>, Tapco Report ER 3957, Thompson Ramo Wooldridge, 1960.

4. <u>High-Energy, Low Thrust Jupiter Missions</u>, ARS Paper, 15th Annual Meeting, American Rocket Society, December 5-8, 1960.

5. <u>Requirements for the Exploration of Jupiter and its Moons</u>, Advances in the Astronautical Sciences, Vol 6, National Aeronautics and Space Administration, 1961.

1. Electric propulsion
2. Nuclear propulsion
3. Controlled-fusion propulsion
4. Controlled-thermonuclear reactions

I. AFSC Project 5350, Task 53501
II. R. L. Verga, R. F. Cooper
III. Not avail tr OTS
IV. In ASTIA collection

Aeronautical Systems Division, Dir/Aeromechanics, Propulsion Laboratory, Wright-Patterson AFB, Ohio.
Rpt Nr ASD-TDR-62-696, MISSION ANALYSIS FOR A CONTROLLED FUSION PROPULSION SYSTEM. Apr 63, 84p. incl illus., 5 refs.

Unclassified Report

This report presents a discussion of the relationships existing between engine, vehicle, and mission parameters of a typical controlled-fusion propulsion (CFP) system. The low specific weight (α) obtainable with a CFP device allows extremely high payload fractions in large vehicles. The CFP
(over)

system is compared with other electric propulsion systems, and the CFP system is shown to possess inherent advantages for the performance of high ΔV missions.